UCGE Reports

Number 20257

Department of Geomatics Engineering

Interference Effects on GPS L2C Signal Acquisition and Tracking

(URL: http://www.geomatics.ucalgary.ca/research/publications/GradTheses.html)

by

Donghua Yao

August 2007

THE UNIVERSITY OF CALGARY

Interference Effects on GPS L2C Signal Acquisition and Tracking

by

Donghua Yao

A THESIS

SUBMITTED TO THE FACULTY OF GRADUATE STUDIES

IN PARTIAL FULFILLMENT OF THE REQUIREMENTS FOR THE

DEGREE OF MASTER OF SCIENCE

DEPARTMENT OF GEOMATICS ENGINEERING

CALGARY, ALBERTA

August, 2007

Abstract

GPS L2C signals are now being transmitted from the new-generation IIR-M satellites. L2C signals are easily affected by RF and are often distorted by RF interference. Therefore, the performance of L2C signal acquisition and tracking is influenced by RF interference. The interferences of additive white Gaussian noise and unwanted L2C signals are always accompanied with incoming desired L2C signals. In this thesis, the effects of cross-correlation and additive white Gaussian noise (AWGN) on the performances of the L2C signal acquisition and tracking are analyzed in four parts: L2C signal detection, maximum error probability of information data estimation, signal-to-noise ratio, and PLL tracking errors.

In L2C signal detection, a large cross-correlation value is used to estimate the detection probabilities. Cross-correlation will affect L2C signal detection performance. The cross-correlations increase the error probability of information data estimation. The average signal-to-noise ratio is derived under the effects of cross-correlation and AWGN. The SNR is reduced when there is more cross-correlation or when the unwanted signal power from another satellite is higher than the desired signal power. In the PLL error analysis, the PLL error is estimated by using the linear method under the cross-correlation and AWGN. Simulations are also done for the analyses of the cross-correlation and AWGN

effects on L2C signal acquisition and tracking.

Acknowledgements

My foremost thanks go to my supervisors, Professor Gérard Lachapelle and Professor Susan Skone. Their patient guidance and constant encouragement have been invaluable and made this thesis a reality.

I am grateful to my wife and my daughter for their unconditional love, endless support, and constant encouragement in my career. I thank also my parents and other family members for their love and encouragement during my study.

I would like to express my thanks to research associates and graduate students, particularly Mr. Rob Watson, for their efforts and patience during my many inquiries; their technical feedback greatly helped to improve this thesis. I thank Wei Yu for his help in a numerical experiment. Many thanks go to Bo Zheng, Gang Mao, Ning Luo, Zhi Jiang, Wouter van der Wal, Changlin Ma, Jianning Qiu, Surendran Shanmugam, Moncton Gao and Tao Hu for helpful discussions and advices. I also thank other PLAN group members, Mark Petovello, John Schleppe, as well as many others for their valuable assistances during the period of my study.

Table of Contents

List of Tables

List of Figures

Notation

List of Abbreviations

AM	Amplitude Modulation
AWGN	Additive White Gaussian Noise
BPSK	Binary Phase-Shift Keying
C/A	GPS Coarse/Acquisition Code
CL	GPS Civil Long Code
CM	GPS Civil Moderate Code
C/N_0	Carrier-to-Noise density ratio
CW	Continuous Wave
dB	Decibel
dBW	Decibel Watt
DLL	Delay Locked Loop
FM	Frequency Modulation
GPS	Global Positioning System
L2C	L2 Civil
MRSRG	Multiple Return Shift Register Generator
NCO	Numerical Controlled Oscillator
PLL	Phase Locked Loop

PN	Pseudonoise
PRN	Pseudorandom Noise
PSD	Power Spectral Density
P(Y)	Precision Code
RF	Radio Frequency
RMS	Root Mean Square
SNR	Signal to Noise Ratio
VCO	Voltage Controlled Oscillator

List of Symbols

N_0	One Side PSD of thermal noise
P_D	Probability of Detection
P_{fa}	Probability of false alarm
P_k	L2C signal power for satellite k
τ_k	Code delay of satellite k
ϕ_k	Phase offset of satellite k
Φ	Standard Gaussian cumulative distribution function

Chapter 1

Introduction

1.1 Background

In a pseudonoise (PN) spread-spectrum system, the spreading of the message signal is achieved by modulating it with a PN sequence before transmission. At the receiver, the incoming signal is despread by correlating it with the local PN sequence (Holmes 1990). Radio frequency (RF) interference may affect the link between a transmitter and a receiver in a PN spread-spectrum system. As a PN spread-spectrum system, the Global Positioning System (GPS) is also affected by RF interference. RF interference on GPS signals received by a GPS receiver will distort the signal and affect the performance of acquisition and tracking of receivers. RF interference will cause an increase in noise in receivers and decrease the signal to noise ratio (SNR) of signals; therefore they will affect the detection level. If the RF interference is very large, receivers cannot acquire signals and will lose tracking capabilities.

Many users worldwide depend on GPS for their positioning. In real-world applications, both the accuracy and reliability of GPS under non-ideal circumstances should be known to these users. RF interference affects both

accuracy and reliability of receivers and it is therefore important to study RF interference in detail.

Generally, RF interference includes cross-correlation (wideband spread spectrum), additive white Gaussian noise (AWGN), wideband phase/frequency modulation, wideband pulse, narrowband continuous wave, narrowband phase/frequency modulation, and narrowband swept continuous wave. Any radio navigation system can be disrupted by sufficiently high power interference (Parkinson 1996). Although receivers can take advantage of the spread spectrum of GPS codes, the signal can be disrupted by RF interference that is beyond a certain threshold level (Parkinson 1996).

The GPS signal consists of two components: L1 at a centre frequency of 1575.42 MHz and L2 at a centre frequency of 1227.6 MHz. The L1 signal has an in-phase carrier component which is modulated by a 10.23 MHz clock rate precision (P) signal and a quadrature carrier component that is modulated by a 1.023 MHz civil C/A signal (Kaplan 1996). The L2 carrier is biphase modulated by the P code. The new L2C signal modulates the quadrature carrier component of the L2 carrier with 1.023 MHz chip rate (Cho et al 2004). L2C uses two different PN codes for every satellite: one is the civil moderate (CM) code, which repeats every 10,230 chips, the other is the civil long (CL) code, which repeats every 767,250 chips. The L2C signal is formed by the chip-by-chip multiplexing of the

CM (with data) and CL codes (Tran et al 2003).

1.2 Radio Frequency Interference

Some research studies about the effects of RF interference on receivers in the environment of L1 with C/A code have been performed by others and are introduced as follows.

1.2.1 Cross-Correlation Interference

Cross-correlation is a type of interference in a weak signal environment. The cross-correlation properties of the L1 C/A and L2C codes are such that in a weak signal environment, the presence of a strong signal may cause a cross-correlation peak that exceeds the autocorrelation peak of the weak signal. The interference will lead to a false alarm, because the cross-correlation peak is acquired as an autocorrelation peak. Acquiring the incorrect cross-correlation peak will have a negative impact on acquisition performance as the value of the Doppler frequency and the code delay acquired are inaccurate. In the tracking loop, if the desired signal is being tracked, the cross-correlation of C/A code causes more tracking errors, in the situation of Doppler crossovers and large Doppler offsets between two satellites. Cross-correlation errors are affected by, amongst others, correlator spacing, integration time, and tracking loop filtering (Zhu & van Graas 2005).

Generally, in the analyses of C/A codes, C/A codes are assumed to be random. The power spectral density (PSD) of the signals is assumed to be $(\sin(x)/x)^2$. In theory, $(\sin(x)/x)^2$ is the PSD of codes that are maximal length PN codes and have very long periods. The C/A codes are not the maximal length PN codes and do not have sufficiently long periods to be considered purely random. Therefore the C/A codes have different autocorrelation and cross-correlation properties compared with random codes (Kumar et al 1999). Moreover, if the Doppler frequency differences are well outside the tracking loop bandwidth, cross-correlation errors will reach maximum values (Zhu & van Graas 2005)

1.2.2 Pulsed Interference

The effects of pulsed interference on receivers can vary widely depending on the characteristics of the interfering signal (peak power, duty cycle, pulse width) and the exact implementation of the receiver (Hegarty et al 2000). But in the situation of low power pulsed interference, the noise power variation is only affected minimally by coherent and non-coherent integration, and the low power pulsed interference effect on the noise power is negligible (Deshpande et al 2004a). The low power pulsed interference has no effect on the signal processing section (Deshpande et al 2004a).

1.2.3 Continuous Wave Interference

Continuous wave (CW) interference will also cause loss of lock in a signal tracking loop. In acquisition mode, the probability of detection can be strongly decreased by CW interference. The C/A code has a few strong lines in the PSD above the $(\sin(x)/x)^2$ envelope (nearly 8 dB above), which makes it more vulnerable to a continuous wave RF interference at these line frequencies than its maximum length PN sequence counterpart (Kaplan 1996). The reason is that the incoming CW interference power spread by the local code replica is not the same as the ideal PSD envelope. For the line frequencies with higher PSD than the envelope, the real CW interference powers (after spreading) are larger than the ideal powers.

Deshpande (2004a) demonstrates that for acquisition, although the continuous wave interference results in an increase in noise power when the coherent integration time and non-coherent integration time are increased, the SNR can still be raised by increasing the coherent and non-coherent integration time. With longer coherent and non-coherent integration time, receivers are able to tolerate more continuous wave interference power.

1.2.4 AM Interference

An AM signal is a continuous wave signal whose amplitude varies as a function of the modulating signal. The amount of modulation present in the signal is

determined by the modulation depth. The correlation process in acquisition and tracking spreads the interference signal and decreases the signal power to reduce the effect of the interference signal. In the presence of AM interference, the noise power increases for higher modulation depths because more modulation signals are present. The noise power increase raises the detection threshold, thereby reducing the possibility of acquisition. Therefore, with an increase of the interference power at different modulation depths, the SNR decreases and the successful acquisition percentage decreases (Deshpande et al 2004b). After correlation, the de-spread interference signal causes non-Gaussian noise. This increases the noise with an increase in the pre-detection integration period. But the SNR increases with an increase of the coherent integration time. The longer coherent integration time provides better tolerance to high noise power (Deshpande et al 2004b).

1.2.5 FM Interference

An FM signal is a CW signal whose frequency varies as a function of the modulating signal. Higher deviations of frequency result in the increase of noise power. Longer coherent integration times can increase the signal peak and allow successful acquisition. Non-coherent integration can improve the interference tolerance. For example, a coherent integration time of 20 ms is sufficient to tolerate

10 dB of interference power. A non-coherent integration factor of five and a coherent integration time beyond 8 ms can tolerate 20 dB interference power (Deshpande et al 2004b). By increasing the non-coherent integration factor, non-coherent integration improves the interference tolerance to 30 dB (Deshpande et al 2004b).

1.3 Motivation and Objective

The first new generation GPS IIR-M satellite was launched in September 2005. From this satellite, two signals are transmitted: L1 (including L1 C/A code, P(Y) code and M code) and L2 (L2C code, P(Y) and M code). A new L2 civil signal has been developed which is especially designed to provide better cross-correlation interference protection relative to the current C/A codes. Therefore, it is important to consider the cross-correlation interference and white Gaussian noise interference on this new signal.

The major objective of this thesis is to analyse the effects of the cross-correlation and white Gaussian noise interference on L2C acquisition and tracking performance. This includes

1. Evaluate the ability of detection under the AWGN and cross-correlation, especially under the weak signal environment.

2. Estimate the maximum error probability of information data estimation, especially under the weak desired incoming signal.

3. Estimate the average signal-to-noise ratio of the correlator output after integration under the normal or weak desired signal.

4. Evaluate the phase locked loop error with cross-correlation and AWGN combined and the error changes with cross-correlations under weak desired signal.

To achieve the objectives, the following tasks are carried out in this thesis:

1. To analyse the L2C signal structure including properties of the CM and CL codes and how the CM and CL codes combine into the L2C code.

2. To theoretically analyse the effects of L2C cross-correlations and AWGN interferences on L2C signal detection.

3. To estimate the error probability of the information (navigation) data estimation under the worst cross-correlation and AWGN effects and the average SNR of the correlator output under cross-correlation and AWGN.

4. To theoretically derive the PLL jitter of L2C cross-correlation and white Gaussian noise, and analyse the tracking loop performance under different noise power and cross-correlation in the weak signal environment.

5. To generate the simulated cross-correlation data of L2C signal and AWGN data.

6. To process the L2C signals with cross-correlation interference and AWGN interference by using base-band simulation method including probability of detection, average SNR of correlator output and PLL jitter.

7. To analyse the differences between the theoretical results and the output of the base-band simulation.

To realize the objectives, the theoretical analyses of the interference effects will first be carried out: analysing the effects of cross-correlation interference on L2C acquisition, error probability of the information estimation and PLL tracking performance, determining the L2C acquisition, error probability and PLL tracking performance with AWGN interference.

Second, a base-band simulation for L2C cross-correlation and AWGN interference is provided. In the simulation, the error probability and the SNR of the correlator output with and without cross-correlation are considered. In the PLL tracking loops, the PLL errors are simulated with and without cross-correlation.

Finally, the differences between the simulation and the theoretical results are analysed taking into account the limitations of the theoretical models.

1.4 Thesis Outline

In Chapter 2 of this thesis, the L2C signal structure, the output of correlator and L2C cross-correlation and AWGN interference effects on L2C signal detection are analysed.

The error probability of information data estimation under worst cross-correlation effects and the SNR of the correlator output with cross-correlation and AWGN interference are analysed in Chapter 3. A simulation is used to support this analysis. The SNR of the correlator output is derived theoretically. Then according to the SNR theoretical model, the SNR as a function of L2C signal power from other satellites is computed. In the later simulation part, by using simulated cross-correlation and white Gaussian noise interference data, the SNR is computed under the presence of cross-correlation and AWGN. Lastly, results of theoretical SNR derivations and simulated SNR are analysed.

The L2C cross-correlation and AWGN interference effects on PLL tracking loops are studied in Chapter 4. In this part, the PLL jitter is derived under the cross-correlation and AWGN interference. Furthermore, throughout the theoretical model, the theoretical PLL error is calculated. Then, by using second order PLL tracking loops and simulated cross-correlation and AWGN interference data, the PLL errors are simulated. At the end of the chapter, the results of theoretical and

simulated PLL errors are analysed.

Chapter 5 contains conclusions and recommendations.

Chapter 2

Cross-Correlation and White Gaussian Noise Effects on Acquisition

In this chapter, the structure of the L2C signal is analysed and the model of correlator output is derived. Given that during acquisition the most important task is to detect a desired L2C signal in the input signals, the probability of detection in L2C acquisition is also estimated.

2.1 L2C Code Structure

The new signal is modulated on the L2 carrier at a frequency of 1227.60 MHz. The new signal structure was augmented by the addition of the enhanced L2C code. The L2C signal is composed of two multiplexed code signals, which include the moderate length code (CM) signal with a 10,230 chip sequence repeating every 20 ms, and the long length code (CL) signal which has a 767,250 chip sequence repeating every 1.5 seconds (Fontana et al 2001). Thus, the CL code is 75 times longer than CM code. Both CM and CL codes are generated from a single multiple return shift register generator (MRSRG) (Holmes 1990). Figure 2.1 shows the L2C code generator (IS-GPS-200D 2004). Its polynomial is $1+x^3+x^4+x^5+x^6+x^9+x^{11}+x^{13}+x^{16}+x^{19}+x^{21}+x^{24}+x^{27}$ (IS-GPS-200D

2004). This polynomial is considered to be a “primitive polynomial” (Peterson 1962) and the output sequence produced by the MRSRG is an m-sequence (Holmes 1990). That is, the output sequence is a PN code with maximal length of $2^{27}-1$. Simulation studies confirm that every CM code or CL code is a part of the same PN code sequence that is shown in Table 2.1 and 2.2.

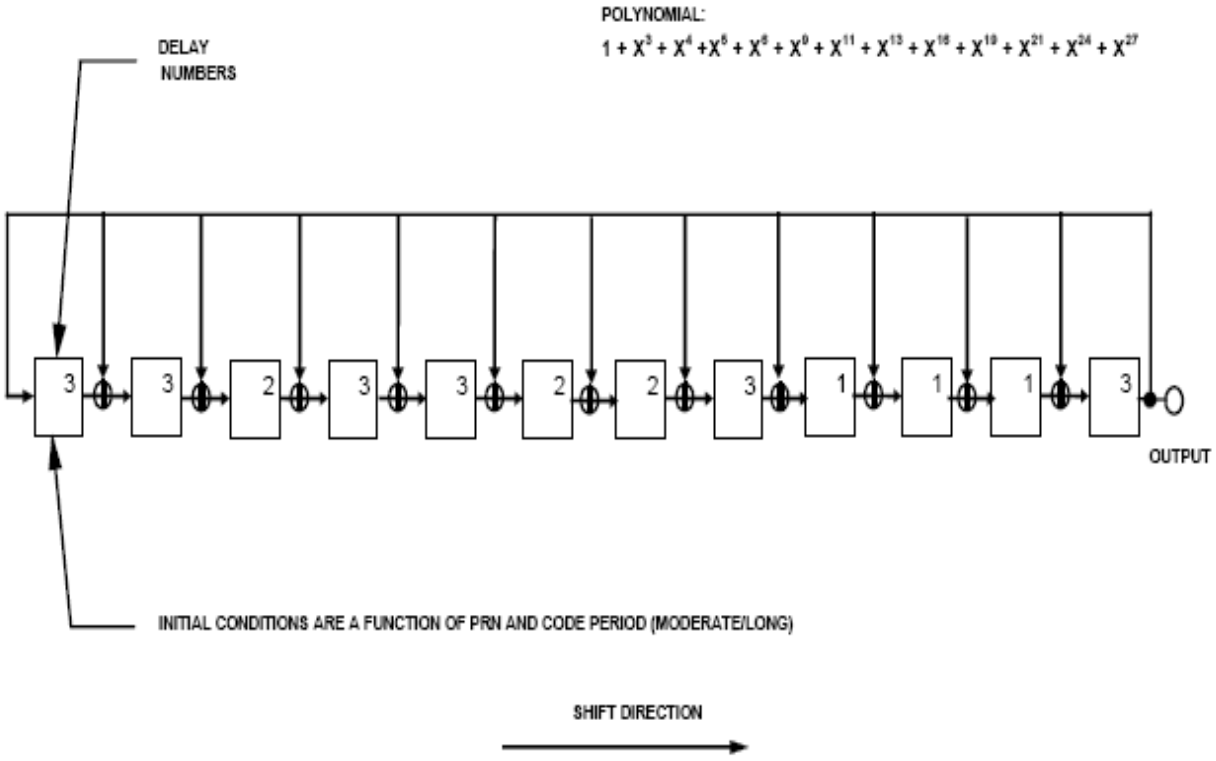

Figure 2.1 L2C Code Generator (IS-GPS-200D 2004)

Assuming that the PN code begins from the CM code with PRN 1, Figure 2.2 shows the positions of the CM and CL code area in the PN code. The area from CM1 to CL37 occupies about one-third of the PN code sequence.

Figure 2.2 Positions of CM and CL Code Area in the PN Code

Figure 2.3 shows that CM codes are distributed in order of PRN number. There is an interval between any two adjacent CM codes, except for CM4 to CM5 and CM34 to CM35, but there is no overlap. Also, CL codes are distributed in order of PRN number, with an interval between any two adjacent CL codes.

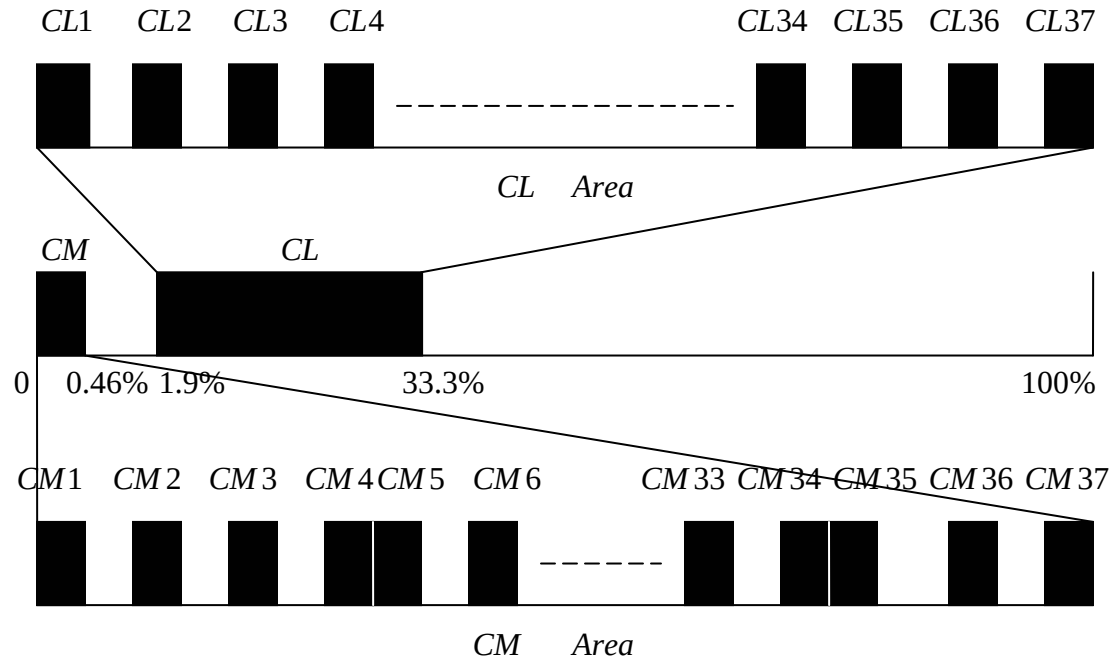

Figure 2.3 Positions of CM and CL Codes in the CM and CL Code Area

Table 2.1 provides the chip positions of CM codes in the PN code and Table 2.2 gives the chip positions of CL codes in the same PN code. Table 2.1 shows that there is no interval between CM4 and CM5 and between CM34 and CM35.

The navigation data (CNAV) on L2C is a stream of 50 symbols per second (sps). This stream is modulo-2 added and synchronized to a CM code of 10,230 chips (20 ms) which has a chip rate of 511.5 Kchips/s. The CL code has the same chip rate of 511.5 Kchips/s. A combined sequence is generated at 1.023 Mchips/s via chip-by-chip multiplexing of 75 CM codes with one CL code (the odd chips of the combined sequence are the chips of the CM code, while the chips of the CL code constitute the even chips of the combined sequence). Subsequently, this sequence is Binary Phase-Shift Keying (BPSK) modulated on the L2 carrier frequency of 1227.6 MHz to generate the GPS L2C signal. For an L2C code, the related positions of the CM and the CL codes are shown in Figure 2.4. Figure 2.5 displays the first 8 chips of an L2C code.

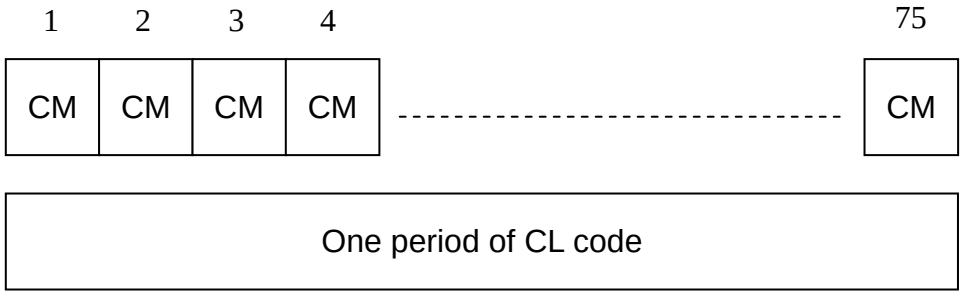

Figure 2.4 Related Positions of CM and CL Codes in the L2C Code

CM0	CL0	CM1	CL1	CM2	CL2	CM3	CL3

Figure 2.5 The Chip Positions of CM and CL Codes in the L2C Code

If the CM and CL codes are considered separately, Figure 2.6 gives the CM code and CL codes respectively.

CM0	0	CM1	0	CM2	0	CM3	0
0	CL0	0	CL1	0	CL2	0	CL3

Figure 2.6 Chips of CM and CL Codes

The CM code is interspersed with zeros: for instance, the CM code starts with the first chip of the CM code followed by a zero, followed by the second chip of CM code, etc. The CL code is also interspersed with zeros but the CL code starts with a zero, followed by the first chip of the CL code, followed by another zero, then followed by the second chip of the CL code, etc. Now the real CM code includes 20,460 chips. Half of them are zeros. The real CL code includes 1,534,500 chips and half of them are also zeros.

Table 2.1 Chip Positions of the CM Codes in the PN Code

PRN	Start Chip	End Chip	PRN	Start Chip	End Chip
CM1	1	10230	CM20	358159	368388
CM2	24669	34898	CM21	368563	378792
CM3	46159	56388	CM22	379671	389900
CM4	58357	68586	CM23	390029	400258
CM5	68587	78816	CM24	407162	417391
CM6	79923	90152	CM25	420550	430779
CM7	93620	103849	CM26	445145	455374
CM8	107201	117430	CM27	455377	465606
CM9	131569	141798	CM28	465704	475933
CM10	174842	185071	CM29	485565	495794
CM11	204213	214442	CM30	502101	512330
CM12	215951	226180	CM31	513281	523510
CM13	243924	254153	CM32	525874	536103
CM14	254666	264895	CM33	545269	555498
CM15	267233	277462	CM34	555504	565733
CM16	287283	297512	CM35	565734	575963
CM17	314872	325101	CM36	576174	586403
CM18	328577	338806	CM37	609080	619309
CM19	345852	356081			

Table 2.2 Chip Positions of the CL Codes in the PN Code

PRN	Start Chip	End Chip	PRN	Start Chip	End Chip
CL1	2572874	3340123	CL20	25086060	25853309
CL2	3611748	4378997	CL21	25860042	26627291
CL3	4776698	5543947	CL22	26632841	27400090
CL4	5549911	6317160	CL23	27404480	28171729
CL5	6600950	7368199	CL24	28479640	29246889
CL6	7693046	8460295	CL25	29461932	30229181
CL7	8490864	9258113	CL26	30527913	31295162
CL8	9813391	10580640	CL27	31463955	32231204
CL9	11318511	12085760	CL28	32255663	33022912
CL10	12301506	13068755	CL29	33084255	33851504
CL11	13089158	13856407	CL30	34138540	34905789
CL12	13856747	14623996	CL31	35770969	36538218
CL13	15831362	16598611	CL32	36613325	37380574
CL14	17989992	18757241	CL33	38779316	39546565
CL15	18836507	19603756	CL34	39872698	40639947
CL16	20185827	20953076	CL35	40649710	41416959
CL17	20963478	21730727	CL36	43057237	43824486
CL18	22095019	22862268	CL37	43893760	44661009
CL19	23196321	23963570			

2.2 L2C Signal Acquisition

The CL code period is 1.5 seconds. Direct acquisition of the CL code is therefore difficult. Since the CM code period is 20 ms, a good way to acquire the L2C signal

is to acquire and track the CM code first, then the known relationship between CM and CL code can be used to acquire and track CL code.

2.2.1 L2C Signal

If there are K satellites, the k-th navigation data signal $d_k(t)$ is a sequence of unit amplitude, positive and negative rectangular pulses with duration T (T =20 ms is the pre-integration time). The data signal $d_k(t)$ can be expressed as (Pursley 1977)

$$d_k(t) = \sum_{l=-\infty}^{\infty} d_{k,l}\, p_T(t - lT)\,. \tag{2-1}$$

Here, $p_T(t) = 1$ for $0 \le t < T$ and $p_T(t) = 0$ otherwise, and $d_{k,l} \in \{+1,-1\}$. The k-th L2C code comprises moderate and long code segments termed $CM_k(t)$ and $CL_k(t)$. The $CM_k(t)$ code consists of a 20 ms periodic sequence of unit amplitude, positive and negative rectangular pulses of duration T_c (T_c =1/20460 ms). The $CL_k(t)$ code has identical characteristics, but has a 1.5 s repetition period. If P_k represents the signal powers then the L2C signal transmitted from the k-th satellite is

$$S_k = \sqrt{2P_k}\,[d_k(t)CM_k(t) + CL_k(t)]\cos[2\pi f_{L2}t + \theta_k]\,. \tag{2-2}$$

where P_k is the L2C signal power from satellite k, $\sqrt{2P_k}$ is the amplitude of L2C

signal, $d_k(t)$ is the navigation data on the CM code and f_{L2} is the L2 carrier frequency. The variable θ_k is the carrier phase, $CM_k(t)$ represents the CM code and $CL_k(t)$ represents the CL code.

Considering that there are several satellites in view simultaneously and that there is channel noise which can be assumed to be $n(t)$ (an additive white Gaussian noise (AWGN) with a two-sided spectral density $N_0/2$), the received signal can be written as

$$r(t) = \sum_{k=1}^{K} \sqrt{2P_k}\,[d_k(t-\tau_k)CM_k(t-\tau_k) + CL_k(t-\tau_k)] \times \cos[2\pi(f_{L2} + f_{dk})t + \phi_k] + n(t) \quad (2\text{-}3)$$

where K is the number of satellites in view, f_d is the Doppler frequency of the incoming signal and $\phi_k = \theta_k - 2\pi(f_{L2} + f_d)\tau_k$ where τ_k is the code time delay.

2.2.2 Model of the Correlator Output for CM Code Acquisition

Assuming that the local signal includes the carrier and CM code replica, the local CM replica is $CM_i(t)$ which is one period of the CM code. The local in-phase carrier is $\cos[2\pi(f_{L2} + \hat{f}_{di})t]$ and the local quadrature phase carrier is $\sin[2\pi(f_{L2} + \hat{f}_{di})t]$. Here, $\hat{f}_{di}$ is the Doppler estimate for the local carrier. This estimate is in the range –4 kHz to +4 kHz, with a search step of about 33 Hz (the pre-integration time is 20 ms). The step is equal to 2/(3T) (Kaplan 1996) to find the

raw incoming Doppler. A circular correlation method is then used to find the code delay. This is achieved by first multiplying the incoming signal with the local in-phase carrier and quadrature phase carriers and correlating them with the local replica $CM_i(t)$.

The correlator outputs are

$$I_i = \int_0^T r(t) CM_i(t) \cos[2\pi(f_{L2} + \hat{f}_{di})t] dt . \tag{2-4}$$

$$Q_i = \int_0^T r(t) CM_i(t) \sin[2\pi(f_{L2} + \hat{f}_{di})t] dt . \tag{2-5}$$

which can be rewritten as

$$I_i = \int_0^T \left\{ \sum_{k=1}^{K} \sqrt{2P_k} [d_k(t-\tau_k) CM_k(t-\tau_k) + CL_k(t+mT-\tau_k)] \cos[2\pi(f_{L2} + f_{dk})t + \phi_k] + n(t) \right\} \times CM_i(t) \cos[2\pi(f_{L2} + \hat{f}_{di})t] dt \tag{2-6}$$

$$Q_i = \int_0^T \left\{ \sum_{k=1}^{K} \sqrt{2P_k} [d_k(t-\tau_k) CM_k(t-\tau_k) + CL_k(t+mT-\tau_k)] \cos[2\pi(f_{L2} + f_{dk})t + \phi_k] + n(t) \right\} \times CM_i(t) \sin[2\pi(f_{L2} + \hat{f}_{di})t] dt \tag{2-7}$$

where m = 0, 1, 2, 3,…, 74. Because the integration time is 20 ms, every 20 ms there is an integration output. For local CM code, the integration from 1 to T (T=20 ms) is one CM code period, but for incoming CL code, the integration from 1 to T is

only 1/75 period of CL code. Supposing the code delay is zero, the integration of incoming CL code is not only from $CL_k(0)$ to $CL_k(T)$, it is also possible from $CL_k(T)$ to $CL_k(2T)$, from $CL_k(2T)$ to $CL_k(3T)$,..., and from $CL_k(74T)$ to $CL_k(75T)$. That is from $CL_k(0+mT)$ to $CL_k(T+mT)$, m = 0, 1, 2, 3,…, 74, or integration is on $CL_k(t+mT)$, t is from 0 to T, m = 0, 1, 2, 3,…, 74. Now if there is a code delay τ_k, the integration will be on $CL_k(t+mT-\tau_k)$, t is from 0 to T, m = 0, 1, 2, 3,…, 74. When m=0 and t is from 0 to T, the incoming $CL_k(t-\tau_k)$ includes the last part of CL code (from $CL_k(75T-\tau_k)$ to $CL_k(75T)$) and the first part of CL code (from $CL_k(0)$ to $CL_k(T-\tau_k)$). In fact $CL_k(t+75T-\tau_k)=CL_k(t-\tau_k)$. The mT and code delay τ_k can give which part of CL code is correlated with the local CM code.

According to Viterbi (1966), supposing the AWGN $n(t)$ has been passed through a symmetric wideband bandpass filter with centre frequency ω_0 (where ω_0 is the incoming desired signal frequency), a band-limited WGN $n_b(t)$ is given which can be expressed as

$$n_b(t)=\sqrt{2}[n_1(t)\sin\omega_0 t+n_2(t)\cos\omega_0 t]. \qquad (2\text{-}8)$$

where $n_1(t)$ and $n_2(t)$ are independent Gaussian processes of zero mean and same identical spectral densities as the spectral density of $n(t)$ but their centre frequency is about zero. The processes $n_1(t)$ and $n_2(t)$ are also band-limited

WGN (Holmes 1990).

The components I and Q can be written as

$$I_i = \sum_{k=1}^{K} \sqrt{P_k / 2}[d_k M_k(\tau_k) + L_k(mT, \tau_k)]\cos(\Delta\phi_k)\frac{\sin(\pi\Delta f_k T)}{\pi\Delta f_k T} + n_I . \qquad (2\text{-}9)$$

$$Q_i = \sum_{k=1}^{K} \sqrt{P_k / 2}[d_k M_k(\tau_k) + L_k(mT, \tau_k)]\sin(\Delta\phi_k)\frac{\sin(\pi\Delta f_k T)}{\pi\Delta f_k T} + n_Q . \qquad (2\text{-}10)$$

where n_I and n_Q are centred Gaussian correlator output noise with power $\sigma_{nI}^2 = \sigma_{nQ}^2 = \frac{N_0 T}{8}$. $M_k(\tau_k) = \int_0^T CM_k(t-\tau_k)CM_i(t)dt$ is the cross-correlation between $CM_k(t-\tau_k)$ and $CM_i(t)$, $L_k(mT, \tau_k) = \int_0^T CL_k(t+mT-\tau_k)CM_i(t)dt$ is the cross-correlation between $CL_k(t+mT-\tau_k)$ and $CM_i(t)$, τ_k is the difference between the local delay and the incoming code delay, $\Delta\phi_k$ is the difference between phases of the local carrier and of the incoming signal carrier, and Δf_k is the difference between the frequency of the local carrier and that of the incoming carrier.

The centred Gaussian correlator output noise power is derived from the following formulas:

$$\sigma_{nI}^2 = Var\{\int_0^T n(t)CM_i(t)\cos(2\pi(f_{L2} + \hat{f}_{di})t + \hat{\phi}_i)dt\} . \qquad (2\text{-}11)$$

$$\sigma_{nQ}^2 = Var\{\int_0^T n(t)CM_i(t)\sin(2\pi(f_{L2} + \hat{f}_{di})t + \hat{\phi}_i)dt\}. \quad (2\text{-}12)$$

where $Var(X) = E\{(X - E(X))^2\} = E(X^2) - [E(X)]^2$, such that

$$E\{\int_0^T n(t)CM_i(t)\cos(2\pi(f_{L2} + \hat{f}_{di})t + \hat{\phi}_i)dt\} = \int_0^T E\{n(t)\}CM_i(t)\cos(2\pi(f_{L2} + \hat{f}_{di})t + \hat{\phi}_i)dt = 0$$

and

$$E\{\int_0^T n(t)CM_i(t)\sin(2\pi(f_{L2} + \hat{f}_{di})t + \hat{\phi}_i)dt\} = \int_0^T E\{n(t)\}CM_i(t)\sin(2\pi(f_{L2} + \hat{f}_{di})t + \hat{\phi}_i)dt = 0.$$

Therefore

$$\sigma_{nI}^2 = E\left\{\int_0^T n(t)CM_i(t)\cos(2\pi(f_{L2} + \hat{f}_{di})t + \hat{\phi}_i)dt\}^2\right\}. \quad (2\text{-}13)$$

$$\sigma_{nQ}^2 = E\left\{\int_0^T n(t)CM_i(t)\sin(2\pi(f_{L2} + \hat{f}_{di})t + \hat{\phi}_i)dt\}^2\right\}. \quad (2\text{-}14)$$

This result can be expressed as

$$
\begin{aligned}
\sigma_{nI}^2 &= E\left\{\int_0^T n(t)CM_i(t)\cos(2\pi(f_{L2}+\hat{f}_{di})t+\hat{\phi}_i)dt\int_0^T n(s)CM_i(s)\cos(2\pi(f_{L2}+\hat{f}_{di})s+\hat{\phi}_i)ds\right\} \\
&= E\left\{\int_0^T \sqrt{2}[-\frac{1}{2}n_1(t)\sin(2\pi\hat{f}_{di}t+\hat{\phi}_i)+\frac{1}{2}n_2(t)\cos(2\pi\hat{f}_{di}t+\hat{\phi}_i)]CM_i(t)dt\cdot\right. \\
&\quad \left.\int_0^T \sqrt{2}[-\frac{1}{2}n_1(s)\sin(2\pi\hat{f}_{di}s+\hat{\phi}_i)+\frac{1}{2}n_2(s)\cos(2\pi\hat{f}_{di}s+\hat{\phi}_i)]CM_i(s)ds\right\} \\
&= \int_0^T\int_0^T E[\frac{1}{2}n_1(t)n_1(s)\sin(2\pi\hat{f}_{di}t+\hat{\phi}_i)\sin(2\pi\hat{f}_{di}s+\hat{\phi}_i)+ \\
&\quad \frac{1}{2}n_2(t)n_2(s)\cos(2\pi\hat{f}_{di}t+\hat{\phi}_i)\cos(2\pi\hat{f}_{di}s+\hat{\phi}_i)]CM_i(t)CM_i(s)dtds \\
&= \int_0^T\int_0^T [\frac{1}{2}\frac{N_0}{2}\delta(t-s)\sin(2\pi\hat{f}_{di}t+\hat{\phi}_i)\sin(2\pi\hat{f}_{di}s+\hat{\phi}_i)+ \\
&\quad \frac{1}{2}\frac{N_0}{2}\delta(t-s)\cos(2\pi\hat{f}_{di}t+\hat{\phi}_i)\cos(2\pi\hat{f}_{di}s+\hat{\phi}_i)]CM_i(t)CM_i(s)dtds \\
&= \int_0^T \frac{N_0}{4}CM_i(t)CM_i(t)[\sin^2(2\pi\hat{f}_{di}t+\hat{\phi}_i)+\cos^2(2\pi\hat{f}_{di}t+\hat{\phi}_i)]dt \\
&= \frac{N_0}{4}\int_0^T CM_i(t)CM_i(t)dt \\
&= \frac{N_0T}{8}
\end{aligned}
$$

(2-15)

In the above equation, $n_1(t)$ and $n_2(t)$ are independent Gaussian processes with respect to each other, so $E[n_1(t)n_2(s)]=0$. Half of the $CM_i(t)$ chips are assumed to be zeros, and the property $\int_0^T CM_i(t)CM_i(t)dt=\frac{T}{2}$ is used. The double frequency component is ignored, because $(f_{L2}+\hat{f}_{di}) >> \frac{1}{T}$ and is filtered out.

With similar reasoning, Equation (2-14) can also be written as

$$\sigma_{nQ}^2 = \frac{N_0 T}{8}. \tag{2-16}$$

Suppose the difference between the local code delay and the desired incoming code delay is zero ($\tau_i = 0$) and the desired PRN is i, the correlation between the i-th received desired signal and the local signal (when $k = i$) is

$$I_{id} = \sqrt{P_i / 2}[d_{i,0} M_i(\tau_i) + L_i(mT, \tau_i)]\cos(\Delta\phi_i)\frac{\sin(\pi\Delta f_i T)}{\pi\Delta f_i T}. \tag{2-17}$$

$$Q_{id} = \sqrt{P_i / 2}[d_{i,0} M_i(\tau_i) + L_i(mT, \tau_i)]\sin(\Delta\phi_i)\frac{\sin(\pi\Delta f_i T)}{\pi\Delta f_i T}. \tag{2-18}$$

Considering the property $M_i(\tau_i) = \int_0^T CM_i(t)CM_i(t)dt = \frac{T}{2}$ (e.g. considering that half of the chips of CM code are zero), and the property $L_i(mT, \tau_i) = \int_0^T CM_i(t)CL_i(t + mT)dt = 0$ (e.g. considering the chips with value zero), Equations (2-17) and (2-18) can be rewritten as

$$I_{id} = \sqrt{P_i / 2}\,\frac{T}{2} d_{i,0}\cos(\Delta\phi_i)\frac{\sin(\pi\Delta f_i T)}{\pi\Delta f_i T}. \tag{2-19}$$

$$Q_{id} = \sqrt{P_i / 2}\,\frac{T}{2} d_{i,0}\sin(\Delta\phi_i)\frac{\sin(\pi\Delta f_i T)}{\pi\Delta f_i T}. \tag{2-20}$$

and the I_i and Q_i can be written as

$$I_i = \sqrt{P_i/2}\,\frac{T}{2}\,d_{i,0}\cos(\Delta\phi_i)\,\frac{\sin(\pi\Delta f_i T)}{\pi\Delta f_i T} + \sum_{\substack{k=1\\k\neq i}}^{K}\sqrt{P_k/2}\,[d_k(t-\tau_k)M_k(\tau_k)+L_k(mT,\tau_k)]\cos(\Delta\phi_k)\,\frac{\sin(\pi\Delta f_k T)}{\pi\Delta f_k T} + n_{\mathrm{I}} \quad . \tag{2-21}$$

$$Q_i = \sqrt{P_i/2}\,\frac{T}{2}\,d_{i,0}\sin(\Delta\phi_i)\,\frac{\sin(\pi\Delta f_i T)}{\pi\Delta f_i T} + \sum_{\substack{k=1\\k\neq i}}^{K}\sqrt{P_k/2}\,[d_k(t-\tau_k)M_k(\tau_k)+L_k(mT,\tau_k)]\cos(\Delta\phi_k)\,\frac{\sin(\pi\Delta f_k T)}{\pi\Delta f_k T} + n_{Q} \quad . \tag{2-22}$$

The CM code can be defined as (Pursley 1977)

$$CM_k(t) = \sum_{j=-\infty}^{\infty} a_{k,j}^{M}\, p_{Tc}(t - jT_c)\,. \tag{2-23}$$

where $P_{Tc}(t) = 1$ for $0 \le t < T_c$, and $P_{Tc}(t) = 0$ otherwise. If the CM and CL codes are considered separately, from Figure 2.6, the chips of the real CM code include zeros when the chip number is even. Therefore $a_{k,j}^{M} = 0$ when j is even. Otherwise $a_{k,j}^{M}$ is the sequence of code chips in the set [+1, -1] which has a period $N = T/T_c$. T_c is the duration of a chip.

The CL code can be defined as (Pursley 1977)

$$CL_k(t) = \sum_{j=-\infty}^{\infty} a_{k,j}^{L}\, p_{Tc}(t - jT_c)\,. \tag{2-24}$$

where the chips of real CL code include zeros when the chip number is odd, i.e. $a_{k,j}^{L} = 0$ when j is odd. In other cases $a_{k,j}^{L}$ is also the sequence of code chips in the set [+1, -1], which has a period $N_L N = T_L/T_c = 75T/T_c$. T_c is also the

duration of a CL chip. Equations (2-21) and (2-22) can be rewritten as

$$I_i = \sqrt{P_i/2}\frac{T}{2}d_{i,0}\cos(\Delta\phi_i)\frac{\sin(\pi\Delta f_i T)}{\pi\Delta f_i T} + \sum_{\substack{k=1\\k\neq i}}^{K}\sqrt{P_k/2}[d_{k,-1}R_{k,i}^{M}(\tau_k) + d_{k,0}\hat{R}_{k,i}^{M}(\tau_k) + R_{k,i}^{L}(\tau_k, mNT_C)]\cos(\Delta\phi_k)\frac{\sin(\pi\Delta f_k T)}{\pi\Delta f_k T} + n_I \quad (2\text{-}25)$$

$$Q_i = \sqrt{P_i/2}\frac{T}{2}d_{i,0}\sin(\Delta\phi_i)\frac{\sin(\pi\Delta f_i T)}{\pi\Delta f_i T} + \sum_{\substack{k=1\\k\neq i}}^{K}\sqrt{P_k/2}[d_{k,-1}R_{k,i}^{M}(\tau_k) + d_{k,0}\hat{R}_{k,i}^{M}(\tau_k) + R_{k,i}^{L}(\tau_k, mNT_C)]\sin(\Delta\phi_k)\frac{\sin(\pi\Delta f_k T)}{\pi\Delta f_k T} + n_Q \quad (2\text{-}26)$$

where the continuous-time partial cross-correlation is defined as (Pursley 1977)

$$R_{k,i}^{M}(\tau_k) = \int_0^{\tau_k} CM_k(t-\tau_k)CM_i(t)dt\,. \quad (2\text{-}27)$$

$$\hat{R}_{k,i}^{M}(\tau_k) = \int_{\tau_k}^{NTc} CM_k(t-\tau_k)CM_i(t)dt\,. \quad (2\text{-}28)$$

for $0 \le \tau_k \le T$. Because of the code delay τ_k, d_k may take a different value $d_{k,-1}$ or $d_{k,0}$ (+1 or -1).

The continuous-time partial cross-correlation between the CM code CL code is defined by

$$R_{k,i}^{L}(\tau_k, mNT_C) = \int_0^{NTc} CL_k(t+mNT_C-\tau_k)CM_i(t)dt\,. \quad (2\text{-}29)$$

where m = 0, 1, 2, …, 74. The length of the CL code is 75 times that of CM code. When the code delay is fixed, the cross-correlation between the CM and CL code has 75 possibilities because of the 75 different values of m.

According to Pursley (1977), for $0 \le \tau_k < T$, there is an l that fits $0 \le lT_c \le \tau_k \le (l+1)T_c < T$, so the continuous-time partial cross-correlation can be expressed as

$$R_{k,i}^{M}(\tau_k) = C_{k,i}(l-N)T_c + [C_{k,i}(l+1-N) - C_{k,i}(l-N)](\tau_k - lT_c)\,. \qquad (2\text{-}30)$$

$$\hat{R}_{k,i}^{M}(\tau_k) = C_{k,i}(l)T_c + [C_{k,i}(l+1) - C_{k,i}(l)](\tau_k - lT_c)\,. \qquad (2\text{-}31)$$

where

$$C_{k,i}(l) = \begin{cases} \sum_{j=0}^{N-1-l} a_{k,j}^{M} a_{i,j+l}^{M}, & 0 \le l \le N-1 \\ \sum_{j=0}^{N-1+l} a_{k,j-l}^{M} a_{i,j}^{M}, & 1-N \le l < 0\,. \\ 0, & |l| \ge N \end{cases} \qquad (2\text{-}32)$$

Given Equations (2-23) and (2-24), the cross-correlation function between CL and CM can be written as

$$R_{k,i}^{L}(\tau_k, mNT_c) = \int_0^{NT_C} CL_k(t + mNT_c - \tau_k)\,CM_i(t)\,dt$$
$$= \int_0^{NT_C} \sum_{j=-\infty}^{\infty} \sum_{n=-\infty}^{\infty} a_{k,j}^{L} \cdot P_{Tc}[t + mNT_c - jT_c - \tau_k] \cdot a_{i,n}^{M} \cdot P_{Tc}[t - nT_c] \cdot dt\,.$$

From time 0 to time $T = NT_C$, there are N chips. The integration can be done on every chip time. Furthermore, supposing a code delay $\tau_k = lT_c + \Delta\tau$, and because the $\Delta\tau$ may not be zero, the code chip of the incoming signal is not matched with a chip of the local signal. The correlations on the two parts are different. The integration on every local chip time can be on the two different incoming chips. Therefore the integration can be divided into two parts: one is from the beginning of the chip time to $\Delta\tau$, and the other from $\Delta\tau$ to the end of the chip time T_C. This cross-correlation function can be written as

$$
\begin{aligned}
R_{k,i}^{L}(\tau_k, mNT_c) &= \sum_{\mathrm{r}=0}^{\mathrm{N}-1} \int_{rTc}^{(r+1)Tc} \sum_{j=-\infty}^{\infty} \sum_{n=-\infty}^{\infty} a_{k,j}^{L} P_{Tc}[t + mNT_c - jT_c - lT_c - \Delta\tau] a_{i,n}^{M} P_{Tc}[t - nT_c]\,dt \\
&= \sum_{r=0}^{N-1} a_{i,r}^{M} \int_{rTc}^{rTc+\Delta\tau} \sum_{j=-\infty}^{\infty} a_{k,j}^{L} P_{Tc}[t + mNT_c - jT_c - lT_c - \Delta\tau]\,dt \\
&\quad + \sum_{r=0}^{N-1} a_{i,r}^{M} \int_{rTc+\Delta\tau}^{(r+1)Tc} \sum_{j=-\infty}^{\infty} a_{k,j}^{L} P_{Tc}[t + mNT_c - jT_c - lT_c - \Delta\tau]\,dt
\end{aligned}
\quad .
$$

where $0 \le l \le N-1$, $0 \le \Delta\tau < T_c$.

In the chip time range from rT_c to $(r+1)T_c$, $P_{Tc}[t - nT_c] = 1$ when $n = r$. Therefore $a_{i,n}^{M} = a_{i,r}^{M}$. But on the same time interval [rT_c , $(r+1)T_c$], $P_{Tc}[t + mNT_c - jT_c - lT_c - \Delta\tau] = 1$ when $0 \le t + mNT_c - jT_c - lT_c - \Delta\tau < T_c$. This condition requires that the time interval be divided into two parts: $[rT_c, rT_c + \Delta\tau]$ and $[rT_c + \Delta\tau, (r+1)T_c]$. In the two time intervals, j will take different values. In the first part, $rT_c \le t < rT_c + \Delta\tau$, $j = r + mN - l - 1$. In the second part,

$rT_c + \Delta\tau \le t < (r+1)T_c$, $j = r + mN - l$. Therefore, the cross-correlation function between the CM and CL code can be written as

$$\begin{aligned} R_{k,i}^{L}(\tau_k, mNT_C) &= \sum_{r=0}^{N-1} a_{i,r}^{M} \int_{rTc}^{rTc+\Delta\tau} \sum_{j=-\infty}^{\infty} a_{k,j}^{L} P_{Tc}[t + mNT_c - jT_c - lT_c - \Delta\tau]dt \\ &\quad + \sum_{r=0}^{N-1} a_{i,r}^{M} \int_{rTc+\Delta\tau}^{(r+1)Tc} \sum_{j=-\infty}^{\infty} a_{k,j}^{L} P_{Tc}[t + mNT_c - kT_c - lT_c - \Delta\tau]dt \\ &= \sum_{r=0}^{N-1} a_{i,r}^{M} \int_{rTc}^{rTc+\Delta\tau} a_{k,r+mN-l-1}^{L} dt + \sum_{r=0}^{N-1} a_{i,r}^{M} \int_{rTc+\Delta\tau}^{(r+1)Tc} a_{k,r+mN-l}^{L} dt \\ &= \sum_{r=0}^{N-1} a_{i,r}^{M} a_{k,r+mN-l-1}^{L} \cdot \Delta\tau + \sum_{r=0}^{N-1} a_{i,r}^{M} a_{k,r+mN-l}^{L} \cdot (T_c - \Delta\tau) \\ &= \sum_{r=0}^{N-1} a_{i,r}^{M} a_{k,r+mN-l}^{L} \cdot T_c + [\sum_{r=0}^{N-1} a_{i,r}^{M} a_{k,r+mN-l-1}^{L} - \sum_{r=0}^{N-1} a_{i,r}^{M} a_{k,r+mN-l}^{L}] \cdot (\tau_k - lT_c) \\ &= W_{k,i}(m,l) \cdot T_c + [W_{k,i}(m,l+1) - W_{k,i}(m,l)] \cdot (\tau_k - lT_c) \end{aligned} \quad . \text{ (2-33)}$$

where

$$W_{k,i}(m,l) = \sum_{r=0}^{N-1} a_{i,r}^{M} a_{k,r+mN-l}^{L}, 0 \le l \le N-1, \ \tau_k - lT_c = \Delta\tau, \ m = 0, 1, 2, \ldots, 74.$$

when $m = 75$, $a_{k,r+75N-l}^{L} = a_{k,r-l}^{L}$.

2.2.3 Largest Cross-Correlation

The cross-correlation components are considered: $d_{k,-1}R_{k,i}^{M}(\tau_k)$, $d_{k,0}\hat{R}_{k,i}^{M}(\tau_k)$ and $R_{k,i}^{L}(\tau_k, mNT_C)$. Because the code delay τ_k can be changed in the range of 0 to T and m can be taken to be 0, 1, 2,…,74, the values of $d_{k,-1}R_{k,i}^{M}(\tau_k)$, $d_{k,0}\hat{R}_{k,i}^{M}(\tau_k)$ and $R_{k,i}^{L}(\tau_k, mNT_C)$ vary with τ_k and m. In the worst-case scenario

$d_{k,-1}R^M_{k,i}(\tau_k) + d_{k,0}\hat{R}^M_{k,i}(\tau_k) + R^L_{k,i}(\tau_k, mNT_C)$ will have the largest absolute values; in such cases the effect of the cross-correlation is maximum.

The chips in the CM code with even numbers and the chips in the CL code with odd numbers are all zeros. For the continuous time partial cross-correlations $R^M_{k,i}(\tau_k)$, $\hat{R}^M_{k,i}(\tau_k)$, and $R^L_{k,i}(\tau_k, mNT_C)$, because N is an even number the following are derived for cases in which l is an odd number.

$C_{k,i}(l) = \sum_{j=0}^{N-1-l} a^M_{k,j} a^M_{j,+l} = 0$, $C_{k,i}(l-N) = \sum_{j=0}^{l-1} a^M_{k,j-l+N} a^M_{i,j} = 0$ and

$W_{k,i}(m, l+1) = \sum_{r=0}^{N-1} a^M_{i,r} a^L_{k,r+mN-l-1} = 0$.

The three continuous time cross-correlations

$R^M_{k,i}(\tau_k) = C_{k,i}(l-N)T_c + [C_{k,i}(l+1-N) - C_{k,i}(l-N)](\tau_k - lT_c)$,

$\hat{R}^M_{k,i}(\tau_k) = C_{k,i}(l)T_c + [C_{k,i}(l+1) - C_{k,i}(l)](\tau_k - lT_c)$, and

$R^L_{k,i}(\tau_k, mNT_C) = W_{k,i}(m,l)\cdot T_c + [W_{k,i}(m,l+1) - W_{k,i}(m,l)]\cdot(\tau_k - lT_c)$

can be rewritten as

$$R^M_{k,i}(\tau_k) = C_{k,i}(l+1-N)\cdot\Delta\tau. \quad (2\text{-}34)$$

$$\hat{R}^M_{k,i}(\tau_k) = C_{k,i}(l+1)\cdot\Delta\tau. \quad (2\text{-}35)$$

$$R_{k,i}^{L}(\tau_k, mNT_C) = W_{k,i}(m,l)\cdot(T_c - \Delta\tau)\,. \tag{2-36}$$

where $\Delta\tau = \tau_k - lT_c$, $0 \le \Delta\tau \le T_c$.

For cases in which l is an even number the following expressions are derived.

$C_{k,i}(l+1) = \sum_{j=0}^{N-2-l} a_{k,j}^{M} a_{i,j+l+1}^{M} = 0$, $C_{k,i}(l+1-N) = \sum_{j=0}^{l} a_{k,j-l-1+N}^{M} a_{i,j}^{M} = 0$ and

$W_{k,i}(m,l) = \sum_{r=0}^{N-1} a_{i,r}^{M} a_{k,r+mN-l}^{L} = 0$.

The three continuous time cross-correlations can be rewritten as

$$R_{k,i}^{M}(\tau_k) = C_{k,i}(l-N)\cdot(T_c - \Delta\tau)\,. \tag{2-37}$$

$$\hat{R}_{k,i}^{M}(\tau_k) = C_{k,i}(l)\cdot(T_c - \Delta\tau)\,. \tag{2-38}$$

$$R_{k,i}^{L}(\tau_k, mNT_C) = W_{k,i}(m,l+1)\cdot\Delta\tau\,. \tag{2-39}$$

where $\Delta\tau = \tau_k - lT_c$, $0 \le \Delta\tau \le T_c$.Given the first two terms of the cross-correlation $d_{k,-1}R_{k,i}^{M}(\tau_k) + d_{k,0}\hat{R}_{k,i}^{M}(\tau_k) + R_{k,i}^{L}(\tau_k, mNT_C)$, and assuming that l is an even number, the cross-correlation between the local and incoming CM code (with navigation data) can be written as follows when taking Equations (2-37) and (2-38) into account:

$$d_{k,-1}R_{k,i}^{M}(\tau_k)+d_{k,0}\hat{R}_{k,i}^{M}(\tau_k)=d_{k,-1}C_{k,i}(l-N)\cdot(T_c-\Delta\tau)+d_{k,0}C_{k,i}(l)\cdot(T_c-\Delta\tau)$$
$$=\begin{cases}d_{k,-1}[C_{k,i}(l-N)+C_{k,i}(l)]\cdot(T_c-\Delta\tau); d_{k,-1}=d_{k,0}\\ d_{k,-1}[C_{k,i}(l-N)-C_{k,i}(l)]\cdot(T_c-\Delta\tau); d_{k,-1}=-d_{k,0}\end{cases}.$$

The above equation shows that the cross-correlation between the local and incoming CM code is a straight line over the time area [lT_C, $(l+1)T_C$]. When $d_{k,-1}=d_{k,0}$, the slope of the line is $-d_{k,-1}[C_{k,i}(l-N)+C_{k,i}(l)]$. When $d_{k,-1}=-d_{k,0}$, the slope is $-d_{k,-1}[C_{k,i}(l-N)-C_{k,i}(l)]$. When $\tau_k=lT_C$ (e.g. $\Delta\tau=0$ on the left boundary) the cross-correlation reaches its extreme value of $d_{k,-1}[C_{k,i}(l-N)+C_{k,i}(l)]T_c$ or $d_{k,-1}[C_{k,i}(l-N)-C_{k,i}(l)]T_c$. On the right boundary, when $\tau_k=(l+1)T_C$ (e.g. $\Delta\tau=T_C$) the cross-correlation is zero.

Assuming that l is an odd number, from Equations (2-34) and (2-35) the cross-correlation between the local and incoming CM code with navigation data can be written as

$$d_{k,-1}R_{k,i}^{M}(\tau_k)+d_{k,0}\hat{R}_{k,i}^{M}(\tau_k)=d_{k,-1}C_{k,i}(l+1-N)\cdot\Delta\tau+d_{k,0}C_{k,i}(l+1)\cdot\Delta\tau$$
$$=\begin{cases}d_{k,-1}[C_{k,i}(l+1-N)+C_{k,i}(l+1)]\cdot\Delta\tau; d_{k,-1}=d_{k,0}\\ d_{k,-1}[C_{k,i}(l+1-N)-C_{k,i}(l+1)]\cdot\Delta\tau; d_{k,-1}=-d_{k,0}\end{cases}.$$

The cross-correlation between the two codes is also a straight line over the time interval [lT_C , $(l+1)T_C$]. When $d_{k,-1}=d_{k,0}$, the slope of the line is $d_{k,-1}[C_{k,i}(l+1-N)+C_{k,i}(l+1)]$. When $d_{k,-1}=-d_{k,0}$, the slope is $d_{k,-1}[C_{k,i}(l+1-N)-C_{k,i}(l+1)]$. At the left boundary, when $\Delta\tau=0$, the cross-correlation is zero. At the right boundary, when $\Delta\tau=T_C$, the

cross-correlation reaches its extreme value, namely $d_{k,-1}[C_{k,i}(l+1-N)+C_{k,i}(l+1)]T_C$, or $d_{k,-1}[C_{k,i}(l+1-N)-C_{k,i}(l+1)]T_C$. Through these analyses, we know that the cross-correlation between the local and incoming CM code from another satellite will have many cases of extreme values. In the code delay period [0, T], when the code delay is an even integer multiple of T_C , $\tau_k = lT_C$, $l = 0, 2, 4, \ldots, N-2$ is an even number and the cross-correlation reaches the following extreme value

$$d_{k,-1}[C_{k,i}(l-N)+C_{k,i}(l)]T_C = \lambda_{ki} \cdot T_C .$$

or

$$d_{k,-1}[C_{k,i}(l-N)-C_{k,i}(l)]T_C = \hat{\lambda}_{ki} \cdot T_C .$$

When the code delay is an odd integer multiple of T_C , $\tau_k = lT_C$, $l = 1, 3, 5, \ldots, N-1$ is an odd number, and the cross-correlation becomes zero. Therefore, the maximum value of the cross-correlation $d_{k,-1}R_{k,i}^{M}(\tau_k)+d_{k,0}\hat{R}_{k,i}^{M}(\tau_k)$ is the highest one of these extreme values.

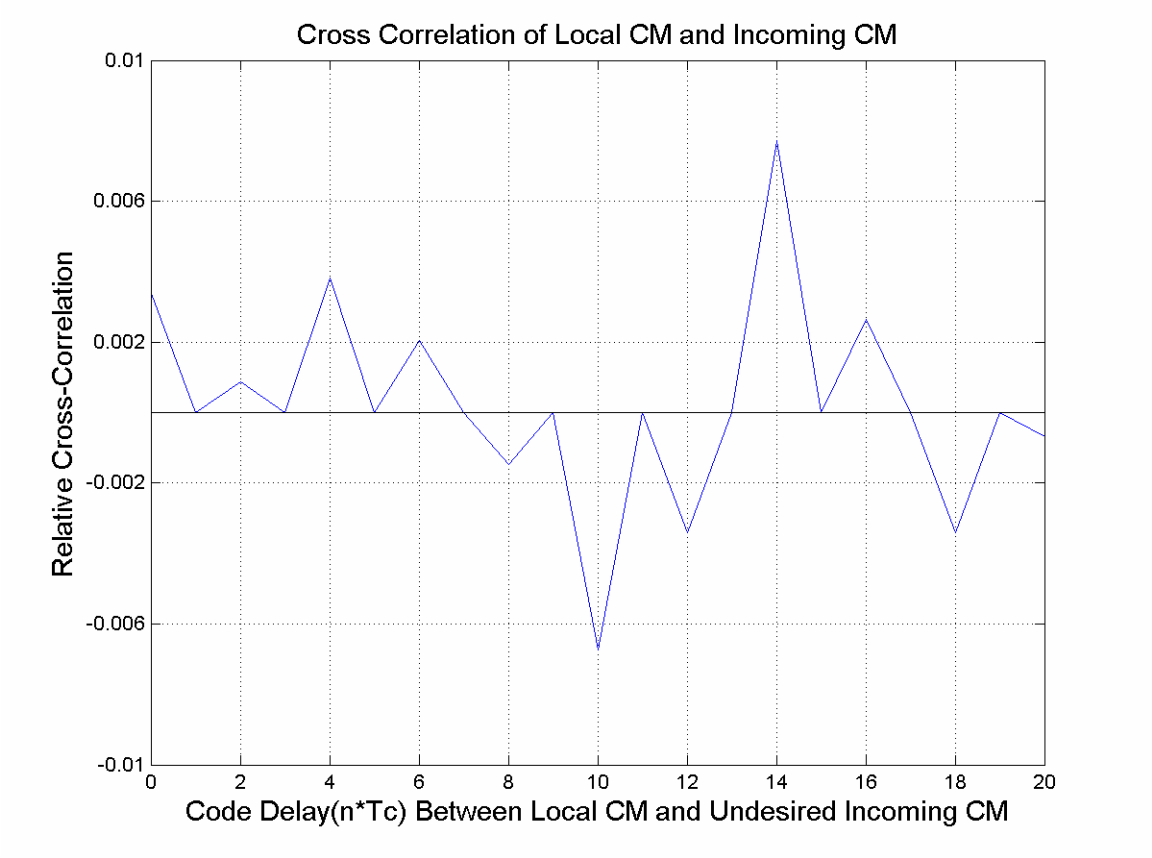

Figure 2.7 Variation of Cross-Correlation between Local and Incoming CM Code with Delays Ranging from 0 to 20 T_C

Figure 2.7 displays the simulated cross-correlation between the local CM code for PRN=1 and the incoming CM code for PRN=2. This figure gives only the cross-correlation with code delay [0, $20T_C$]. The relative cross-correlation is the value of the cross-correlation related to the value of the auto-correlation. It shows that when the code delay is an odd integer multiple of T_C, the cross-correlation is zero. When the code delay is an even integer multiple of T_C, the cross-correlation takes its extreme value.

The cross-correlation between the local and incoming CM code is affected by the navigation data. Assuming that the navigation data $d_{k,-1}$ and $d_{k,0}$ can be 1 or -1 with the same probabilities, any value of the cross-correlation can be positive or negative, so the cross-correlation between the local and incoming CM code with navigation data is symmetrical. The maximum cross-correlation (should be positive) equals the absolute value of the minimum cross-correlation.

Now, consider the cross-correlation between a local CM code and an incoming CL code from another satellite. Given the last term of the cross-correlation $d_{k,-1}R^M_{k,i}(\tau_k) + d_{k,0}\hat{R}^M_{k,i}(\tau_k) + R^L_{k,i}(\tau_k, mNT_C)$ and assuming l is an even number, from Equation (2-39), the cross-correlation between the local CM code and the incoming CL code can be written as

$$R^L_{k,i}(\tau_k, mNT_C) = W_{k,i}(m, l+1) \cdot \Delta\tau \ .$$

This cross-correlation is a straight line in the time interval [$mT + lT_C$, $mT + (l+1)T_C$]. The slope of the line is $W_{k,i}(m, l+1)$. The cross-correlation reaches the extreme value $W_{k,i}(m, l+1) \cdot T_C$ at the right boundary $\Delta\tau = T_C$, $\tau_k = (l+1)T_C$. At the left boundary, the cross-correlation becomes zero ($\Delta\tau = 0$, $\tau_k = lT_C$).

Assuming that l is an odd number, from Equation (2-36), the cross-correlation can be given by

$$R_{k,i}^{L}(\tau_k, mNT_C) = W_{k,i}(m,l)\cdot(T_c - \Delta\tau).$$

The cross-correlation is also a straight line in the time interval [$mT + lT_C$, $mT + (l+1)T_C$]. The slope of the line is $W_{k,i}(m,l)$. The cross-correlation reaches the extreme value $W_{k,i}(m,l)\cdot T_C$ on the left boundary. On the right boundary, the cross-correlation becomes zero.

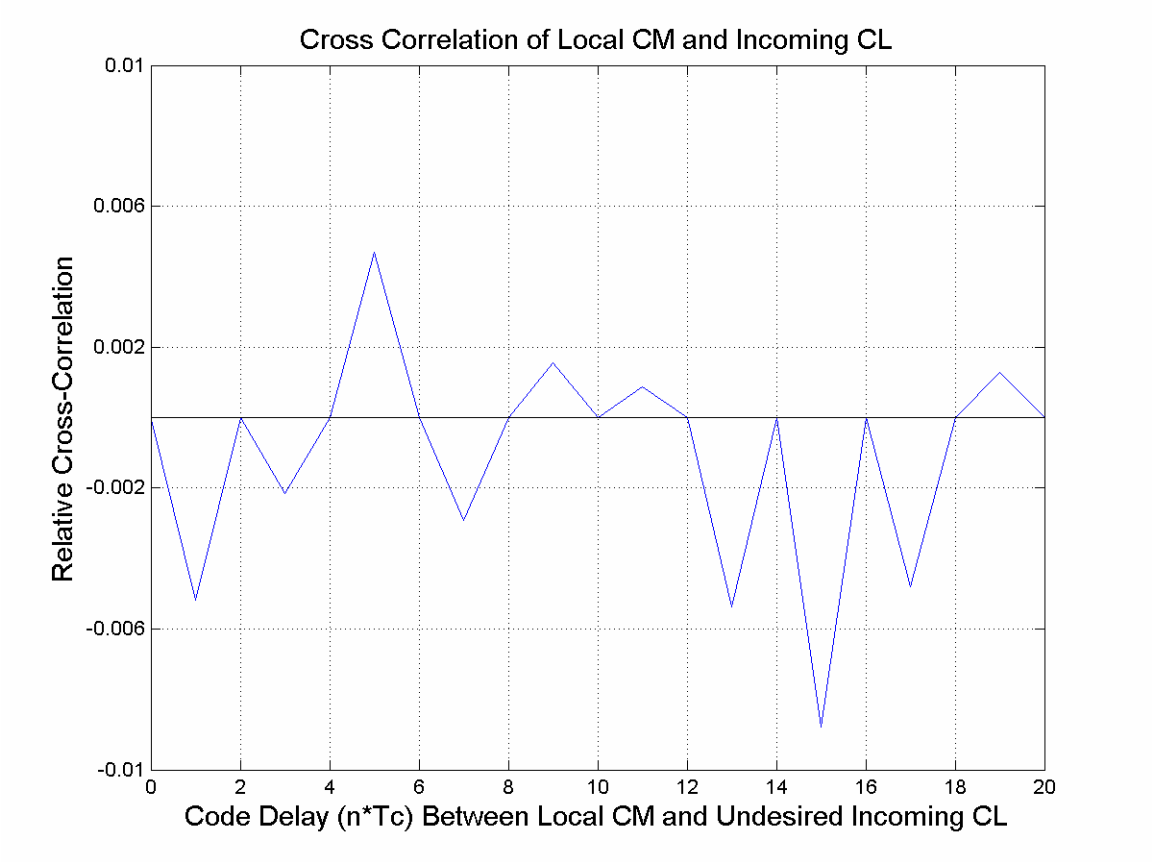

Figure 2.8 Variation of Cross-Correlation between CM and CL Code with Delays Ranging from 0 to 20 T_C

Figure 2.8 displays the cross-correlation between the local CM code for PRN=1 and incoming CL code for PRN=2 with the code delay only ranging from 0 to 20 T_C .

When the code delay is an odd integer multiple of T_C, $\tau_k = lT_C$, $l = 1, 3, 5,\ldots,$ $N-1$ is an odd number, $m = 0, 1, 2,\ldots,74$, and the cross-correlation $R_{k,i}^{L}(\tau_k, mNT_C)$ takes its extreme value:

$$W_{k,i}(m,l)\cdot T_C = \eta_{ki}\cdot T_C .$$

The cross-correlation $R_{k,i}^{L}(\tau_k, mNT_C)$ becomes zeros when the code delay is an even integer multiple of T_C, $\tau_k = lT_C$, $l = 0, 2, 4,\ldots,$ and $N-2$ is an odd integer. The maximum value of the cross-correlation $R_{k,i}^{L}(\tau_k, mNT_C)$ is the largest one of these extreme values.

Because there are no navigation data on the incoming CL code, the cross-correlation $R_{k,i}^{L}(\tau_k, mNT_C)$ may not be symmetrical, so the maximum (positive) value of $R_{k,i}^{L}(\tau_k, mNT_C)$ may be different from the absolute minimum value (the minimum value should be negative) of $R_{k,i}^{L}(\tau_k, mNT_C)$.

The cross-correlations $d_{k,-1}R_{k,i}^{M}(\tau_k) + d_{k,0}\hat{R}_{k,i}^{M}(\tau_k)$ and $R_{k,i}^{L}(\tau_k, mNT_C)$ are all straight lines in any one range of [$mT + lT_C$, $mT + (l+1)T_C$]. Therefore, the summation of the cross-correlations $d_{k,-1}R_{k,i}^{M}(\tau_k) + d_{k,0}\hat{R}_{k,i}^{M}(\tau_k)$ and $R_{k,i}^{L}(\tau_k, mNT_C)$ is also a straight line in the same range.

The maximum value of $d_{k,-1}R_{k,i}^{M}(\tau_k) + d_{k,0}\hat{R}_{k,i}^{M}(\tau_k) + R_{k,i}^{L}(\tau_k, mNT_C)$ for all values of l and m can be found by comparing $d_{k,-1}R_{k,i}^{M}(\tau_k) + d_{k,0}\hat{R}_{k,i}^{M}(\tau_k)$ and

$R_{k,i}^{L}(\tau_k, mNT_C)$ values. When $d_{k,-1}R_{k,i}^{M}(\tau_k) + d_{k,0}\hat{R}_{k,i}^{M}(\tau_k)$ reaches its extreme value $\lambda_{k,i}T_C$ or $\hat{\lambda}_{k,i}T_C$, $R_{k,i}^{L}(\tau_k, mNT_C)$ becomes zero; when $R_{k,i}^{L}(\tau_k, mNT_C)$ reaches its extreme value $\eta_{k,i}T_C$, $d_{k,-1}R_{k,i}^{M}(\tau_k) + d_{k,0}\hat{R}_{k,i}^{M}(\tau_k)$ becomes zero. Therefore the maximum value of $[d_{k,-1}R_{k,i}^{M}(\tau_k) + d_{k,0}\hat{R}_{k,i}^{M}(\tau_k) + R_{k,i}^{L}(\tau_k, mNT_C)]/T_C$ is defined by

$$\begin{aligned}\gamma_{k,i} &= \max\left\{\left[d_{k,-1}R_{k,i}^{M}(\tau_k) + d_{k,0}\hat{R}_{k,i}^{M}(\tau_k) + R_{k,i}^{L}(\tau_k, mNT_C)\right]/T_C\right\} \\ &= \max\{\max(\lambda_{k,i}, \eta_{k,i}), \max(\hat{\lambda}_{k,i}, \eta_{k,i})\} \\ &= \max\{\theta_{\mathrm{k,i}}, \hat{\theta}_{k,i}\}\end{aligned}$$

where $\theta_{k,i} = \max(\lambda_{k,i}, \eta_{k,i})$ or $\hat{\theta}_{k,i} = \max(\hat{\lambda}_{k,i}, \eta_{k,i})$.

Therefore, to choose the maximum value of $d_{k,-1}R_{k,i}^{M}(\tau_k) + d_{k,0}\hat{R}_{k,i}^{M}(\tau_k) + R_{k,i}^{L}(\tau_k, mNT_C)$ is equivalent to choosing

$$\gamma_{k,i} = \max\{\theta_{k,i}, \hat{\theta}_{k,i},\} = \max\{\max(\lambda_{k,i}), \max(\hat{\lambda}_{k,i}), \max(\eta_{k,i})\}. \qquad (2\text{-}40)$$

By using a similar approach, the minimum value of $[d_{k,-1}R_{k,i}^{M}(\tau_k) + d_{k,0}\hat{R}_{k,i}^{M}(\tau_k) + R_{k,i}^{L}(\tau_k, mNT_C)]/T_C$ for all values of l and m is defined by

$$\begin{aligned}\hat{\gamma}_{k,i} &= \min\left\{\left[d_{k,-1}R_{k,i}^{M}(\tau_k) + d_{k,0}\hat{R}_{k,i}^{M}(\tau_k) + R_{k,i}^{L}(\tau_k, mNT_C)\right]/T_C\right\} \\ &= \min\{\min(\lambda_{k,i}, \eta_{k,i}), \min(\hat{\lambda}_{k,i}, \eta_{k,i})\} \\ &= \min\{\mu_{\mathrm{k,i}}, \hat{\mu}_{k,i}\}\end{aligned}$$

where $\mu_{k,i} = \min(\lambda_{k,i}, \eta_{k,i})$ or $\hat{\mu}_{k,i} = \min(\hat{\lambda}_{k,i}, \eta_{k,i})$.

Therefore, to choose the minimum value of $d_{k,-1}R_{k,i}^{M}(\tau_k) + d_{k,0}\hat{R}_{k,i}^{M}(\tau_k) + R_{k,i}^{L}(\tau_k, mNT_C)$ is equivalent to choosing

$$\hat{\gamma}_{k,i} = \min\{\mu_{k,i}, \hat{\mu}_{k,i},\} = \min\{\min(\lambda_{k,i}), \min(\hat{\lambda}_{k,i}), \min(\eta_{k,i})\}. \qquad (2\text{-}41)$$

Because the $\lambda_{k,i}$ and $\hat{\lambda}_{k,i}$ are symmetrical, Equation (2-41) can be written as

$$\hat{\gamma}_{k,i} = \min\{\mu_{k,i}, \hat{\mu}_{k,i},\} = \min\{-\max|\lambda_{k,i}|, -\max|\hat{\lambda}_{k,i}|, \min(\eta_{k,i})\}. \qquad (2\text{-}42)$$

Finally, the largest cross-correlation is the larger value of $\gamma_{k,i}$ and $|\hat{\gamma}_{k,i}|$.

2.2.4 Simulation Approach for the Largest Cross-Correlation

In the simulation, Matlab is used to do the numerical experiment. The purpose of the simulation is to find the largest absolute value of the cross-correlation. First step is to generate local CM code and incoming CM and CL code. Then, the outputs of cross-correlations are simulated with several different variations. Code delays $\tau_k = T_C, 2T_C, ..., 20460T_C$ are simulated because the extreme values of cross-correlation only take place in these cases, with navigation data transitions and the cross-correlations between local CM code and the incoming CM and CL code for different m; $m = 0, 1, 2, ..., 74$. At last, these outputs of cross-correlations are compared to obtain the one with largest absolute value.

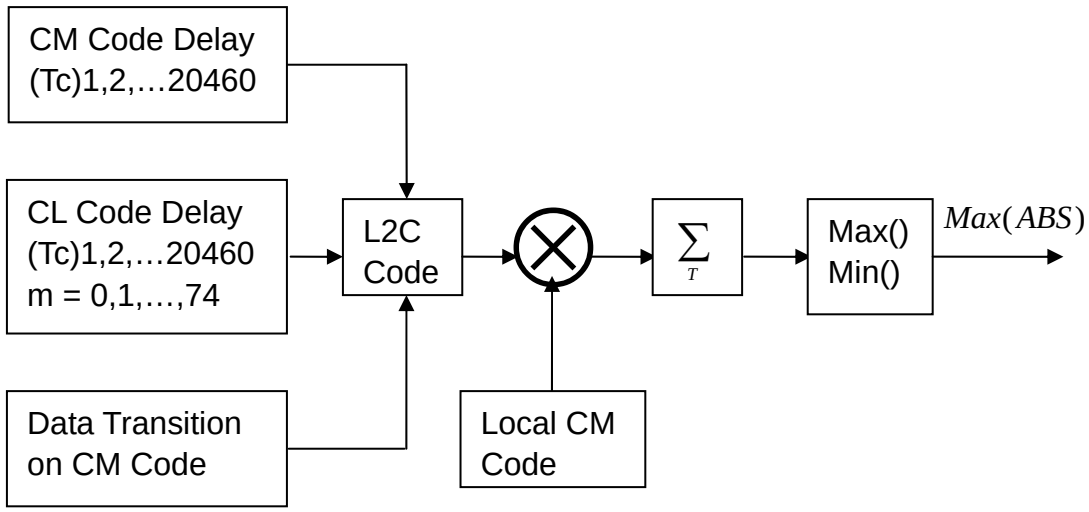

Figure 2.9 Scheme to Find The Maximum Cross-Correlation

Figure 2.9 displays the simulation process. The code delay is only taken as an integer multiple of T_C. In this way, one can obtain the extreme values of the cross-correlation; by comparing these extreme values, the maximum and minimum values are obtained. For the incoming CM code, there are data transitions to consider. Two cases are analysed here: with and without data transition. On the incoming CL code, there is no data. After integration, it is necessary to compare the maximum and minimum absolute values of the cross-correlation because the cross-correlation between the incoming CL code and local CM code is not symmetrical.

Table 2.3 displays the result of the maximum cross-correlation where $i = 1$ was chosen.

Table 2.3 Maximum Cross-Correlation

k	τ_k	m	$\hat{\gamma}_{k,1}$	$\gamma_{k,1}$	CM-CL	CM-CM
2	10414	74	-446	418	Yes	No
3	5670	11	-450	410	Yes	No
4	18776	10	-450	406	Yes	No
5	10710	58	-430	400	Yes	No

Explanation: Yes: With largest cross-correlation. No: Without largest cross-correlation

From Table 2.3, after comparing the cross-correlations, it is found that the largest absolute cross-correlation values between the local CM code and incoming CL code are greater than the largest cross-correlation between the local and incoming CM code. The cross-correlation with the largest absolute value is negative (Local PRN=1, for incoming CM and CL code, PRN=2, 3, 4, 5). After comparing all largest absolute cross-correlations with each other, the largest value is the cross-correlation between the local CM code (with PRN=26) and incoming CL code (with PRN=4) where $\hat{\gamma}_{4,26} = -570$ and the cross-correlation is -31.1 dB.

2.2.5 Signal Detection

In Figure 2.10, S represents the number of samples acquired during the integration time and M is the non-coherent integration number.

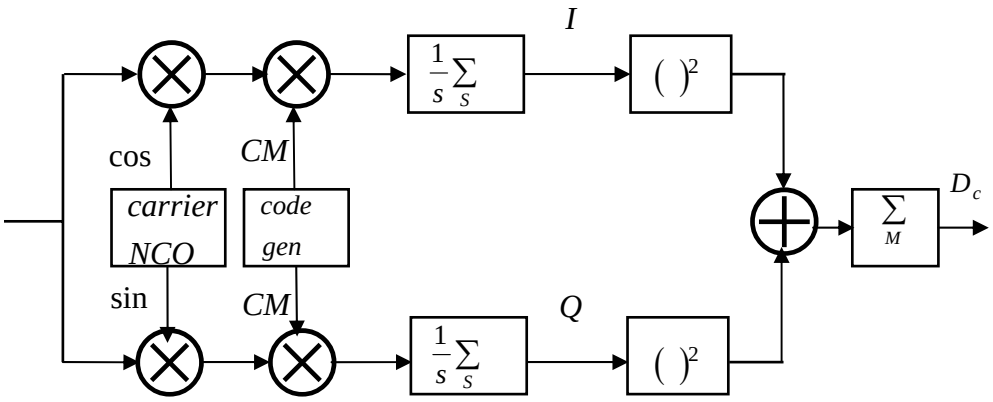

Figure 2.10 Generic CM Code Acquisition Model

The classical acquisition structure for only one cross-correlation is considered. The cross-correlation output of the correlator is integrated over the interval T and the integrated samples can be written as (Bastide et al 2002)

$$I_{ik} = \sqrt{P_k/2}\frac{1}{T}[d_{k,-1}R^M_{k,i}(\tau_k) + d_{k,0}\hat{R}^M_{k,i}(\tau_k) + R^L_{k,i}(\tau_k, mNT_C)] \times \cos(\Delta\phi_k)\frac{\sin(\pi\Delta f_k T)}{\pi\Delta f_k T} + n_{Ik} \quad (2\text{-}43)$$

$$Q_{ik} = \sqrt{P_k/2}\frac{1}{T}[d_{k,-1}R^M_{k,i}(\tau_k) + d_{k,0}\hat{R}^M_{k,i}(\tau_k) + R^L_{k,i}(\tau_k, mNT_C)] \times \sin(\Delta\phi_k)\frac{\sin(\pi\Delta f_k T)}{\pi\Delta f_k T} + n_{Qk} \quad (2\text{-}44)$$

where there is a factor $\frac{1}{T}$ in every equation (considered the normalized cross-correlation for the integration time T), and n_{Ik} and n_{Qk} are centred Gaussian correlator output noise with power $\sigma_n^2 = \frac{N_0}{8T}$.

Signal acquisition can include coherent and non-coherent integration. Coherent integration is the correlation between incoming signal and local replica. When the signal code phase and frequency offset are matched, the SNR of the predetection integration is enhanced. The longer the predetection integration time, the larger the value of SNR for the integrator output. Because the band-limited white Gaussian noise is random and its mean is zero, it can be reduced over the integration time. Generally, the CM code predetection integration interval is 20 ms. This integration time is long enough for the signal to be detected, because the SNR can be relatively large for the case of a 20 ms integration time. Sometimes if the incoming signal is very weak, for example indoor signal reception, non-coherent integration can be added to improve the SNR. Although non-coherent integration suffers from a squaring loss, it still increases the SNR.

The hypothesis test of the signal detection includes (Bastide et al 2002): Hypothesis H0 (the desired signal is not present) and Hypothesis H1 (the desired signal is present). The test statistic is compared to a threshold. The detection decision will be made under a false alarm probability P_{fa} and detection probability P_d. The relevant test statistic is

$$D = \sum_{M} (I_i^2 + Q_i^2) \,. \tag{2-45}$$

where M is the non-coherent time number. This test statistic includes coherent and non-coherent integration.

Next, signal detection is analysed for the cases of band-limited WGN effects only and one cross-correlation combined with band-limited WGN effects.

2.2.5.1 Band-Limited WGN Effects Only on Signal Detection

Hypothesis H0: no desired signal

Considering only the white Gaussian noise, the test statistic can be written as (Bastide et al 2002)

$$D_0 = \sum_{M} (n_{Ik}^2 + n_{Qk}^2) \,. \tag{2-46}$$

Because n_{Ik} and n_{Qk} represent the Gaussian distribution, then D_n / σ_n^2 is a central χ^2 (chi square) distribution, and 2M represents the degrees of freedom of the central χ^2 chi square distribution.

The false alarm probability is given as follows (Bastide et al 2002):

$$P_{fa} = \Pr\{D_n > Th\} = \int_{Th}^{\infty} p_{D_n}(u) du \,. \tag{2-47}$$

where Th is the threshold, P_{fa} is false alarm probability, and $P_{D_n}(u)$ is the probability density function of the test statistic and of the central χ^2 distribution. If

the P_{fa} value is chosen as $P_{fa}=10^{-3}$, the classical value, then from the central χ^2 distribution the Th value is determined with different M values by calculating the inverse function of Equation (2-47). If $P_{fa}=10^{-3}$ and M is 1, from the central χ^2 distribution, the threshold Th is about 13.8. When M is 2, the threshold Th should be about 18.5. And when M is 3, the threshold Th is about 22.5. The error is less than 0.05.

Hypothesis H1: a desired signal is present

In the case of a useful signal with white Gaussian noise being present, from Equations (2-17) and (2-18) and considering the factor $\frac{1}{T}$, the test statistic is derived as follows (Bastide et al 2002).

$$D_s=\sum_M\left\{\left[\sqrt{P_i/2}\,\frac{1}{T}[d_{i,0}M_i(\tau_i)+L_i(mT+\tau_i)]\cos(\Delta\phi_i)\frac{\sin(\pi\Delta f_iT)}{\pi\Delta f_iT}+n_{Ik}\right]^2\right.$$
$$\left.+\left[\sqrt{P_i/2}\,\frac{1}{T}[d_{i,0}M_i(\tau_i)+L_i(mT+\tau_i)]\sin(\Delta\phi_i)\frac{\sin(\pi\Delta f_iT)}{\pi\Delta f_iT}+n_{Qk}\right]^2\right\} \quad (2\text{-}48)$$

D_s/σ_n^2 is a non-central χ^2 distribution. The degree of freedom is 2M. The expected value of the non-centrality parameter is given as (Bastide et al 2002)

$$\lambda_s=\frac{4MP_i}{N_0T}[d_iM_i(\tau_i)+L_i(mT+\tau_i)]^2\left(\frac{\sin(\pi\Delta f_iT)}{\pi\Delta f_iT}\right)^2. \quad (2\text{-}49)$$

where the function $[d_iM_i(\tau_i)+L_i(mT+\tau_i)]$ is the autocorrelation between the local CM code and the desired incoming L2C signal.

From the analysis above, it is clear that the probability of the detection is related to a non-central χ^2 distribution and the detection threshold Th. The value of the non-centrality parameter shows that the non-central χ^2 distribution depends on the carrier-to-noise density ratio (C/N_0) (here, it is P_i/N_0), pre-detection integration time T, non-coherent integration number M, the difference between the frequency of the local carrier and the desired incoming carrier, the difference between phase of the local carrier and of the desired incoming signal carrier, and the difference between the local code delay and the desired incoming code delay.

If one only considers that the difference between the local code delay and the desired incoming code delay is zero ($\tau_i = 0$), the difference between the phase of the local carrier and that of the desired incoming signal carrier is zero ($\Delta\phi_i = 0$) and the difference between the frequency of the local carrier and of the desired incoming carrier is zero ($\Delta f_i = 0$). Equation (2-48) can then be written as follows (considering Equations (2-19) and (2-20)).

$$D_s = \sum_M \left\{ \left[\sqrt{P_i/2}\,\frac{1}{2} d_{i,0} + n_{Ik} \right]^2 + \left[\sqrt{P_i/2}\,\frac{1}{2} d_{i,0} + n_{Qk} \right]^2 \right\}. \qquad (2\text{-}50)$$

Equation (2-49) can be written as

$$\lambda_s = \frac{MTP_i}{N_0}. \qquad (2\text{-}51)$$

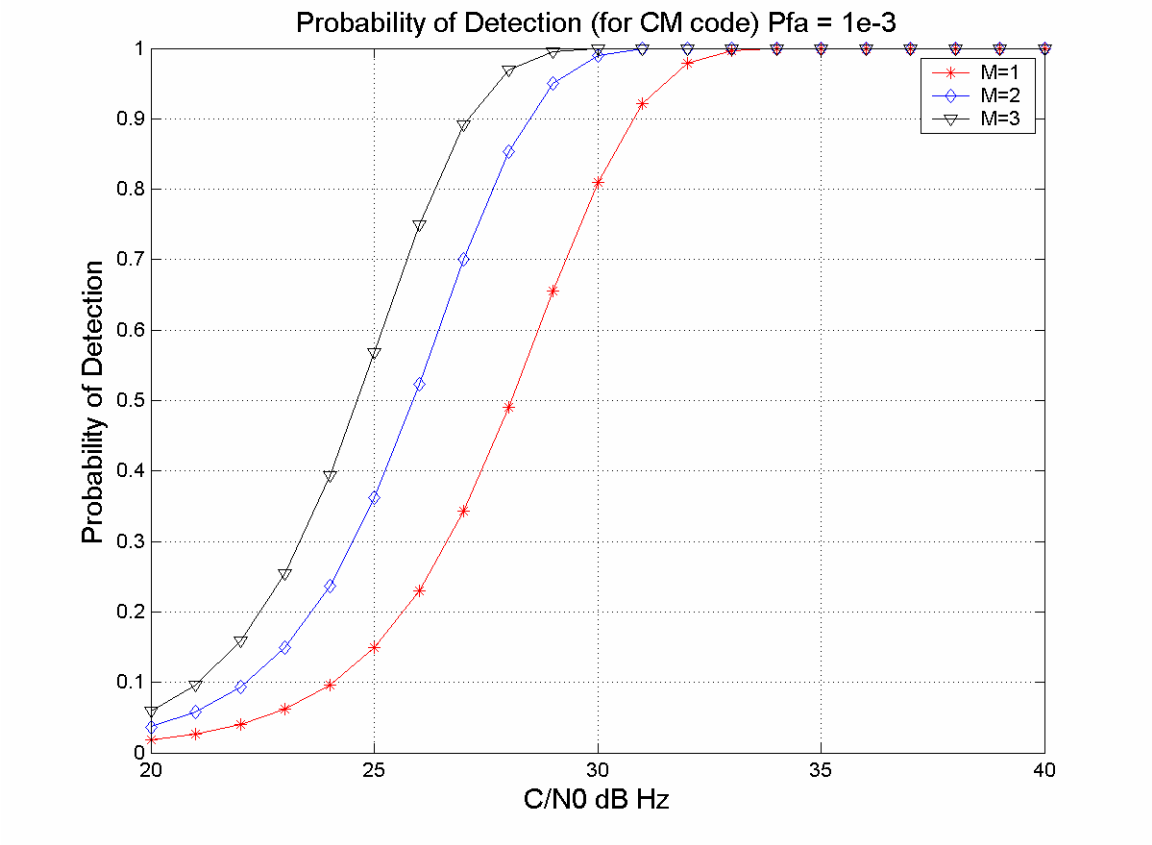

Figure 2.11 Probability of Detection of Total (I+Q)C/N_0 at the Antenna Output

Figure 2.11 displays the probability of detection depending on the total (I+Q)C/N_0 at the antenna output. When the probability of false alarm (P_{fa}) is chosen as 0.001, the relationship between the probability of detection and the C/N_0 ranging from 20 dB-Hz to 33 dB-Hz is shown. The pre-detection integration T is 20 ms. The three curves express the relationship with the non-coherent integration number M=1, 2 and 3. In the figure, the effects of front-end are not considered and the code, frequency, and phase uncertainties are assumed to be zero. More non-coherent

integrations will yield higher detection capabilities if the effects of code Doppler can be ignored. The non-coherent integration with M=3 has a 3 to 4 dB-Hz better ability to detect the desired signal; that is, with a C/N_0 which can be 3 to 4 dB-Hz lower than the one with M=1. Under the weak desired signal environment, when M=1, the probability of detection can reach 0.9 with C/N_0 equal to 30.8 dB-Hz. When C/N_0 equals 29.9 dB-Hz, the probability of detection can reach 0.8. When M=3, the probability of detection can be 0.9 with C/N_0 equal to 27.1 dB-Hz and 0.8 with C/N_0 equal to 26.3 dB-Hz

2.2.5.2 Band-Limited WGN and One Cross-Correlation Effects on Signal Detection

Hypothesis H0: no desired signal

If a cross-correlation interference peak is considered (the worst case of cross-correlation), the test statistic becomes (Bastide et al 2002)

$$D_{0,c} = \sum_{M} \left\{ \left[\sqrt{P_k/2}\,\frac{1}{T}[d_{k,-1}R^M_{k,i}(\tau_k) + d_{k,0}\hat{R}^M_{k,i}(\tau_k) + R^L_{k,i}(\tau_k, mNT_C)]\frac{\sin(\pi\Delta f_k T)}{\pi\Delta f_k T}\cos(\Delta\phi_k) + n_{Ik} \right]^2 + \left[\sqrt{P_k/2}\,\frac{1}{T}[d_{k,-1}R^M_{k,i}(\tau_k) + d_{k,0}\hat{R}^M_{k,i}(\tau_k) + R^L_{k,i}(\tau_k, mNT_C)]\frac{\sin(\pi\Delta f_k T)}{\pi\Delta f_k T}\sin(\Delta\phi_k) + n_{Qk} \right]^2 \right\} \quad (2\text{-}52)$$

$D_{0,c}/\sigma_n^2$ is a non-central χ^2 distribution. The degree of freedom is 2M. The

non-centrality parameter of the χ^2 distribution is calculated as follows (Bastide et al 2002).

$$\begin{aligned}\lambda_c &= \sum_M \{(\sqrt{P_k/2}\,\frac{1}{T}[d_{k,-1}R^M_{k,i}(\tau_k)+d_{k,0}\hat{R}^M_{k,i}(\tau_k)+R^L_{k,i}(\tau_k,mNT_C)]\frac{\sin(\pi\Delta f_k T)}{\pi\Delta f_k T}\cos(\Delta\phi_k))^2 \\ &\quad +(\sqrt{P_k/2}\,\frac{1}{T}[d_{k,-1}R^M_{k,i}(\tau_k)+d_{k,0}\hat{R}^M_{k,i}(\tau_k)+R^L_{k,i}(\tau_k,mNT_C)]\frac{\sin(\pi\Delta f_k T)}{\pi\Delta f_k T}\sin(\Delta\phi_k))^2\}/\sigma_n^2 \\ &= \frac{4MP_k}{N_0 T}[d_{k,-1}R^M_{k,i}(\tau_k)+d_{k,0}\hat{R}^M_{k,i}(\tau_k)+R^L_{k,i}(\tau_k,mNT_C)]^2\left(\frac{\sin(\pi\Delta f_k T)}{\pi\Delta f_k T}\right)^2\end{aligned}$$

(2-53)

where the function $\frac{1}{T^2}[d_{k,-1}R^M_{k,i}(\tau_k)+d_{k,0}\hat{R}^M_{k,i}(\tau_k)+R^L_{k,i}(\tau_k,mNT_C)]^2$ is the normalized cross-correlation between the local CM code and the k-th incoming L2C signal. The false alarm probability must be associated with a precise $\frac{P_k}{N_0T^2}[d_{k,-1}R^M_{k,i}(\tau_k)+d_{k,0}\hat{R}^M_{k,i}(\tau_k)+R^L_{k,i}(\tau_k,mNT_C)]^2$ that represents the worst real case. From Section 2.2.4, the worst cross-correlation of $\frac{1}{T^2}[d_{k,-1}R^M_{k,i}(\tau_k)+d_{k,0}\hat{R}^M_{k,i}(\tau_k)+R^L_{k,i}(\tau_k,mNT_C)]^2$ is -31.1 dB. Then, the term $\frac{P_k}{N_0T^2}[d_{k,-1}R^M_{k,i}(\tau_k)+d_{k,0}\hat{R}^M_{k,i}(\tau_k)+R^L_{k,i}(\tau_k,mNT_C)]^2$ can be chosen as 11.7dB-Hz, ($\frac{P_k}{N_0}=42.8\,dB-Hz$), which is the worst L2C case for a 20 ms pre-detection integration.

Hypothesis H1: a desired signal is present

If, in the case of the useful signal, cross-correlation and white Gaussian noise are present, the test statistic is given as follows (Bastide et al 2002).

$$
\begin{aligned}
D_s = \sum_M \{ & (\sqrt{P_i/2}\,\frac{1}{T}[d_i M_i(\tau_i) + L_i(mT+\tau_i)]\frac{\sin(\pi\Delta f_i T)}{\pi\Delta f_i T}\cos(\Delta\phi_i) \\
& + \sqrt{P_k/2}\,\frac{1}{T}[d_{k,-1}R^M_{k,i}(\tau_k) + d_{k,0}\hat{R}^M_{k,i}(\tau_k) + R^L_{k,i}(\tau_k, mNT_C)]\frac{\sin(\pi\Delta f_k T)}{\pi\Delta f_k T}\cos(\Delta\phi_k) + n_{Ik})^2 \\
& + (\sqrt{P_i/2}\,\frac{1}{T}[d_i M_i(\tau_i) + L_i(mT+\tau_i)]\frac{\sin(\pi\Delta f_i T)}{\pi\Delta f_i T}\sin(\Delta\phi_i) \\
& + (\sqrt{P_k/2}\,\frac{1}{T}[d_{k,-1}R^M_{k,i}(\tau_k) + d_{k,0}\hat{R}^M_{k,i}(\tau_k) + R^L_{k,i}(\tau_k, mNT_C)]\frac{\sin(\pi\Delta f_k T)}{\pi\Delta f_k T}\sin(\Delta\phi_k) + n_{Qk})^2 \}
\end{aligned}
\tag{2-54}
$$

D_s/σ_n^2 is a non-central χ^2 distribution and the degree of freedom is 2M. The expected value of the non-centrality parameter is (Bastide et al, 2002)

$$
\begin{aligned}
\lambda_s = & \frac{4MP_i}{N_0 T}[d_i M_i(\tau_i) + L_i(mT+\tau_i)]^2\left(\frac{\sin(\pi\Delta f_i T)}{\pi\Delta f_i T}\right)^2 \\
& + \frac{4MP_k}{N_0 T}[d_{k,-1}R^M_{k,i}(\tau_k) + d_{k,0}\hat{R}^M_{k,i}(\tau_k) + R^L_{k,i}(\tau_k, mNT_C)]^2\left(\frac{\sin(\pi\Delta f_k T)}{\pi\Delta f_k T}\right)^2
\end{aligned}
\tag{2-55}
$$

where the function $\frac{1}{T}[d_i M_i(\tau_i) + L_i(mT+\tau_i)]$ is the normalized autocorrelation between the local CM code and the desired incoming L2C code. If τ_i is assumed to be zero, $\frac{1}{T}L_i(mT+\tau_i)$ is equal to zero and $\frac{1}{T}M_i(\tau_i)$ is equal to $\frac{1}{2}$.

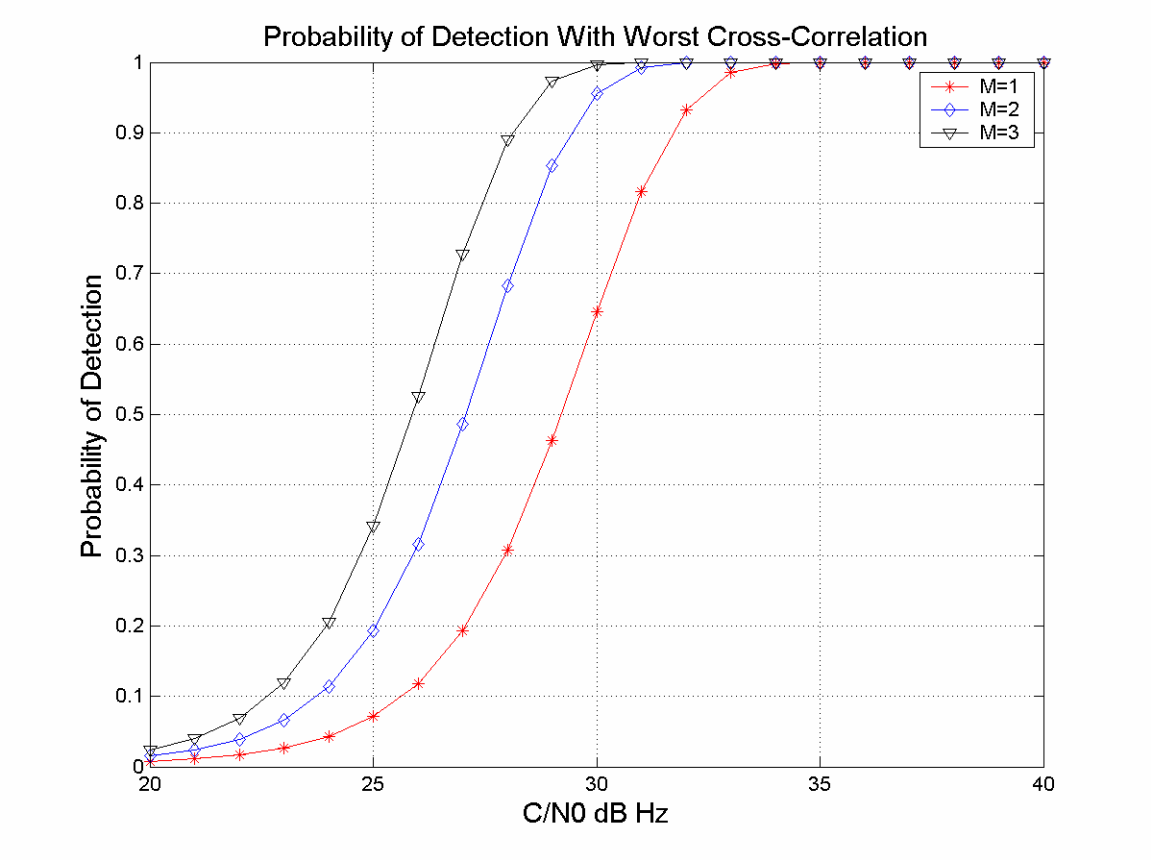

Figure 2.12 Probability of Detection of Total (I+Q)C/N_0 at the Antenna Output for 20 ms Coherent Integration Time (No Uncertainty and No Front End Filtering Effects are Considered)

In this case, results are almost identical to the case shown in Figure 2.11 except that the cross-correlation false alarm probability is 0.001. In Figure 2.12, the false alarm probability (P_{fa}) is still 0.001, but the worst cross-correlation case has been considered. Pre-integration time is 20 ms. The non-coherent integration number is M=1,2 and 3. The effects of the front-end are not considered and the code, frequency, and phase uncertainties are assumed to be zero. Additional non-coherent integration will result in better detection if the Doppler effects on

incoming code can be ignored. The non-coherent method with M=3 has a 3 to 4 dB-Hz higher ability to detect the desired signal than the one with M=1. Comparing Figure 2.11 with Figure 2.12, with the presence of cross-correlation the detection probabilities are degraded. With the same non-coherent integration number M, the detection capability under band-limited WGN only is about 1 dB-Hz higher than the detection capabilities under one worst cross-correlation and band-limited WGN combined. Under the weak desired signal environment, when M=1, the probability of detection can reach 0.9 with C/N_0=31.7 dB-Hz and 0.8 with C/N_0=30.8 dB-Hz. When M=3, the probability of detection can reach 0.9 with C/N_0=28.1 dB-Hz and 0.8 with C/N_0=27.4 dB-Hz. The detection probabilities are mostly decreased by approximately 0.20 for M=1 at C/N_0=29 dB-Hz, by approximately 0.21 for M=2 at C/N_0=27 dB-Hz, and by approximately 0.22 for M=3 at C/N_0=26 dB-Hz.

2.3 Conclusions

The CM and CL codes of the L2C signal are generated from one PN code with maximal length of $2^{27}-1$. The largest cross-correlation of -31.1 dB is between a local CM code (PRN=26) and incoming CL code (PRN=4). For any cross-correlation of the local and incoming CM code, when the code delay is an odd integer multiple of T the cross-correlation is zero. When the code delay is an even integer multiple of T, the cross-correlation reaches its extreme values. For

any cross-correlation of the local CM code and incoming CL code, when the code delay is an odd integer multiple of T the cross-correlations have extreme values. When the code delay is an even integer multiple of T, the cross-correlations are zero. Under band-limited WGN only, the non-coherent integration with M=3 has a 3 to 4 dB-Hz better ability to detect the desired signal than the case for M=1. Under band-limited WGN and one worst case cross-correlation combined, the non-coherent integration with non-coherent integration number M=3 also has a 3 to 4 dB-Hz better ability to detect the desired signal than the one with M=1. Under the weak desired signal environment, with the same non-coherent integration number M, the detection capabilities under band-limited WGN only is about 1 dB-Hz higher than the detection capabilities under one worst cross-correlation and band-limited WGN combined.

Chapter 3

Cross-Correlation and White Gaussian Noise Effects on Signal-To-Noise Ratio

The signal-to-noise ratio is a critical parameter in receivers. The SNR of the incoming signal and the SNR of the output of the correlator affect the detection performance. After decoding and wiping-off the code on the desired incoming signal, the output of a correlator includes the desired signal, cross-correlations with unwanted signals, and the spread band-limited WGN in the cases being considered. The cross-correlations cause SNR degradation as compared to the situation without cross-correlations.

3.1 Worst Case Performance

For the L2C signal, given the analysis in Chapter 2, consider that there are several satellites in view simultaneously. If the Doppler effects are not considered ($\Delta f_i = \Delta f_k = 0$) and the local carrier is matched with the incoming desired signal ($\Delta\phi_i = 0$), Equation (2-25) can be written as

$$I_i = \sqrt{P_i/2}\,\frac{T}{2}d_{i,0} + \sum_{\substack{k=1\\k\neq i}}^{K}\sqrt{P_k/2}[d_{k,-1}R_{k,i}^{M}(\tau_k) + d_{k,0}\hat{R}_{k,i}^{M}(\tau_k) + R_{k,i}^{L}(\tau_k, mNT_C)]\cos(\Delta\phi_k) + n_I \quad . \tag{3-1}$$

Now consider the cross-correlation terms in Equation (3-1):

$$\sum_{\substack{k=1 \\ k\neq i}}^{K}\sqrt{P_k/2}[d_{k,-1}R_{k,i}^{M}(\tau_k)+d_{k,0}\hat{R}_{k,i}^{M}(\tau_k)+R_{k,i}^{L}(\tau_k,mNT_C)]\cos(\Delta\phi_k)\,.$$

$v_{k,i}(\tau_k,m)$ is defined by

$$v_{k,i}(\tau_k,m)=[d_{k,-1}R_{k,i}^{M}(\tau_k)+d_{k,0}\hat{R}_{k,i}^{M}(\tau_k)+R_{k,i}^{L}(\tau_k,mNT_C)]\cos(\Delta\phi_k)\,. \qquad (3\text{-}2)$$

In Equation (3-2), when the difference between the phase of the local carrier and that of the incoming signal carrier become zero ($\Delta\phi_k=0$), the largest value of $\cos(\Delta\phi_k)$ occurs ($\cos(\Delta\phi_k)=1$).

The output of a correlator is sent to a discriminator. If a discriminator of type $\Psi(\theta)=sign(I_i)\cdot Q_i$ is used, $sign(I_i)$ is critical. In Equation (3-1), if the sign of I_i is different from that of $d_{i,0}$ under the effects of cross-correlation and white Gaussian noise, errors of information data estimation occur. These error probabilities are defined by $P_r(I_i>0\,|\,d_{i,0}=-1)$ and $P_r(I_i<0\,|\,d_{i,0}=+1)$ (Pursley 1977). When $d_{i,0}=-1$, the maximum error probability for the information data estimation corresponds to the maximum value of $v_{k,i}(\tau_k,m)$ for each $k\neq i$. When $d_{i,0}=1$, the maximum error probability for the information data estimation corresponds to the minimum value of $v_{k,i}(\tau_k,m)$ for each $k\neq i$.

According to the analyses in Chapter 2, if $d_{i,0}=-1$, the maximum value of the cross-correlation can be estimated by

$$\gamma_{k,i} = \max\{\max(\lambda_{k,i}), \max(\hat{\lambda}_{k,i}), \max(\eta_{k,i})\}.$$

If $d_{i,0} = 1$, the minimum value of the cross-correlation can be estimated by

$$\hat{\gamma}_{k,i} = \min\{-\max|\lambda_{k,i}|, -\max|\hat{\lambda}_{k,i}|, \min(\eta_{k,i})\}.$$

Finally, the worst case is to choose the larger values of $\gamma_{k,i}$ and $|\hat{\gamma}_{k,i}|$. When $\gamma_{k,i}$ is larger, the condition $d_{i,0} = -1$ is considered. When $|\hat{\gamma}_{k,i}|$ is larger, the condition $d_{i,0} = 1$ is considered.

Suppose that

$$\Lambda = \max\{\sqrt{\frac{P_k}{2}}\gamma_{k,i}T_C, \sqrt{\frac{P_k}{2}}|\hat{\gamma}_{k,i}|T_C\},$$

and this is the worst case of cross-correlation.

If the cross-correlation is generated from more than one signal, that is $K \geq 3$, and noting that $\gamma_{k,i}$ is not symmetrical according to Equation (3-1), the expressions $\sum_{\substack{k=1 \\ k\neq i}}^{K} \sqrt{\frac{P_k}{2}}\gamma_{k,i}T_C$ and $\sum_{\substack{k=1 \\ k\neq i}}^{K} \sqrt{\frac{P_k}{2}}|\hat{\gamma}_{k,i}|T_C$ can be compared. When $\sum_{\substack{k=1 \\ k\neq i}}^{K} \sqrt{\frac{P_k}{2}}\gamma_{k,i}T_C$ is larger, $d_{i,0} = -1$ is considered. When $\sum_{\substack{k=1 \\ k\neq i}}^{K} \sqrt{\frac{P_k}{2}}|\hat{\gamma}_{k,i}|T_C$ is larger, $d_{i,0} = 1$ is considered. Now

$$\Lambda = \max\{\sum_{\substack{k=1 \\ k\neq i}}^{K} \sqrt{\frac{P_k}{2}}\gamma_{k,i}T_C, \sum_{\substack{k=1 \\ k\neq i}}^{K} \sqrt{\frac{P_k}{2}}|\hat{\gamma}_{k,i}|T_C\}. \quad (3\text{-}3)$$

The maximum value of probability $P_{\max}$ can be given by (Pursley 1977)

$$\begin{aligned} P_{\max} &= 1-\Phi\{[1-(\frac{\Lambda}{T}\sqrt{\frac{8}{P_i}})]\sqrt{P_iT/N_0}\} \\ &= 1-\Phi\{[1-\max(\sum_{\substack{k=1\\k\neq i}}^{K}\frac{2\gamma_{k,i}}{N}\sqrt{\frac{P_k}{P_i}},\sum_{\substack{k=1\\k\neq i}}^{K}\frac{2|\hat{\gamma}_{k,i}|}{N}\sqrt{\frac{P_k}{P_i}})]\sqrt{P_iT/N_0}\} \end{aligned} \tag{3-4}$$

where Φ is the standard Gaussian cumulative distribution function.

3.2 Numerical Simulation for Worst Case Performance

For the worst-case performance, because the largest cross-correlation is considered, the cross-correlation is not variable. The output of the correlator is sent to the discriminator, thus the sign of the in-phase component is critical. If the evaluation of the in-phase component sign is different from in the real case, a tracking error will occur. When $d_{i,0}=-1$ or $d_{i,0}=1$, the largest positive cross-correlation or the largest negative cross-correlation will lead to more effects on the information data estimation of desired signal.

3.2.1 Simulation Scheme

The simulation scheme is shown in Figure 3.1. In the simulation, by using Matlab, the incoming signal is simulated which includes the desired signal (CM code) and band-limited WGN. Then, the integration is done after the correlation between the local CM code and incoming signal. After integration, a minimum cross-correlation

(the absolute value is the largest from the simulation in Chapter 2) is added to the output of the integration. Because the minimum cross-correlation is used, $d_{1,0}$ is chosen to be +1. If the output I_i is negative which is different with the sign of the desired signal, an error of information data estimation occurs. Here, in the simulation, K is chosen to be 1, 3, and 5, which means no cross-correlation, two cross-correlations, and four cross-correlations. Then, the error probability of information data estimation is calculated under different C/N_0 including under the weak desired signal.

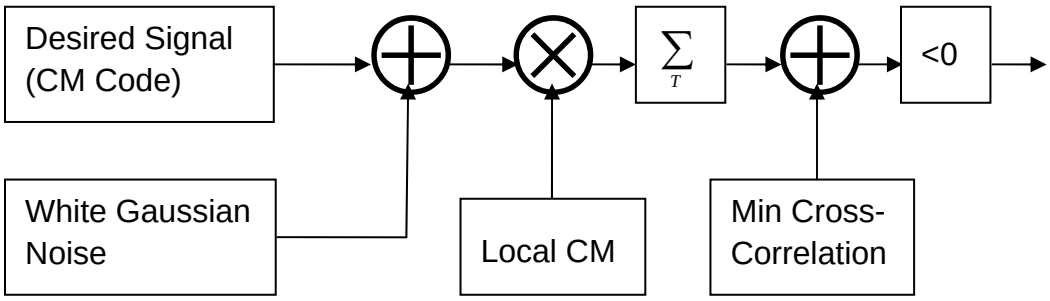

Figure 3.1 Method Used to Estimate the Largest Error Probability

3.2.2 Result Analysis

Figure 3.2 displays the maximum error probabilities of information data estimation for the worst cases. In this figure, the lowest two curves are the maximum error probabilities for the theoretical value and simulated result with band-limited WGN

only (K=1). The other curves are the theoretical results and simulation results with band-limited WGN and two worst cross-correlations (K=3), and the results with four cross-correlations (K=5).

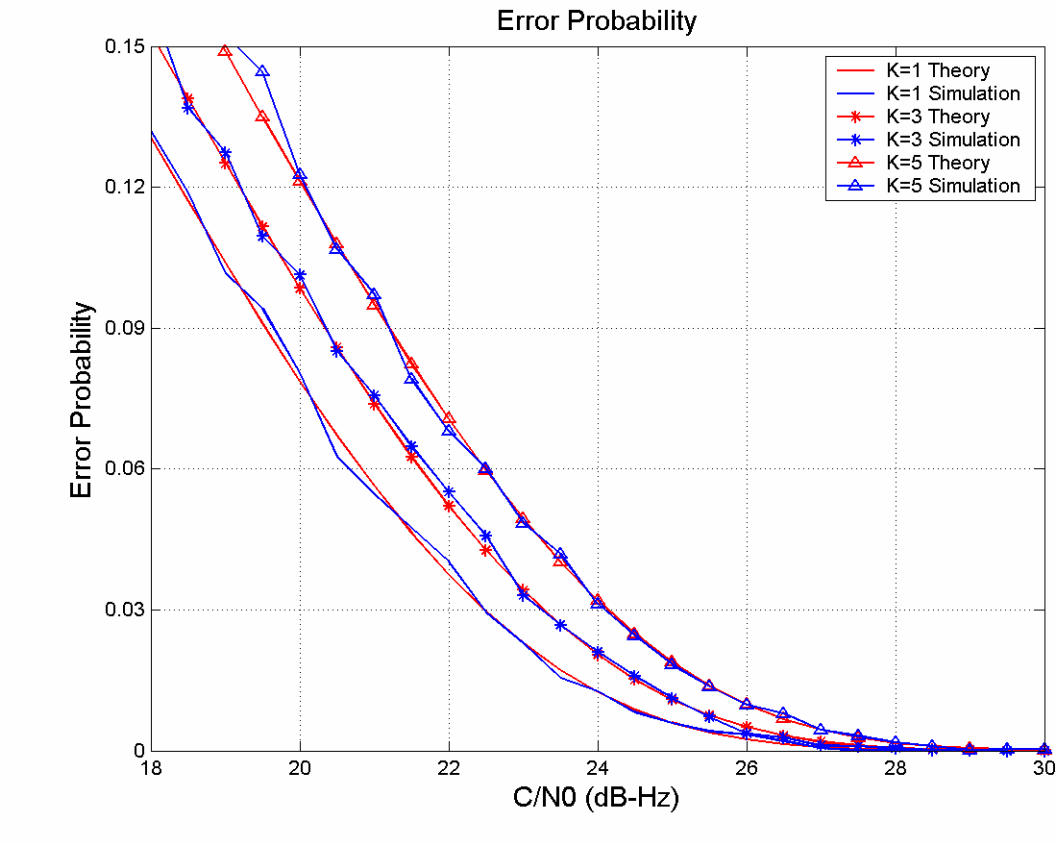

Figure 3.2 Maximum Error Probabilities

In the simulation, the maximum error probabilities of information data estimation increase with the reduction of the C/N_0. When the C/N_0 is less than 26 dB-Hz, the maximum error probabilities cannot be ignored. From the figure, when there are cross-correlations, the error probabilities are larger than the case with band-limited WGN only. In the case above, the power of the desired signal is the same as the

power of the undesired signal power. The difference of the error probabilities generated by the cross-correlations is not very great. The main effect on maximum error probabilities comes from band-limited WGN.

Figure 3.3 shows that when C/N_0 is chosen to be 26 dB-Hz, the maximum error probabilities vary with the ratio of the desired signal power to the undesired signal powers.

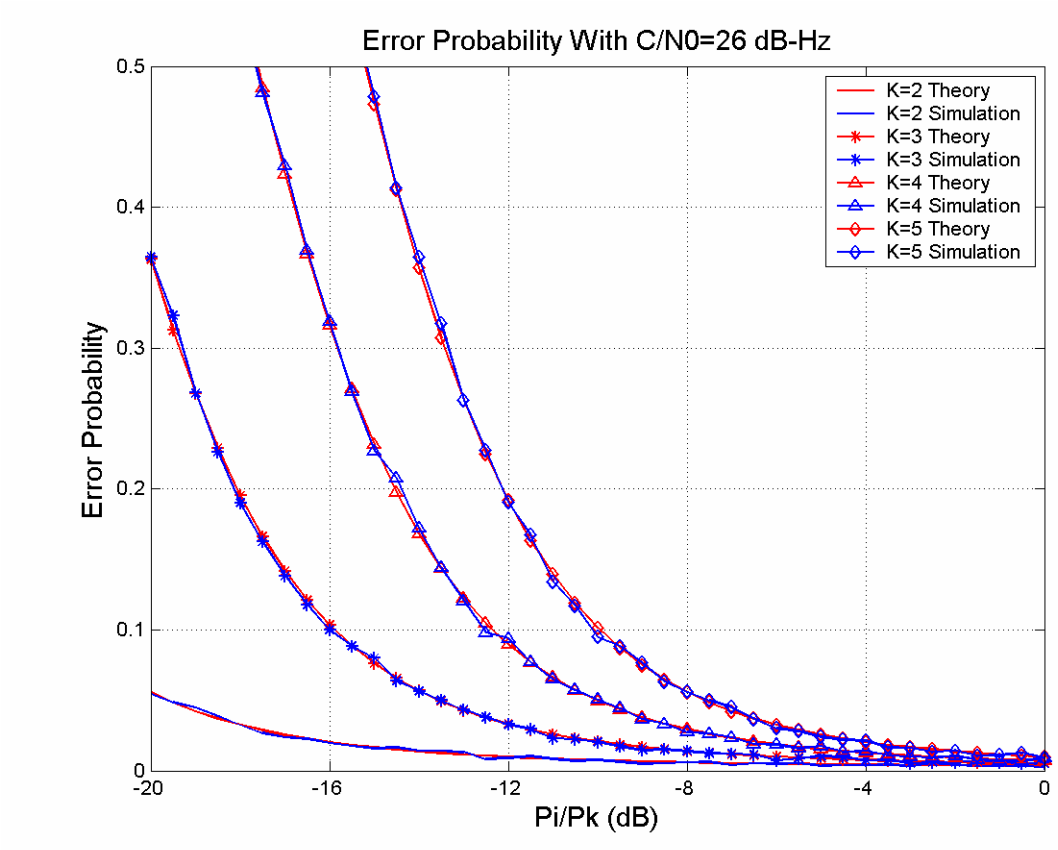

Figure 3.3 Maximum Error Probabilities with White Gaussian Noise and Cross-Correlation

The results in Figure 3.3 show that when the ratio (in dB) of Pi power to Pk power is

less than about -8 dB, the effects of cross-correlations on the maximum error probabilities become very large, especially when $K \geq 4$. That is, under the situation of weak desired signal (C/N_0 is 26 dB-Hz), the strong undesired signal (about 8 dB larger or more than the desired signal), which leads to the large cross-correlation, is a significant source of the information data estimation error probabilities.

3.3 Theoretical Analysis of Average Signal-To-Noise Ratio

In Equation (3-1), $d_{i,0}$ can be +1 or -1. The two probabilities are considered symmetrical. There is no loss in generality in assuming $d_{i,0} = +1$; thus the desired signal component of I_i is $\sqrt{P_i/2}\,\frac{T}{2}$.

To get the average signal-to-noise ratio, it is necessary to derive the variance of the noise. First, the average of the I_i can be written as

$$\begin{aligned} E(I_i) = \sqrt{P_i/2}\,\frac{T}{2} + \sum_{\substack{k=1 \\ k\neq i}}^{K} \sqrt{P_k/2}\,[E(d_{k,-1})E(R_{k,i}^{M}(\tau_k)) + E(d_{k,0})E(\hat{R}_{k,i}^{M}(\tau_k)) \\ + E(R_{k,i}^{L}(\tau_k - mNT_C))]E(\cos(\Delta\phi_k)) \\ + \int_0^T E(n(t))CM_i(t)\cos(2\pi(f_{L2} + \hat{f}_{di})t + \hat{\phi}_i)dt \end{aligned} \tag{3-5}$$

Suppose that $\Delta\phi_k$ and τ_k are uniformly distributed in the range $[0, 2\pi]$ and $[0, T]$. Because $E(\cos(\Delta\phi_k))$ and $E(n(t))$ are equal to zero, Equation (3-5) can be written as

$$E(I_i) = \sqrt{P_i/2}\,\frac{T}{2}. \tag{3-6}$$

The I_i^2 average is

$$\begin{aligned}
E(I_i^2) = {} & \frac{P_i T^2}{8} + E\{2\sqrt{P_i/2}\,\frac{T}{2}\cdot\sum_{\substack{k=1\\k\neq i}}^{K}\sqrt{P_k/2}[d_{k,-1}R_{k,i}^{M}(\tau_k) + d_{k,0}\hat{R}_{k,i}^{M}(\tau_k) + R_{k,i}^{L}(\tau_k, mNT_C)]\cos(\Delta\phi_k)\} \\
& + E\{2\sqrt{P_i/2}\,\frac{T}{2}\cdot\int_0^T n(t)CM_i(t)\cos(2\pi(f_{L2}+\hat{f}_{di})t+\hat{\phi}_i)dt\} \\
& + E\{\sum_{\substack{k=1\\k\neq i}}^{K}\sqrt{P_k/2}[d_{k,-1}R_{k,i}^{M}(\tau_k) + d_{k,0}\hat{R}_{k,i}^{M}(\tau_k) + R_{k,i}^{L}(\tau_k, mNT_C)]\cos(\Delta\phi_k)\cdot \\
& \sum_{\substack{k=1\\k\neq i}}^{K}\sqrt{P_k/2}[d_{k,-1}R_{k,i}^{M}(\tau_k) + d_{k,0}\hat{R}_{k,i}^{M}(\tau_k) + R_{k,i}^{L}(\tau_k, mNT_C)]\cos(\Delta\phi_k)\} \\
& + E\{2\sum_{\substack{k=1\\k\neq i}}^{K}\sqrt{P_k/2}[d_{k,-1}R_{k,i}^{M}(\tau_k) + d_{k,0}\hat{R}_{k,i}^{M}(\tau_k) + R_{k,i}^{L}(\tau_k, mNT_C)]\cos(\Delta\phi_k)\cdot \\
& \int_0^T n(t)CM_i(t)\cos(2\pi(f_{L2}+\hat{f}_{di})t+\hat{\phi}_i)dt\} \\
& + E\{[\int_0^T n(t)CM_i(t)\cos(2\pi(f_{L2}+\hat{f}_{di})t+\hat{\phi}_i)dt]^2\}
\end{aligned} \tag{3-7}$$

In Equation (3-7), $E(\cos(\Delta\phi_k)) = 0$ and $E(n(t)) = 0$, so the cross terms are zero as follows:

$$E\{2\sqrt{P_i/2}\,\frac{T}{2}\cdot\sum_{\substack{k=1\\k\neq i}}^{K}\sqrt{P_k/2}[d_{k,-1}R_{k,i}^{M}(\tau_k) + d_{k,0}\hat{R}_{k,i}^{M}(\tau_k) + R_{k,i}^{L}(\tau_k, mNT_C)]\cos(\Delta\phi_k)\} = 0.$$

$$E\{2\sqrt{P_i/2}\,\frac{T}{2}\cdot\int_0^T n(t)CM_i(t)\cos(2\pi(f_{L2}+\hat{f}_{di})t+\hat{\phi}_i)dt\}=0\,.$$

$$E\{2\sum_{\substack{k=1\\k\neq i}}^{K}\sqrt{P_k/2}[d_{k,-1}R_{k,i}^{M}(\tau_k)+d_{k,0}\hat{R}_{k,i}^{M}(\tau_k)+R_{k,i}^{L}(\tau_k,mNT_C)]\cos(\Delta\phi_k)\cdot$$
$$\int_0^T n(t)CM_i(t)\cos(2\pi(f_{L2}+\hat{f}_{di})t+\hat{\phi}_i)dt\}=0$$

Considering these zero terms, Equation (3-7) can be rewritten as

$$E(I_i^2)=\frac{P_iT^2}{8}+E\{\sum_{\substack{k=1\\k\neq i}}^{K}\frac{P_k}{2}[d_{k,-1}R_{k,i}^{M}(\tau_k)+d_{k,0}\hat{R}_{k,i}^{M}(\tau_k)+R_{k,i}^{L}(\tau_k,mNT_C)]\cos(\Delta\phi_k)\cdot$$
$$\sum_{\substack{j=1\\j\neq i}}^{K}\frac{P_j}{2}[d_{j,-1}R_{j,i}^{M}(\tau_j)+d_{j,0}\hat{R}_{j,i}^{M}(\tau_j)+R_{j,i}^{L}(\tau_j,mNT_C)]\cos(\Delta\phi_j)\}$$
$$+E\{[\int_0^T n(t)CM_i(t)\cos(2\pi(f_{L2}+\hat{f}_{di})t+\hat{\phi}_i)dt]^2\}$$

(3-8)

In Equation (3-8), there are still cross terms in the cross-correlation term. If we take

$E(d_{k,-1})=0$, $E(d_{k,0})=0$, $E(d_{k,-1}d_{j,0})=E(d_{k,-1})E(d_{j,0})=0$,

$E(d_{k,-1}d_{j,-1})=E(d_{k,-1})E(d_{j,-1})=0$, $j\neq k$, $E(d_{k,0}d_{j,0})=E(d_{k,0})E(d_{j,0})=0$, $j\neq k$,

$E(d_{k,-1}d_{k,-1})=E(d_{k,0}d_{k,0})=1$, $E(\cos(\Delta\phi_k)\cos(\Delta\phi_j))=E(\cos(\Delta\phi_k))E(\cos(\Delta\phi_j))=0$,

$j\neq k$, $E(d_{k,-1}d_{k,0})=E(d_{k,-1})E(d_{k,0})=0$ and $E(\cos^2(\Delta\phi_k))=\frac{1}{2}$ into account, the following terms are all zero, where $j\neq k$:

$$E[d_{k,-1}R_{k,i}^{M}(\tau_k)d_{k,0}\hat{R}_{k,i}^{M}(\tau_k)\cos^2(\Delta\phi_k)]=0\,.$$

$$E[d_{k,-1}R_{k,i}^{M}(\tau_k)R_{k,i}^{L}(\tau_k, mNT_C)\cos^2(\Delta\phi_k)] = 0 .$$

$$E[d_{k,0}\hat{R}_{k,i}^{M}(\tau_k)R_{k,i}^{L}(\tau_k, mNT_C)\cos^2(\Delta\phi_k)] = 0 .$$

$$E[d_{k,-1}R_{k,i}^{M}(\tau_k)d_{j,0}\hat{R}_{j,i}^{M}(\tau_k)\cos(\Delta\phi_k)\cos(\Delta\phi_j)] = 0 .$$

$$E[d_{k,-1}R_{k,i}^{M}(\tau_k)R_{j,i}^{L}(\tau_j, mNT_C)\cos(\Delta\phi_k)\cos(\Delta\phi_j)] = 0 .$$

$$E[d_{k,0}\hat{R}_{k,i}^{M}(\tau_k)R_{j,i}^{L}(\tau_j, mNT_C)\cos(\Delta\phi_k)\cos(\Delta\phi_j)] = 0 .$$

$$E[d_{k,-1}R_{k,i}^{M}(\tau_k)d_{j,-1}R_{j,i}^{M}(\tau_k)\cos(\Delta\phi_k)\cos(\Delta\phi_j)] = 0 .$$

$$E[d_{k,0}\hat{R}_{k,i}^{M}(\tau_k)d_{j,0}\hat{R}_{j,i}^{M}(\tau_k)\cos(\Delta\phi_k)\cos(\Delta\phi_j)] = 0 .$$

$$E[R_{k,i}^{L}(\tau_k, mNT_C)R_{j,i}^{L}(\tau_j, mNT_C)\cos(\Delta\phi_k)\cos(\Delta\phi_j)] = 0 .$$

The I_i^2 average can be written as

$$E(I_i^2) = \frac{P_i T^2}{8} + \sum_{\substack{k=1 \\ k\neq i}}^{K} \frac{P_k}{4}[E(R_{k,i}^{M}(\tau_k))^2 + E(\hat{R}_{k,i}^{M}(\tau_k))^2 + E(R_{k,i}^{L}(\tau_k, mNT_C))^2] + \frac{N_0 T}{8} \quad (3\text{-}9)$$

Therefore, the variance of the noise component of I_i is

$$\begin{aligned} Var(I_i) &= E\{[I_i - E(I_i)]^2\} = E(I_i^2) - [E(I_i)]^2 \\ &= \sum_{\substack{k=1 \\ k\neq i}}^{K} \frac{P_k}{4}[E(R_{k,i}^{M}(\tau_k))^2 + E(\hat{R}_{k,i}^{M}(\tau_k))^2 + E(R_{k,i}^{L}(\tau_k, mNT_C))^2] + \frac{N_0 T}{8} \end{aligned} \quad (3\text{-}10)$$

Equation (3-10) can be rewritten as (Pursley 1977)

$$Var(I_i) = \sum_{\substack{k=1 \\ k\neq i}}^{K} \frac{P_k}{4T} \int_0^T \{[R_{k,i}^M(\tau_k)]^2 + [\hat{R}_{k,i}^M(\tau_k)]^2 + \frac{1}{N_L}\sum_{m=0}^{N_L-1} [R_{k,i}^L(\tau_k, mNT_C)]^2\} d\tau_k + \frac{N_0 T}{8}$$

$$= \sum_{\substack{k=1 \\ k\neq i}}^{K} \frac{P_k}{4T} \sum_{l=0}^{N-1} \int_{lTc}^{(l+1)Tc} \{[R_{k,i}^M(\tau_k)]^2 + [\hat{R}_{k,i}^M(\tau_k)]^2 + \frac{1}{N_L}\sum_{m=0}^{N_L-1} [R_{k,i}^L(\tau_k, mNT_C)]^2\} d\tau_k + \frac{N_0 T}{8}$$

(3-11)

The integration $\int_{lT_C}^{(l+1)T_C} \{[R_{k,i}^M(\tau_k)]^2 + [\hat{R}_{k,i}^M(\tau_k)]^2 + \frac{1}{N_L}\sum_{m=0}^{N_L-1} [R_{k,i}^L(\tau_k, mNT_C)]^2\} d\tau_k$ can be derived separately as follows. The first term (from Equation (2-30)) is

$$\int_{lT_C}^{(l+1)T_C} (R_{k,i}^M(\tau_k))^2 d\tau_k = \int_{lT_C}^{(l+1)T_C} \{C_{k,i}(l-N)T_c + [C_{k,i}(l+1-N) - C_{k,i}(l-N)](\tau_k - lT_c)\}^2 d\tau_k$$

$$= C_{k,i}^2(l-N)T_c^3 + C_{k,i}(l-N)[C_{k,i}(l+1-N) - C_{k,i}(l-N)]T_c^3$$

$$+ \frac{T_c^3}{3}[C_{k,i}(l+1-N) - C_{k,i}(l-N)]^2$$

$$= \frac{(NT_c)^3}{3N^3}[C_{k,i}^2(l-N) + C_{k,i}(l-N)C_{k,i}(l-N+1) + C_{k,i}^2(l-N+1)]$$

(3-12)

The second term (from Equation (2-31)) is

$$\int_{lT_C}^{(l+1)T_C} (\hat{R}_{k,i}^M(\tau_k))^2 d\tau_k = \int_{lT_C}^{(l+1)T_C} \{C_{k,i}(l)T_c + [C_{k,i}(l+1) - C_{k,i}(l)](\tau_k - lT_c)\}^2 d\tau_k$$

$$= C_{k,i}^2(l)T_c^3 + C_{k,i}(l)[C_{k,i}(l+1) - C_{k,i}(l)]T_c^3$$

$$+ \frac{T_c^3}{3}[C_{k,i}(l+1) - C_{k,i}(l)]^2$$

$$= \frac{(NT_c)^3}{3N^3}[C_{k,i}^2(l) + C_{k,i}(l)C_{k,i}(l+1) + C_{k,i}^2(l+1)]$$

(3-13)

The third term (from Equation (2-33)) is

$$\begin{aligned}\frac{1}{N_L}\sum_{m=0}^{N_L-1}\int_{lT_C}^{(l+1)T_C}(R_{k,i}^{L}(\tau_k,mNT_C))^2\,d\tau_k &= \frac{1}{N_L}\sum_{m=0}^{N_L-1}\int_{lT_C}^{(l+1)T_C}\{W_{k,i}(m,l)T_c+[W_{k,i}(m,l+1)\\ &\quad -W_{k,i}(m,l)](\tau_k-lT_c)\}^2\,d\tau_k\\ &= \frac{1}{N_L}\sum_{m=0}^{N_L-1}\{W_{k,i}^2(m,l)T_c^3+W_{k,i}(m,l)[W_{k,i}(m,l+1)-W_{k,i}(m,l)]T_c^3\\ &\quad +\frac{T_c^3}{3}[W_{k,i}(m,l+1)-W_{k,i}(m,l)]^2\}\\ &= \frac{(NT_c)^3}{3N^3}\frac{1}{N_L}\sum_{m=0}^{N_L-1}[W_{k,i}^2(m,l)+W_{k,i}(m,l)W_{k,i}(m,l+1)+W_{k,i}^2(m,l+1)]\end{aligned} \tag{3-14}$$

Taking Equations (3-12), (3-13) and (3-14) into account, Equation (3-11) can be rewritten as

$$Var(I_i)=\frac{T^2}{12N^3}\sum_{\substack{k=1\\k\neq i}}^{K}P_k[r_{k,i}^{M}+r_{k,i}^{L}]+\frac{N_0T}{8}. \tag{3-15}$$

where

$$r_{k,i}^{M}=\sum_{l=0}^{N-1}\{C_{k,i}^2(l-N)+C_{k,i}(l-N)C_{k,i}(l-N+1)+C_{k,i}^2(l-N+1)+C_{k,i}^2(l)+C_{k,i}(l)C_{k,i}(l+1)+C_{k,i}^2(l+1)\}$$ and

$$r_{k,i}^{L}=\frac{1}{N_L}\sum_{m=0}^{N_L-1}\sum_{l=0}^{N-1}\{W_{k,i}^2(m,l)+W_{k,i}(m,l)W_{k,i}(m,l+1)+W_{k,i}^2(m,l+1)\}.$$

For the CM code, the chips with an even number are zero; therefore, either $C_{k,i}(l-N)$ or $C_{k,i}(l-N+1)$ must be zero. The product of $C_{k,i}(l-N)$ and

$C_{k,i}(l-N+1)$ is zero. For the same reason, either $C_{k,i}(l)$ or $C_{k,i}(l+1)$ must be zero, such that $C_{k,i}(l)C_{k,i}(l+1)$ equals zero.

For the CL code, the chips with an odd number are zero; therefore either $W_{k,i}(m,l)$ or $W_{k,i}(m,l+1)$ must be zero. The product $W_{k,i}(m,l)W_{k,i}(m,l+1)$ equals zero and $r_{k,i}^{M}$ and $r_{k,i}^{L}$ can be rewritten as

$$r_{k,i}^{M} = \sum_{l=0}^{N-1} \{C_{k,i}^2(l-N) + C_{k,i}^2(l-N+1) + C_{k,i}^2(l) + C_{k,i}^2(l+1)\} \text{ and}$$

$$r_{k,i}^{L} = \frac{1}{N_L} \sum_{m=0}^{N_L-1} \sum_{l=0}^{N-1} \{W_{k,i}^2(m,l) + W_{k,i}^2(m,l+1)\}.$$

where

$$\sum_{l=0}^{N-1} C_{k,i}^2(l-N) = \sum_{l=0}^{N-1} C_{k,i}^2(l-N+1), \sum_{l=0}^{N-1} C_{k,i}^2(l) = \sum_{l=0}^{N-1} C_{k,i}^2(l+1) \text{ and}$$

$$\frac{1}{N_L} \sum_{m=0}^{N_L-1} \sum_{l=0}^{N-1} W_{k,i}^2(m,l) = \frac{1}{N_L} \sum_{m=0}^{N_L-1} \sum_{l=0}^{N-1} W_{k,i}^2(m,l+1).$$

Therefore, from the derivation above and Pursley (1977), the average signal-to-noise ratio (SNR) is

$$SNR = \sqrt{P_i/2}\,\frac{T}{2} \Big/ \sqrt{Var(I_i)} = \{(\frac{3}{2}N^3)^{-1} \sum_{\substack{k=1 \\ k\neq i}}^{K} \frac{P_k}{P_i}[r_{k,i}^{M} + r_{k,i}^{L}] + \frac{N_0}{P_i T}\}^{-1/2}. \qquad (3\text{-}16)$$

3.4 The Numerical Simulation for Average SNR

In the numerical simulation of the average SNR, there are cross-correlation and band-limited WGN effects. Three cases are considered here. The first is the situation with band-limited WGN only. The second has cross-correlation only. The third has cross-correlation and band-limited WGN combined.

3.4.1 Simulation Method

SNR is a critical parameter in GPS receivers. The SNR of the correlator output affects the performances of acquisition and of the tracking loop. In this simulation section, the SNR evaluation is done according to the statistical average value over a pre-integration period. The code delays and phase offsets between the local replica and incoming signals from other satellites are supposed to be independent. They are random variables uniformly distributed in the pre-integration time period [0, T] and a phase period [0, 2π]. For the long incoming CL code, there are also 75 cross-correlation possibilities, for which $m = 0, 1, 2, ...74$. The incoming signal includes a desired signal which the local replica matches very well, the signals from other satellites, and band-limited WGN. The undesired signals have different code delays because of the different distances from different satellites to the receiver, and different phase offsets due to the differences between the local and the remote clocks. Figure 3.4 shows the incoming signal simulation, correlation

model, and SNR calculation method.

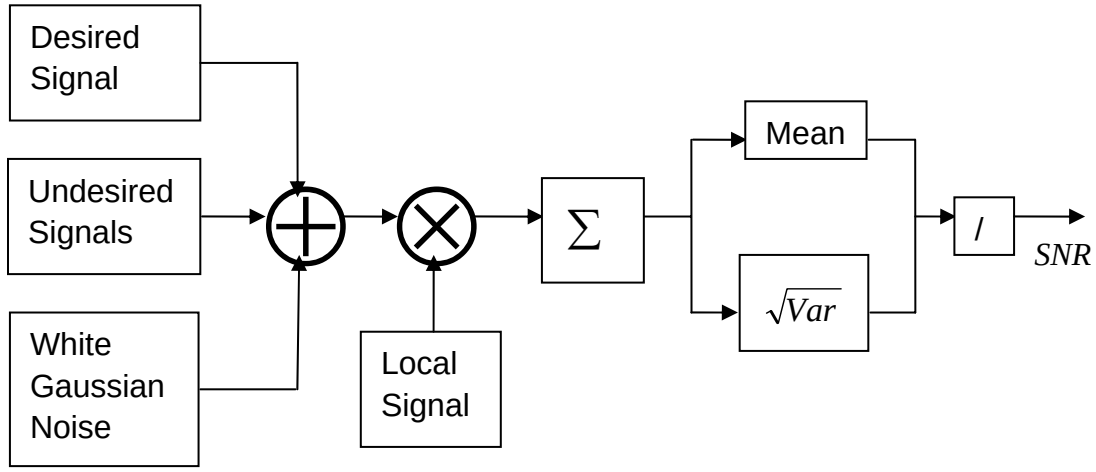

Figure 3.4 Average SNR Scheme Under Cross-Correlation and White Gaussian Noise

Here, by using Matlab, the local signal is the CM code with PRN=1. The desired signal is also the incoming CM code with PRN=1. Because the local and incoming desired CM code are matched exactly, and considering the zero chips in the CM and CL code, the correlation between the incoming CL code with PRN=1 and the local CM code with PRN=1 is zero. It is not necessary to put the CL code in the incoming desired signal. The undesired signals include the incoming CM and CL code with PRN=2, 3, 4, 5. There are code delays and phase offsets in the incoming signal. For the incoming CL code, there is one more parameter $m = 0, 1, 2, ...74$, because the CL code is a long code, which is 75 times the CM code. There are navigation data on the incoming CM code. The data $d_{k,-1}$ and $d_{k,0}$ can be +1 or

-1. The probabilities of having +1 or -1 are equal. The incoming signal is generated which includes desired signal, undesired signals and band-limited WGN. The incoming signal is correlated with the local signal and is integrated. Then, the output average and output variance are calculated. Finally, the SNR is the output average divided by the root square of output variance. The simulations include the SNR with band-limited WGN only, cross-correlations only, and band-limited WGN and cross-correlations combined

3.4.2 Simulated Average SNR Results

When there are no cross-correlation effects, Equation (3-16) can be rewritten as $SNR = [\frac{P_i T}{N_0}]^{1/2}$. If it is presented in dB, then $SNR = 10\log_{10}(P_i T) - 10\log_{10}(N_0)$. There is no loss in generality in assuming $i = 1$.

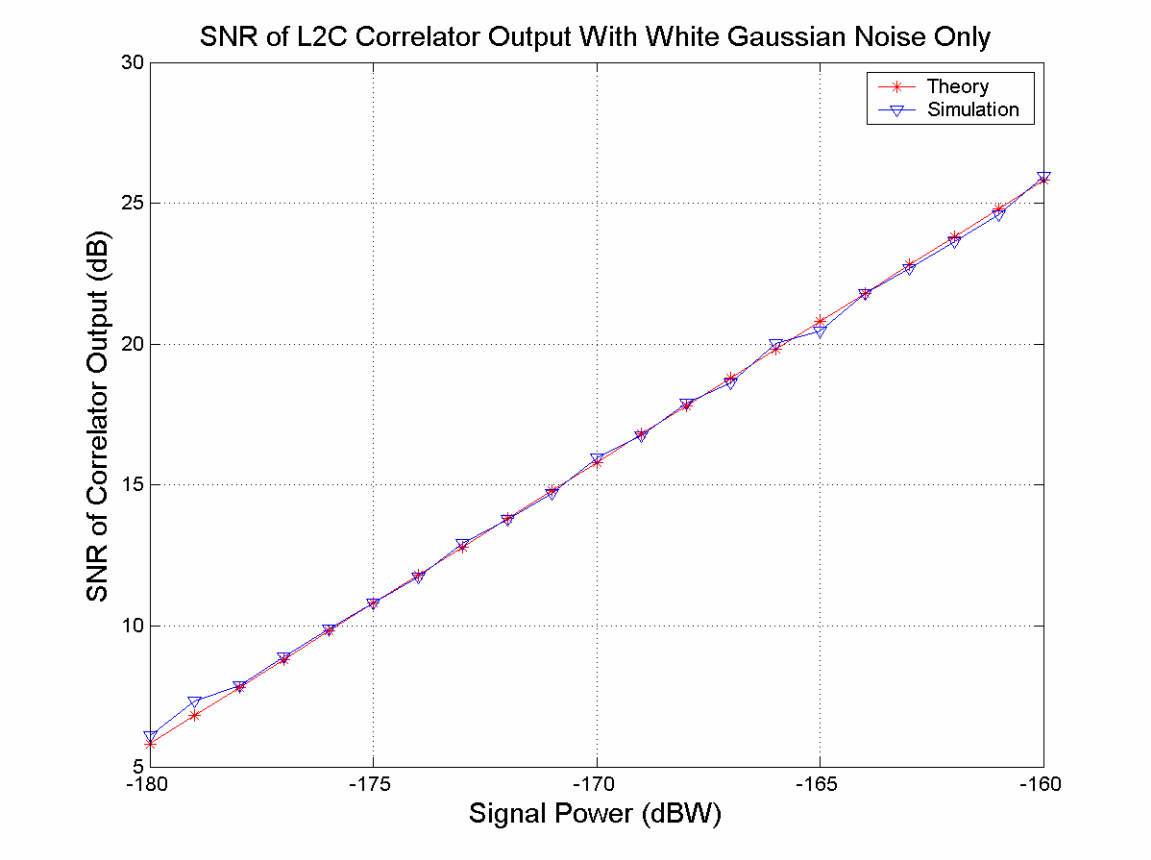

Figure 3.5 Average SNR with White Gaussian Noise Only

Figure 3.5 shows the variation of SNR under the band-limited WGN only with the power of the desired incoming signal. The red line is the theoretical result and the blue line is the simulation result. From the IS-GPS-200D specifications, the L2C power is -160 dBW. Therefore, the simulation area is in the region where the signal power is less than -160 dBW. The SNR is reduced from 26 dB to 6 dB with the deduction of the desired incoming signal power from -160 dBW to -180 dBW. The RMS error of the simulation from Figure 3.5 is less than 0.19 dB.

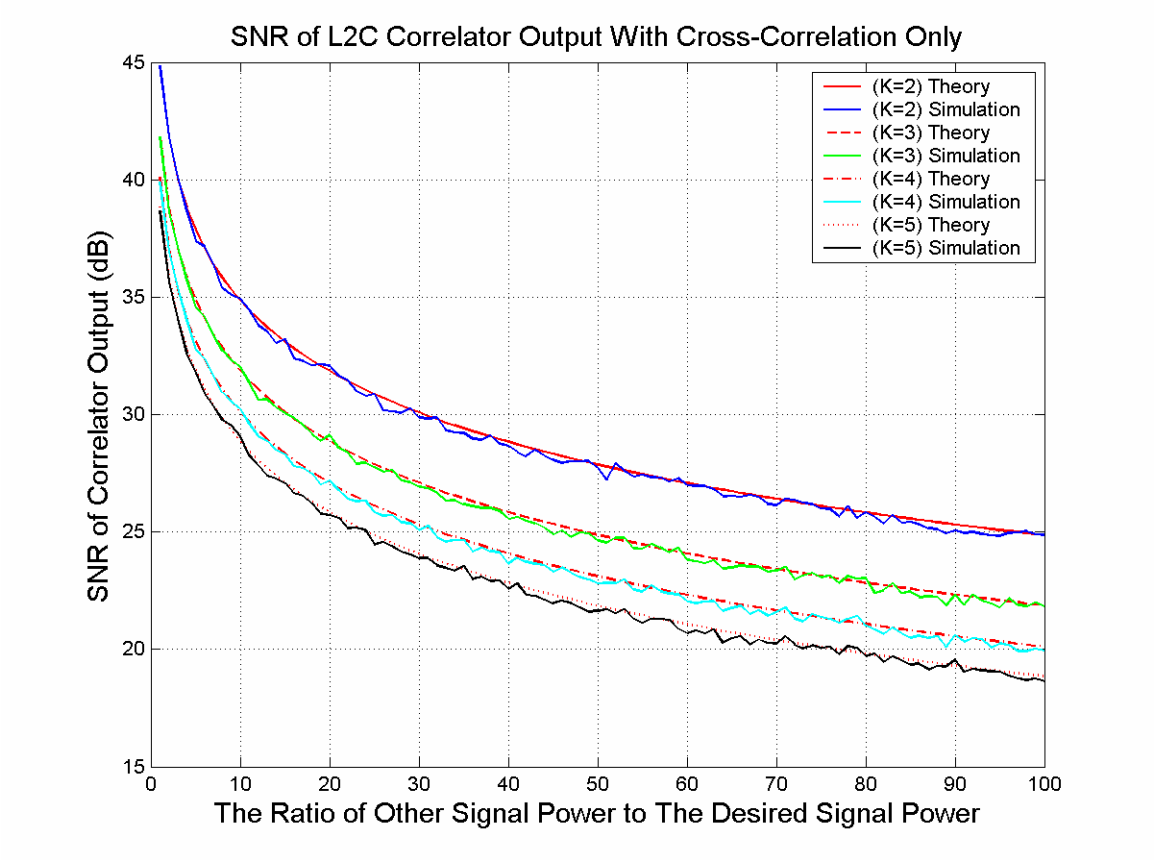

Figure 3.6 Average SNR with Cross-Correlation Only

Figure 3.6 shows the simulation results under the cross-correlations only. In this situation, Equation (3-16) can be rewritten as $SNR = \{(\frac{3}{2}N^3)^{-1}\sum_{\substack{k=1\\k\neq i}}^{K}\frac{P_k}{P_i}[r_{k,i}^M + r_{k,i}^L]\}^{-1/2}$. If it is presented in dB, then

$$SNR = 10\log_{10}\left[\frac{\frac{3}{2}N^3}{\sum_{\substack{k=1\\k\neq i}}^{K}[r_{k,i}^M + r_{k,i}^L]}\right] - 10\log_{10}\left(\frac{P_k}{P_i}\right) \quad (3\text{-}17)$$

$$= 10\log_{10}\left[\frac{3}{2}N^3\right] - 10\log_{10}\left[\sum_{\substack{k=1\\k\neq i}}^{K}[r_{k,i}^M + r_{k,i}^L]\right] - 10\log_{10}\left(\frac{P_k}{P_i}\right)$$

In the simulation, powers from other undesired signals are supposed to be the same ($P_k = P_i, k \neq i$). In Figure 3.6, the ratio of the undesired signal power to desired signal power ranges from 1 to 100. From Equation (3-17), the relationship between SNR in dB and the ratio of undesired signal power to desired signal power is logarithmic. Because the differences between different average cross-correlations are small, the second term in Equation (3-17) is also changed with the logarithm of cross-correlation number if P_k remains constant. The greatest RMS error of the simulation in the four cases (K = 2, 3, 4, 5) is less than 0.23 dB.

Figure 3.7 describes the simulated average SNR results under the cross-correlations and band-limited WGN. Equation (3-16) can be rewritten as (in dB)

$$SNR = -10\log_{10}\left[\frac{\sum_{\substack{k=1 \\ k\neq i}}^{K}\frac{P_k}{P_i}[r_{k,i}^{M} + r_{k,i}^{L}]}{\frac{3}{2}N^3} + \frac{N_0}{P_i T}\right]. \qquad (3\text{-}18)$$

In this simulation, the band-limited WGN and desired incoming signal remain constant. The ratio of undesired signal power and desired signal power is from 1 to 100. There are four cases (K = 2, 3, 4, 5). When K = 2 (that is only one cross-correlation), if the ratio $\frac{P_k}{P_i}$ ranges from 1 to 100 (increase of about 20 dB),

the SNR decreases by about 3.5 dB. When K = 5 (four cross-correlations), in the same range, the SNR decreases by about 7.5 dB.

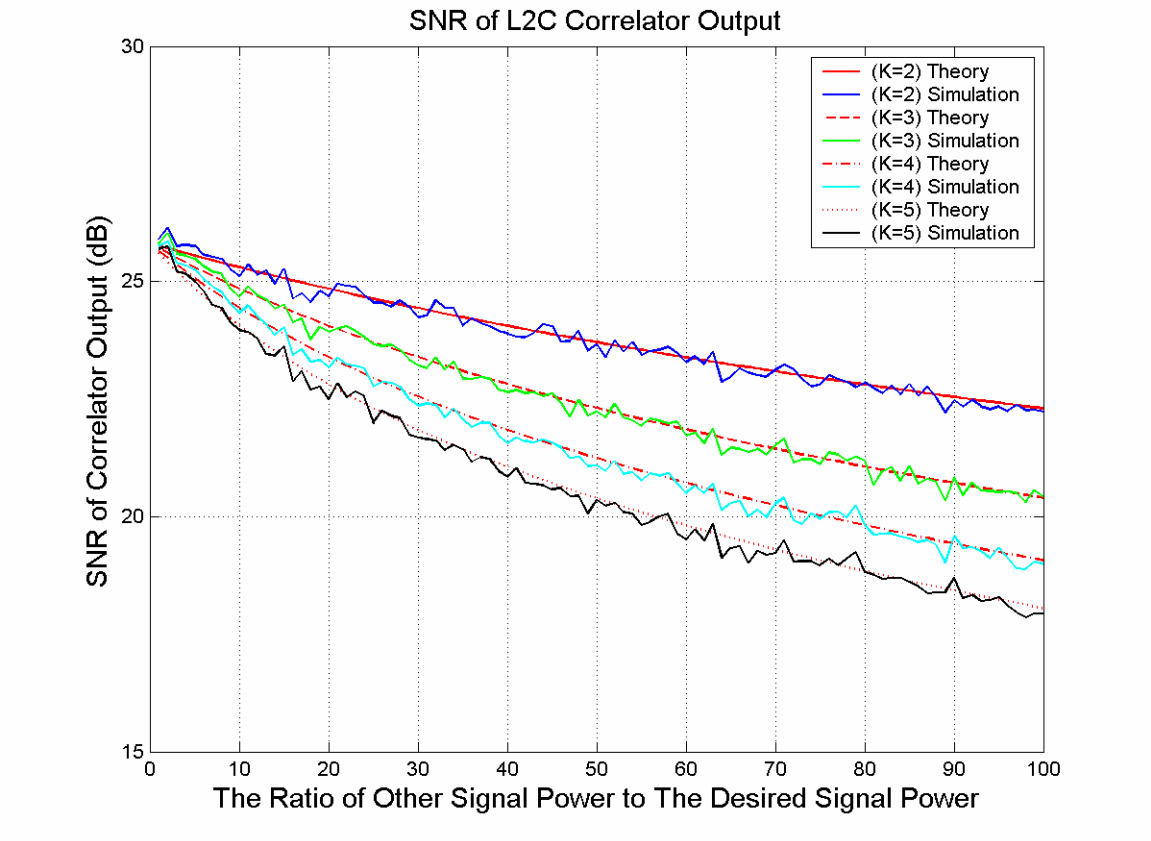

Figure 3.7 Average SNR with Cross-Correlation and White Gaussian Noise

Figure 3.5 shows that when the desired incoming signal power is -160 dBW, the SNR is about 26 dB. In Figure 3.7, on the left hand side, when the unwanted signal power is almost same as the desired signal power, the SNR is near 26 dB. The two results are consistent. The effects from the cross-correlations can be ignored compared to the effects of band-limited WGN. As the ratio of unwanted to desired signal power increases, Figure 3.7 shows that the cross-correlations also increase

their effects on the SNR results.

3.5 Conclusions

The analyses of cross-correlation and band-limited WGN effects on SNR and worst case performance demonstrate the following. If the power of the desired signal is the same as the power of the undesired signal, the maximum error probability difference generated by the cross-correlations is small. The main effects on maximum error probabilities come from the effects of band-limited WGN. In urban areas, the GPS signal can be attenuated by buildings and its strength can be decreased about 32 dBW (Tang and Dodds 2006). Under the weak desired signal situation, if the undesired signal power is larger than the desired signal power (more than 8 dB), the maximum error probability increases rapidly, especially when $K \geq 4$.

In SNR analyses, if there are no cross-correlations, SNR varies linearly with the desired signal power in dBW. If there is no white Gaussian noise, SNR changes with the logarithm of the cross-correlation number or with the logarithm of the ratio of undesired to desired signal power. If the band-limited WGN and desired incoming signal remain constant, under the high ratio of the undesired signal power to desired signal power, cross-correlation becomes the main factor to affect the SNR result.

Chapter 4

Cross-Correlation and White Gaussian Noise Effects on PLL Tracking Loops

Functioning as an automatic phase control system, the phase-locked loop is a closed-loop tracking system capable of tracking the phase of a received signal that has a residual carrier component. The system synchronizes the phase or frequency of its output signal with that of the input signal. When the output signal of the PLL is synchronized with the input signal, an arrangement often referred to as locked state (Best 2003), the phase error between output signal and input signals is zero. Any cross-correlation in the input of the PLL will affect the PLL performance. In this chapter, it is described how the cross-correlations affect such performance.

4.1 Basic Principle of a Phase-Locked Loop

In a phase-locked loop, if a phase error accumulates, a control signal acts on the oscillator in such a way that the phase error is reduced. In this system, the phase of the output signal is locked to the phase of the reference signal.

4.1.1 The Input Signal without Interference

According to Viterbi (1966), a phase-locked loop consists of three major components: a multiplier, a linear time-invariant loop filter, and a voltage-controlled oscillator. Figure 4.1 shows the phase-locked loop for the condition of no interference in the input signal, where $\sqrt{2}A\sin\theta(t)$ is the input signal, A^2 is the input signal power, and $\sqrt{2}K_1\cos\theta'(t)$ is the VCO output signal. The term K_1 is the root-mean-square amplitude of the VCO output signal (Viterbi, 1966) and $e(t)$ is the control signal to the VCO. When $e(t)$ equals zero, the VCO generates a constant-frequency sinusoid with frequency ω_0. Under the control signal $e(t)$, the VCO frequency is $\omega_0 + K_2 e(t)$. The term K_2 is the proportionality constant in radians per second per volt. Then one has (Equation (4-1) to (4-12) are taken from Viterbi (1966)):

$$\frac{d\theta'(t)}{dt} = \omega_0 + K_2 e(t). \tag{4-1}$$

The output of the multiplier is:

$$x(t) = \sqrt{2}A\sin\theta(t)\cdot\sqrt{2}K_1\cos\theta'(t) = AK_1\{\sin[\theta(t)-\theta'(t)] + \sin[\theta(t)+\theta'(t)]\}.$$

The summation component is eliminated by the filter-VCO combination. The output of the linear filter is $e(t) = \int_0^t x(u) f(t-u)du$ and $f(t)$ is the impulse response of the filter.

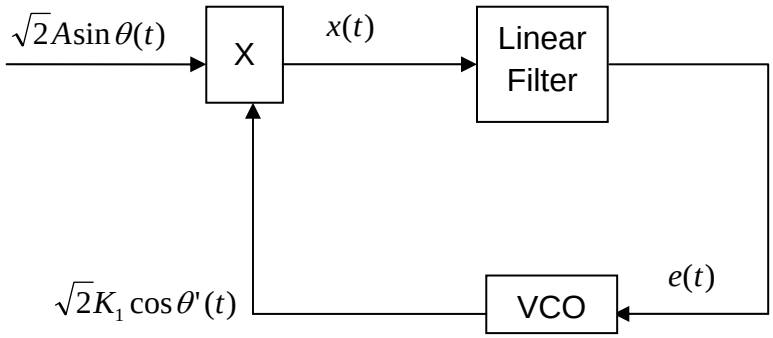

Figure 4.1 Phase-Locked Loop (Viterbi 1966)

Suppose that $\theta_1(t) = \theta(t) - \omega_0 t$ and $\theta_2(t) = \theta'(t) - \omega_0 t$. The phase error is then $\phi(t) = \theta_1(t) - \theta_2(t)$. When $\phi(t)$ is small compared with 1 radian, the approximation $\sin\phi(t) = \phi(t)$ can be used. Then one has the linear equation

$$\frac{d\phi(t)}{dt} = \frac{d\theta_1(t)}{dt} - \frac{d\theta_2(t)}{dt} = \frac{d\theta_1(t)}{dt} - AK\int_0^t f(t-u)\phi(u)du \qquad (4\text{-}2)$$

where $K = K_1K_2$ is the loop gain. Figure 4.2 describes this linear model.

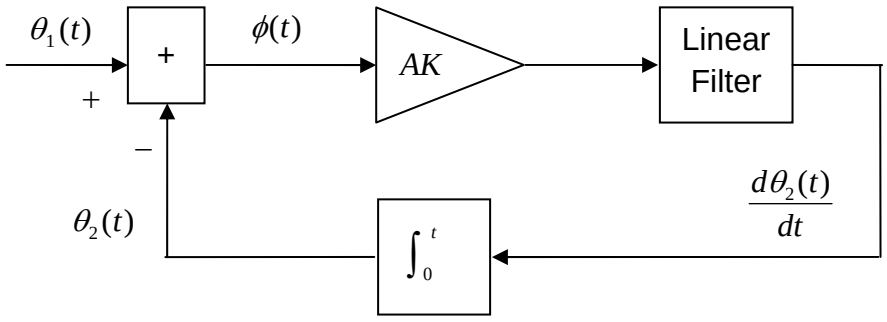

Figure 4.2 Phase-Locked Loop Linear Model (Viterbi 1966)

Assuming the existence of the following Laplace transforms

$\tilde{\theta}_1(s) = \int_0^\infty \theta_1(t)e^{-st}dt; \quad \mathrm{Re}\,al(s) \geq 0$ and

$\tilde{\phi}(s) = \int_0^\infty \phi(t)e^{-st}dt; \quad \mathrm{Re}\,al(s) \geq 0$,

the Equation (4-2) can be written as $\tilde{\phi}(s) = \frac{1}{1 + AKF(s)/s}\tilde{\theta}_1(s)$ and

$\tilde{\theta}_2(s) = \frac{AKF(s)/s}{1 + AKF(s)/s}\tilde{\theta}_1(s)$, where $F(s)$ is the transfer function of the linear filter.

The closed-loop transfer function is

$$H(s) = \frac{\tilde{\theta}_2(s)}{\tilde{\theta}_1(s)} = \frac{AKF(s)/s}{1 + AKF(s)/s}. \tag{4-3}$$

4.1.2 Input Signal with Additive Noise

Suppose that the input signal includes additive thermal noise which is a zero-mean wideband Gaussian process, where the white noise has been passed through a symmetric wide-band bandpass filter with centre frequency ω_0 and a flat passband that passes only frequencies below $2\omega_0$ rad/sec. The Gaussian process can then be expressed as

$$n(t) = \sqrt{2}[n_1(t)\sin(\omega_0 t) + n_2(t)\cos(\omega_0 t)]. \tag{4-4}$$

where $n_1(t)$ and $n_2(t)$ are independent Gaussian processes of zero mean and with two-sided spectral densities of $N_0/2$.

The received signal is

$$\sqrt{2}A\sin\theta(t)+n(t)=\sqrt{2}\{A\sin[\omega_0 t+\theta_1(t)]+n_1(t)\sin(\omega_0 t)+n_2(t)\cos(\omega_0 t)\}. \quad (4\text{-}5)$$

Multiplying by the output signal of the VCO, the output of the multiplier is

$$\begin{aligned}x(t)&=AK_1\sin[\theta_1(t)-\theta_2(t)]-K_1n_1(t)\sin\theta_2(t)+K_1n_2(t)\cos\theta_2(t)\\&\quad+AK_1\sin[2\omega_0 t+\theta_1(t)+\theta_2(t)]+K_1n_1(t)\sin[2\omega_0 t+\theta_2(t)]+K_1n_2(t)\cos[2\omega_0 t+\theta_2(t)]\end{aligned}.$$

The terms with the frequency $2\omega_0$ rad/sec may be neglected. The filtered multiplier output is

$$e(t)=K_1\int_0^t [A\sin\phi(u)-n_1(u)\sin\theta_2(u)+n_2(u)\cos\theta_2(u)]f(t-u)du.$$

If one defines $n'(t)=-n_1(t)\sin\theta_2(t)+n_2(t)\cos\theta_2(t)$, then one has

$$\frac{d\phi(t)}{dt}=\frac{d\theta_1(t)}{dt}-K\int_0^t [A\sin\phi(u)+n'(u)]f(t-u)du. \quad (4\text{-}6)$$

If the phase error $\phi(t)$ is small, then $\sin\phi(t)=\phi(t)$. Equation (4-6) becomes linear

$$\frac{d\phi(t)}{dt}=\frac{d\theta_1(t)}{dt}-K\int_0^t [A\phi(u)+n'(u)]f(t-u)du. \quad (4\text{-}7)$$

Figure 4.3 displays the model of Equation (4-7). According to Viterbi (1966), because of the white Gaussian noise, the spectral density of the phase error is

$$S_\phi(\omega)=\left|\frac{KF(\omega)/i\omega}{1+AKF(\omega)/i\omega}\right|^2 S_n(\omega). \quad (4\text{-}8)$$

where $S_n(\omega)$ is the noise spectral density.

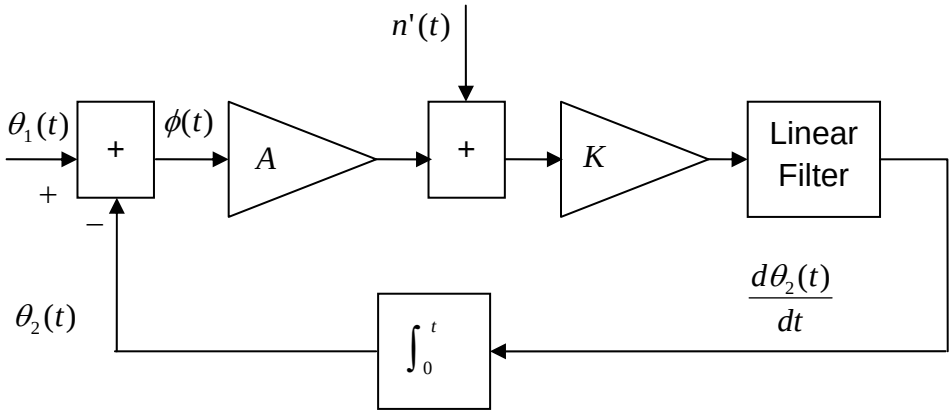

Figure 4.3 Phase-Locked Loop Linear Model (with Additive Noise) (Viterbi 1966)

Given that $H(s) = \dfrac{AKF(s)/s}{1 + AKF(s)/s}$ and $S_n(\omega) = N_0/2$, Equation (4-8) becomes

$$S_\phi(\omega) = \frac{N_0}{2A^2}\left|H(i\omega)\right|^2. \tag{4-9}$$

The phase error variance due to noise is

$$\sigma_\phi^{\,2} = \frac{N_0}{2A^2}\int_{-\infty}^{\infty}\left|H(i\omega)\right|^2\frac{d\omega}{2\pi} = \frac{N_0}{A^2}\int_{0}^{\infty}\left|H(i\omega)\right|^2\frac{d\omega}{2\pi}. \tag{4-10}$$

where N_0 is the one-sided power spectral density of the white Gaussian noise and A^2 is the desired signal power. If the loop-noise bandwidth is defined as

$$B_n = \int_{0}^{\infty}\left|H(i\omega)\right|^2\frac{d\omega}{2\pi}. \tag{4-11}$$

the phase error variance can be rewritten as

$$\sigma_{\phi}^{2} = \frac{N_0 B_n}{A^2}. \tag{4-12}$$

4.2 Theory of Average PLL Phase Error under Cross-Correlation and White Gaussian Noise

If one assumes the PRN of the desired signal $i = 1$, there is no loss in generality. The quadrature-phase component of correlation and integration can be expressed by

$$\begin{aligned} Q_1 &= \int_0^T \{\sum_{k=1}^{K} \sqrt{2P_k}[d_k(t-\tau_k)CM_k(t-\tau_k) + CL_k(t+mT-\tau_k)] \\ &\quad \times \cos(\omega_c t + \phi_k) + n(t)\} CM_1(t)\sin(\omega_c t + \hat{\phi}_1)dt \\ &= d_{1,0}\sqrt{P_1/8}T\sin(\Delta\phi_1) + \sum_{k=2}^{K} \sqrt{P_k/2}[\int_0^T d_k(t-\tau_k)CM_k(t-\tau_k)CM_1(t)dt \\ &\quad + \int_0^T CL_k(t+mT-\tau_k)CM_1(t)dt]\sin(\Delta\phi_k) + \int_0^T n(t)CM_1(t)\sin(\omega_c t + \hat{\phi}_1)dt \end{aligned} \tag{4-13}$$

where $\Delta\phi_1 \neq 0$

Given the discriminator (using this discriminator is because it can be considered as linear function when the phase error is small)

$$\Psi(\theta) = sign(I_1)\cdot Q_1. \tag{4-14}$$

the output of the discriminator is

$$\Psi(\theta) = \hat{d}_{1,0} d_{1,0} \sqrt{P_1/8}T \sin(\Delta\phi_1) + \hat{d}_{1,0} \sum_{k=2}^{K} \sqrt{P_k/2} \left\{ \int_0^T d_k(t-\tau_k) CM_k(t-\tau_k) CM_1(t) dt \right.$$
$$\left. + \int_0^T CL_k(t+mT-\tau_k) CM_1(t) dt \right\} \sin(\Delta\phi_k) + \hat{d}_{1,0} \int_0^T n(t) CM_1(t) \sin(\omega_c t + \hat{\phi}_1) dt$$
$$= \hat{d}_{1,0} d_{1,0} \sqrt{P_1/8}T \sin(\Delta\phi_1) + \Lambda_M(\tau_k) + \Lambda_L(\tau_k) + \Lambda_G(\tau_k) \quad . \tag{4-15}$$

where $\hat{d}_{1,0}$ is the estimation of $sign(I_1)$. In fact, for L2C, it is the estimation of the navigation data on the desired incoming CM code:

$$\Lambda_M(\tau_k) = \hat{d}_{1,0} \sum_{k=2}^{K} \sqrt{P_k/2} \left[\int_0^T d_k(t-\tau_k) CM_k(t-\tau_k) CM_1(t) dt \right] \sin(\Delta\hat{\phi}_k)$$
$$= \hat{d}_{1,0} \sum_{k=2}^{K} \sqrt{P_k/2} Z_{k,1}^M(\tau_k, 0) \sin(\Delta\hat{\phi}_k) \quad .$$

$$\Lambda_L(\tau_k) = \hat{d}_{1,0} \sum_{k=2}^{K} \sqrt{P_k/2} \left[\int_0^T CL_k(t+mT-\tau_k) CM_1(t) dt \right] \sin(\Delta\hat{\phi}_k)$$
$$= \hat{d}_{1,0} \sum_{k=2}^{K} \sqrt{P_k/2} Z_{k,1}^L(\tau_k, 0) \sin(\Delta\hat{\phi}_k) \quad .$$

$$\Lambda_G(\tau_k) = \hat{d}_{1,0} \int_0^T n(t) CM_1(t) \sin(\omega_c t + \hat{\phi}_1) dt \; .$$

The first term in Equation (4-15) is the signal needed by the PLL tracking loop. The other three terms are the interferences generated by cross-correlations and white Gaussian noise. The autocorrelation function of the interferences is

$$R(v) = E\left\{ [\Lambda_M(\tau_k) + \Lambda_L(\tau_k) + \Lambda_G(\tau_k)][\Lambda_M(\tau_k + v) + \Lambda_L(\tau_k + v) + \Lambda_G(\tau_k + v)] \right\}$$
$$= E[\Lambda_M(\tau_k)\Lambda_M(\tau_k + v)] + E[\Lambda_L(\tau_k)\Lambda_L(\tau_k + v)] + E[\Lambda_G(\tau_k)\Lambda_G(\tau_k + v)] \tag{4-16}$$
$$= R_M(v) + R_L(v) + R_G(v)$$

Given that $E(d_{k,-1})=0$, $E(d_{k,0})=0$ and $E(n(t))=0$, then $E(\Lambda_M(\tau_k))=0$ and $E(\Lambda_G(\tau_k))=0$. In Equation (4-16), $\Lambda_M(\tau_k), \Lambda_L(\tau_k)\, and\, \Lambda_G(\tau_k)$ are assumed to be white over the entire loop bandwidth region of interest (Huang 1998), They are independent with each other; therefore $E(\Lambda_L(\tau_k)\Lambda_M(\tau_k+\nu))=0$, $E(\Lambda_G(\tau_k)\Lambda_M(\tau_k+\nu))=0$, $E(\Lambda_M(\tau_k)\Lambda_L(\tau_k+\nu))=0$, $E(\Lambda_G(\tau_k)\Lambda_L(\tau_k+\nu))=0$, $E(\Lambda_M(\tau_k)\Lambda_G(\tau_k+\nu))=0$ and $E(\Lambda_L(\tau_k)\Lambda_G(\tau_k+\nu))=0$.

Given the autocorrelation function of interference, the one-sided power spectral density of the interference can be expressed as:

$$\begin{aligned}\mu &= 2\int_{-NT_C}^{NT_C} R(v)dv = 2\int_{-NT_C}^{NT_C} R_M(v)dv + 2\int_{-NT_C}^{NT_C} R_L(v)dv + 2\int_{-NT_C}^{NT_C} R_G(v)dv \\ &= \mu_{\mathrm{M}} + \mu_L + \mu_G\end{aligned}. \qquad (4\text{-}17)$$

The autocorrelation function $R_G(\nu)$ of the component AWGN can be expressed as (Huang 1998)

$$
\begin{aligned}
R_G(\nu) &= E[\Lambda_G(\tau_k)\Lambda_G(\tau_k+\nu)] \\
&= E[\int_0^{NT_C} n(t)CM_1(t)\sin(\omega_c t+\hat{\phi}_1)dt \int_{|\nu|}^{NT_C+|\nu|} n(u)CM_1(u)\sin(\omega_c u+\hat{\phi}_1)du] \\
&= E[\int_0^{NT_C}\int_{|\nu|}^{NT_C+|\nu|} n(t)n(u)CM_1(t)CM_1(u)\sin(\omega_c t+\hat{\phi}_1)\sin(\omega_c u+\hat{\phi}_1)dtdu \\
&= \int_0^{NT_C}\int_{|\nu|}^{NT_C+|\nu|} \frac{N_0}{2}\delta(t-u)CM_1(t)CM_1(u)\sin(\omega_c t+\hat{\phi}_1)\sin(\omega_c u+\hat{\phi}_1)dtdu \\
&= \int_{|\nu|}^{NT_C} \frac{N_0}{2} CM\ (t)CM_1(t)\sin^2(\omega_c t+\hat{\phi}_1)dt \\
&= \frac{N_0}{2}\int_{|\nu|}^{NT_C} CM_1(t)CM_1(t)[\frac{1}{2}-\frac{1}{2}\cos(2\omega_c t+2\hat{\phi}_1)]dt \\
&= \frac{N_0}{8}(NT_C-|\nu|)
\end{aligned}
\quad . \qquad (4\text{-}18)
$$

Because the component of the AWGN $\Lambda_G(\tau_k)$ is white over the loop filter region of interest and the autocorrelation function is zero at $|\nu| \geq NT_C$ (Huang 1998), the one-side power spectral density of $\Lambda_G(\tau_k)$ can be expressed as

$$
\begin{aligned}
\mu_G &= 2\int_{-NT_C}^{NT_C} R_G(v)dv = 2\int_{-NT_C}^{NT_C}\frac{N_0}{8}(NT_C-|\nu|)dv \\
&= \frac{N_0}{4}[\int_{-NT_C}^{0}(NT_C+v)dv+\int_0^{NT_C}(NT_C-v)dv]\,. \qquad (4\text{-}19) \\
&= \frac{N_0}{4}(NT_C)^2
\end{aligned}
$$

By a similar process, the component of the cross-correlation between the local and incoming CM code is considered. The autocorrelation function of the component $\Lambda_M(\tau_k)$ can be expressed as (Huang 1998)

$$R_M(\nu) = E[\Lambda_M(\tau_k)\Lambda_M(\tau_k+\nu)] = \sum_{k=2}^{K} \frac{P_k}{4} E[Z_{k,1}^M(\tau_k,0)Z_{k,1}^M(\tau_k,\nu)]. \qquad (4\text{-}20)$$

where (Huang 1998)

$$Z_{k,1}^M(\tau_k,0) = \int_0^{NT_C} d_k(t-\tau_k)CM_k(t-\tau_k)CM_1(t)dt = d_{k,-1}R_{k,1}^M(\tau_k) + d_{k,0}\hat{R}_{k,1}^M(\tau_k). \qquad (4\text{-}21)$$

$$\begin{aligned} Z_{k,1}^M(\tau_k,\nu) &= \int_{|\nu|}^{NT_C+|\nu|} d_k(t-\tau_k)CM_k(t-\tau_k)CM_1(t)dt \\ &= B(|\nu|,\tau_k)[d_{k,-1}Q_{k,1}(|\nu|,\tau_k,\tau_k) + d_{k,0}Q_{k,1}(\tau_k,|\nu|+NT_C,\tau_k) \\ &\quad + B(\tau_k,|\nu|)[d_{k,0}Q_{k,1}(|\nu|,\tau_k+NT_C,\tau_k) + d_{k,1}Q_{k,1}(\tau_k,|\nu|,\tau_k)] \end{aligned} \qquad (4\text{-}22)$$

with $B(\alpha,\beta)=1$ for $0 \le \alpha \le \beta$ and $B(\alpha,\beta)=0$ for other cases, and $Q_{k,1}(\alpha,\beta,\gamma) = \int_\alpha^\beta CM_k(t-\gamma)CM_1(t)dt$. The average of $Z_{k,1}^M(\tau_k,0)$ times $Z_{k,1}^M(\tau_k,\nu)$ becomes

$$
\begin{aligned}
E[Z^M_{k,1}(\tau_k,0)Z^M_{k,1}(\tau_k,v)] &= E\{[d_{k,-1}R^M_{k,1}(\tau_k)+d_{k,0}\hat{R}^M_{k,1}(\tau_k)]\{B(|v|,\tau_k)[d_{k,-1}Q_{k,1}(|v|,\tau_k,\tau_k) \\
&\quad d_{k,0}Q_{k,1}(\tau_k,|v|+NT_C,\tau_k)]+B(\tau_k,|v|)[d_{k,0}Q_{k,1}(|v|,\tau_k+NT_C,\tau_k)+ \\
&\quad d_{k,1}Q_{k,1}(\tau_k,|v|,\tau_k)]\}\} \\
&= B(|v|,\tau_k)[R^M_{k,1}(\tau_k)Q_{k,1}(|v|,\tau_k,\tau_k)+\hat{R}^M_{k,1}(\tau_k)Q_{k,1}(\tau_k,|v|+NT_C,\tau_k)]+ \\
&\quad B(\tau_k,|v|)\hat{R}^M_{k,1}(\tau_k)Q_{k,1}(|v|,\tau_k+NT_C,\tau_k) \\
&= B(|v|,\tau_k)[R^M_{k,1}(\tau_k)Q_{k,1}(|v|,\tau_k,\tau_k)-\hat{R}^M_{k,1}(\tau_k)Q_{k,1}(|v|,\tau_k,\tau_k)+ \\
&\quad \hat{R}^M_{k,1}(\tau_k)Q_{k,1}(\tau_k,NT_C,\tau_k)+\hat{R}^M_{k,1}(\tau_k)Q_{k,1}(0,\tau_k,\tau_k)]+ \\
&\quad B(\tau_k,|v|)\hat{R}^M_{k,1}(\tau_k)[Q_{k,1}(\tau_k,NT_C,\tau_k)+Q_{k,1}(0,\tau_k,\tau_k)-Q_{k,1}(\tau_k,|v|,\tau_k)] \\
&= B(|v|,\tau_k)[(\hat{R}^M_{k,1}(\tau_k))^2+\hat{R}^M_{k,1}(\tau_k)R^M_{k,1}(\tau_k)+R^M_{k,1}(\tau_k)Q_{k,1}(|v|,\tau_k,\tau_k)- \\
&\quad \hat{R}^M_{k,1}(\tau_k)Q_{k,1}(|v|,\tau_k,\tau_k)]+B(\tau_k,|v|)[(\hat{R}^M_{k,1}(\tau_k))^2+\hat{R}^M_{k,1}(\tau_k)R^M_{k,1}(\tau_k)- \\
&\quad \hat{R}^M_{k,1}(\tau_k)Q_{k,1}(\tau_k,|v|,\tau_k)] \\
&= (\hat{R}^M_{k,1}(\tau_k))^2+\hat{R}^M_{k,1}(\tau_k)R^M_{k,1}(\tau_k)+[B(|v|,\tau_k)R^M_{k,1}(\tau_k)-\hat{R}^M_{k,1}(\tau_k)]\times \\
&\quad Q_{k,1}(\min\{|v|,\tau_k\},\max\{|v|,\tau_k\},\tau_k)
\end{aligned}
\quad . \tag{4-23}
$$

According to Huang (1998), the interference $\Lambda_M(\tau_k)$ is assumed to be white in the loop bandwidth region and the autocorrelation function is zero at $|v| \geq NT_C$. The power spectral density μ_M can be written as

$$
\mu_M = 2\int_{-NT_C}^{NT_C} R_M(v)dv = \frac{P_1T_C^3}{4N}I_M \,. \tag{4-24}
$$

where

$$
\begin{aligned}
I_M = \frac{1}{3}\sum_{k=2}^{K}\sum_{l=0}^{N-1}\frac{P_k}{P_1}\{&\psi[2C_{k,1}(l),NC_{k,1}(l-N)-D_{k,1}(l-N)]+ \\
&\psi[2C_{k,1}(l),D_{k,1}(l)]+\psi[2C_{k,1}(l-N),D_{k,1}(l-N)]+ \\
&\Theta[C_{k,1}(l),C_{k,1}(l)]+\Theta[C_{k,1}(l-N),C_{k,1}(l-N)]-\Theta[C_{k,1}(l),C_{k,1}(l-N)]\}
\end{aligned}
\quad . \tag{4-25}
$$

with

$$\psi[A(l),B(l)] = A(l)B(l) + \frac{1}{2}A(l)B(l+1) + \frac{1}{2}A(l+1)B(l) + A(l+1)B(l+1) \quad . \tag{4-26}$$

$$\Theta[A(l),B(l)] = \frac{5}{4}A(l)B(l) + \frac{3}{4}A(l+1)B(l+1) + \frac{3}{4}A(l+1)B(l) + \frac{1}{4}A(l)B(l+1) \quad . \tag{4-27}$$

and

$$D_{k,1}(l) = \begin{cases} \sum_{j=0}^{N-1-l} (j+l)a_{k,j}^{M}a_{1,j+l}^{M}, & 0 \le \mathrm{l} \le \mathrm{N}\text{-}1 \\ \sum_{j=0}^{N-1+l} ja_{k,j-l}^{M}a_{1,j}^{M}, & 1\text{-}\mathrm{N} \le \mathrm{l} < 0 \\ 0, & |\mathrm{l}| \ge \mathrm{N} \end{cases} . \tag{4-28}$$

Let us now consider the cross-correlation component between the local CM code and incoming CL code. The autocorrelation function of the component $\Lambda_L(\tau_k)$ can be written as

$$R_L(v) = E[\Lambda_L(\tau_k)\Lambda_L(\tau_k + v)] = \sum_{k=2}^{K} \frac{P_k}{4} E[Z_{k,1}^{L}(\tau_k,0)Z_{k,1}^{L}(\tau_k,v)] . \tag{4-29}$$

where $v = qT_C + \Delta v$, $0 \le \Delta v \le T_C$, and

$$Z_{k,1}^{L}(\tau_k,0) = \int_0^{NT_C} CL_k(t+mT-\tau_k)CM_1(t)dt = W_{k,1}(m,l)T_C + [W_{k,1}(m,l+1) - W_{k,1}(m,l)](\tau_k - lT_C) \quad . \tag{4-30}$$

$$
\begin{aligned}
Z_{k,1}^{L}(\tau_k,\nu) &= \int_{|\nu|}^{NT_C+|\nu|} CL_k(t+mT-\tau_k)CM_1(t)dt \\
&= \int_{|\nu|}^{NT_C+|\nu|} \sum_{j=-\infty}^{\infty} a_{k,j}^{L} P_{T_C}(t+mNT_C-jT_C-\tau_k) \sum_{n=-\infty}^{\infty} a_{1,n}^{M} P_{T_C}(t-nT_C)dt \\
&= \int_{qT_C+\Delta\nu}^{NT_C+qT_C+\Delta\nu} \sum_{j=-\infty}^{\infty} a_{k,j}^{L} P_{T_C}(t+mNT_C-jT_C-\tau_k) \sum_{n=-\infty}^{\infty} a_{1,n}^{M} P_{T_C}(t-nT_C)dt \\
&= \int_{(q+1)T_C}^{(N+q)T_C} \sum_{j=-\infty}^{\infty} a_{k,j}^{L} P_{T_C}(t+mNT_C-jT_C-\tau_k) \sum_{n=-\infty}^{\infty} a_{1,n}^{M} P_{T_C}(t-nT_C)dt + \\
&\quad \int_{qT_C+\Delta\nu}^{(q+1)T_C} \sum_{j=-\infty}^{\infty} a_{k,j}^{L} P_{T_C}(t+mNT_C-jT_C-\tau_k) \sum_{n=-\infty}^{\infty} a_{1,n}^{M} P_{T_C}(t-nT_C)dt + \\
&\quad \int_{(N+q)T_C}^{(N+q)T_C+\Delta\nu} \sum_{j=-\infty}^{\infty} a_{k,j}^{L} P_{T_C}(t+mNT_C-jT_C-\tau_k) \sum_{n=-\infty}^{\infty} a_{1,n}^{M} P_{T_C}(t-nT_C)dt \\
&= \sum_{r=q+1}^{N+q-1} \int_{rT_C}^{(r+1)T_C} \sum_{j=-\infty}^{\infty} a_{k,j}^{L} P_{T_C}(t+mNT_C-jT_C-\tau_k) \sum_{n=-\infty}^{\infty} a_{1,n}^{M} P_{T_C}(t-nT_C)dt + \\
&\quad \int_{qT_C+\Delta\nu}^{(q+1)T_C} a_{1,q}^{M} \sum_{j=-\infty}^{\infty} a_{k,j}^{L} P_{T_C}(t+mNT_C-jT_C-lT_C-\Delta\tau_k)dt + \\
&\quad \int_{(N+q)T_C}^{(N+q)T_C+\Delta\nu} a_{1,N+q}^{M} \sum_{j=-\infty}^{\infty} a_{k,j}^{L} P_{T_C}(t+mNT_C-jT_C-lT_C-\Delta\tau_k)dt
\end{aligned}
\qquad \text{(4-31)}
$$

In the next analyses the average value of $E[Z_{k,1}^{L}(\tau_k,0)Z_{k,1}^{L}(\tau_k,\nu)]$ will be estimated for $\tau_k = lT_C + \Delta\tau$ from 0 to T, that is for l from 0 to N-1 and $\Delta\tau$ from 0 to Tc. $Z_{k,1}^{L}(\tau_k,\nu)$ will take two different values in the different ranges $\Delta\nu \le \Delta\tau \le T_C$ and $0 \le \Delta\tau \le \Delta\nu$. Therefore the integration for $\Delta\tau$ from 0 to Tc should be divided into two parts on $\Delta\nu \le \Delta\tau \le T_C$ and $0 \le \Delta\tau \le \Delta\nu$. After integrations are conducted separately, the two results should be added. Considering Equation (4-31) in the two ranges separately, when $\Delta\nu \le \Delta\tau \le T_C$ Equation (4-31) can be written as

$$
\begin{aligned}
Z_{k,1}^{L}(\tau_k,\nu) = & \sum_{r=q+1}^{N+q-1} a_{1,r}^{M} \int_{rT_C}^{(r+1)T_C} \sum_{j=-\infty}^{\infty} a_{k,j}^{L} P_{T_C}(t+mNT_C - jT_C - lT_C - \Delta\tau_k)dt + \\
& \int_{qT_C+\Delta\nu}^{qT_C+\Delta\tau_k} a_{1,q}^{M} a_{k,q+mN-l-1}^{L} dt + \int_{qT_C+\Delta\tau_k}^{(q+1)T_C} a_{1,q}^{M} a_{k,q+mN-l}^{L} dt + \\
& \int_{(N+q)T_C}^{(N+q)T_C+\Delta\nu} a_{1,N+q}^{M} a_{k,N+q+mN-l-1}^{L} dt \\
= & \sum_{r=q+1}^{N+q-1} a_{1,r}^{M} [\int_{rT_C}^{rT_C+\Delta\tau_k} a_{k,r+mN-l-1}^{L} dt + \int_{rT_C+\Delta\tau_k}^{(r+1)T_C} a_{k,r+mN-l}^{L} dt] + \\
& a_{1,q}^{M} a_{k,q+mN-l-1}^{L} (\Delta\tau_k - \Delta\nu) + a_{1,q}^{M} a_{k,q+mN-l}^{L} (T_C - \Delta\tau_k)] + \\
& a_{1,N+q}^{M} a_{k,N+q+mN-l-1}^{L} \cdot \Delta\nu \\
= & \sum_{r=q}^{N+q-1} a_{1,r}^{M} a_{k,r+mN-l-1}^{L} \cdot \Delta\tau_k + \sum_{r=q}^{N+q-1} a_{1,r}^{M} a_{k,r+mN-l}^{L} \cdot T_C - \\
& \sum_{r=q}^{N+q-1} a_{1,r}^{M} a_{k,r+mN-l}^{L} \cdot \Delta\tau_k + [a_{1,N+q}^{M} a_{k,N+q+mN-l-1}^{L} - \\
& a_{1,q}^{M} a_{k,q+mN-l-1}^{L}] \cdot \Delta\nu \\
= & W_{k,1}(m,l,q) \cdot T_C + [W_{k,1}(m,l+1,q) - W_{k,1}(m,l,q)] \cdot \Delta\tau_k + \\
& [H_{k,1}(m,l+1,N+q) - H_{k,1}(m,l+1,q)] \cdot \Delta\nu \qquad . \quad \text{(4-32)}
\end{aligned}
$$

where $W_{k,1}(m,l,q) = \sum_{r=q}^{N+q-1} a_{1,r}^{M} a_{k,r+mN-l}^{L}$, $H_{k,1}(m,l,q) = a_{1,q}^{M} a_{k,q+mN-l}^{L}$.

When $0 \le \Delta\tau \le \Delta\nu$, Equation (4-31) can be written as

$$
\begin{aligned}
Z_{k,1}^{L}(\tau_k, v) = & \sum_{r=q+1}^{N+q-1} a_{1,r}^{M} \int_{rT_C}^{(r+1)T_C} \sum_{j=-\infty}^{\infty} a_{k,j}^{L} P_{T_C}(t + mNT_C - jT_C - lT_C - \Delta\tau_k)dt + \\
& \int_{qT_C+\Delta v}^{(q+1)T_C} a_{1,q}^{M} a_{k,q+mN-l}^{L} dt + \int_{(N+q)T_C}^{(N+q)T_C+\Delta\tau_k} a_{1,N+q}^{M} a_{k,N+q+mN-l-1}^{L} dt + \\
& \int_{(N+q)T_C+\Delta\tau_k}^{(N+q)T_C+\Delta v} a_{1,N+q}^{M} a_{k,N+q+mN-l}^{L} dt \\
= & \sum_{r=q+1}^{N+q-1} a_{1,r}^{M} [\int_{rT_C}^{rT_C+\Delta\tau_k} a_{k,r+mN-l-1}^{L} dt + \int_{rT_C+\Delta\tau_k}^{(r+1)T_C} a_{k,r+mN-l}^{L} dt] + \\
& a_{1,q}^{M} a_{k,q+mN-l}^{L} (T_C - \Delta v) + a_{1,N+q}^{M} a_{k,N+q+mN-l-1}^{L} \Delta\tau_k + \\
& a_{1,N+q}^{M} a_{k,N+q+mN-l}^{L} \cdot (\Delta v - \Delta\tau_k) \\
= & \sum_{r=q+1}^{N+q} a_{1,r}^{M} a_{k,r+mN-l-1}^{L} \cdot \Delta\tau_k + \sum_{r=q}^{N+q-1} a_{1,r}^{M} a_{k,r+mN-l}^{L} \cdot T_C - \\
& \sum_{r=q+1}^{N+q} a_{1,r}^{M} a_{k,r+mN-l}^{L} \cdot \Delta\tau_k + [a_{1,N+q}^{M} a_{k,N+q+mN-l}^{L} - \\
& a_{1,q}^{M} a_{k,q+mN-l}^{L}] \cdot \Delta v \\
= & W_{k,1}(m,l,q) \cdot T_C + [W_{k,1}(m,l+1,q+1) - W_{k,1}(m,l,q+1)] \cdot \Delta\tau_k + \\
& [H_{k,1}(m,l,N+q) - H_{k,1}(m,l,q)] \cdot \Delta v
\end{aligned}
\quad . \text{(4-33)}
$$

Therefore, when $\Delta v \le \Delta\tau \le T_C$, the average $Z_{k,1}^{L}(\tau_k, 0)$ times $Z_{k,1}^{L}(\tau_k, v)$ becomes

$$
\begin{aligned}
E[Z_{k,1}^{L}(\tau_k,0) Z_{k,1}^{L}(\tau_k, v)] = & E\{\{W_{k,1}(m,l,0) \cdot T_C + [W_{k,1}(m,l+1,0) - W_{k,1}(m,l,0)](\tau_k - lT_C)\} \cdot \\
& \{W_{k,1}(m,l,q) \cdot T_C + [W_{k,1}(m,l+1,q) - W_{k,1}(m,l,q)] \cdot (\tau_k - lT_C) + \\
& [H_{k,1}(m,l+1,N+q) - H_{k,1}(m,l+1,q)] \cdot \Delta v\}\} \\
= & \frac{1}{N_L N T_C} \sum_{m=0}^{N_L-1} \sum_{l=0}^{N-1} \int_{lT_C+\Delta v}^{(l+1)T_C} \{W_{k,1}(m,l,0) W_{k,1}(m,l,q) \cdot T_C^2 + \\
& W_{k,1}(m,l,q)[W_{k,1}(m,l+1,0) - W_{k,1}(m,l,0)] \cdot T_C \cdot (\tau_k - lT_C) + \\
& W_{k,1}(m,l,0)[W_{k,1}(m,l+1,q) - W_{k,1}(m,l,q)] \cdot T_C \cdot (\tau_k - lT_C) + \\
& [W_{k,1}(m,l+1,0) - W_{k,1}(m,l,0)] \cdot [W_{k,1}(m,l+1,q) - W_{k,1}(m,l,q)] \cdot \\
& (\tau_k - lT_C)^2 + W_{k,1}(m,l,0) \cdot [H_{k,1}(m,l+1,N+q) - \\
& H_{k,1}(m,l+1,q)] \cdot T_C \cdot \Delta v + [W_{k,1}(m,l+1,0) - W_{k,1}(m,l,0)] \cdot \\
& [H_{k,1}(m,l+1,N+q) - H_{k,1}(m,l+1,q)] \cdot (\tau_k - lT_C) \cdot \Delta v\} d\tau_k
\end{aligned}
\quad .
$$

(4-34)

After integration, in the range $\Delta\nu \le \Delta\tau \le T_C$, the autocorrelation function can be written as

$$
\begin{aligned}
R_{La}(\nu) &= \sum_{k=2}^{K} \frac{P_k}{4} E[Z_{k,1}^{L}(\tau_k,0) Z_{k,1}^{L}(\tau_k,\nu)] \\
&= \frac{1}{N_L N T_C} \sum_{k=2}^{K} \sum_{m=0}^{N_L-1} \sum_{l=0}^{N-1} \frac{P_k}{4} \{W_{k,1}(m,l,0) W_{k,1}(m,l,q) \cdot T_C^2 [T_C - \Delta\nu] + \\
&\quad W_{k,1}(m,l,q)[W_{k,1}(m,l+1,0) - W_{k,1}(m,l,0)] \cdot (T_C^2 - \Delta\nu^2) \cdot \frac{T_C}{2} + \\
&\quad W_{k,1}(m,l,0)[W_{k,1}(m,l+1,q) - W_{k,1}(m,l,q)] \cdot (T_C^2 - \Delta\nu^2) \cdot \frac{T_C}{2} + \\
&\quad [W_{k,1}(m,l+1,0) - W_{k,1}(m,l,0)] \cdot [W_{k,1}(m,l+1,q) - W_{k,1}(m,l,q)] \cdot \frac{1}{3}(T_C^3 - \Delta\nu^3) + \\
&\quad W_{k,1}(m,l,0) \cdot [H_{k,1}(m,l+1,N+q) - H_{k,1}(m,l+1,q)] \cdot T_C \cdot \Delta\nu \cdot (T_C - \Delta\nu) + \\
&\quad [W_{k,1}(m,l+1,0) - W_{k,1}(m,l,0)][H_{k,1}(m,l+1,N+q) - \\
&\quad H_{k,1}(m,l+1,q)] \cdot \frac{1}{2}(T_C^2 - \Delta\nu^2) \cdot \Delta\nu\}
\end{aligned}
\tag{4-35}
$$

When $0 \le \Delta\tau \le \Delta\nu$, the average $Z_{k,1}^{L}(\tau_k,0)$ times $Z_{k,1}^{L}(\tau_k,\nu)$ becomes

$$
\begin{aligned}
E[Z_{k,1}^{L}(\tau_k,0) Z_{k,1}^{L}(\tau_k,\nu)] &= E\Big\{\{W_{k,1}(m,l,0) \cdot T_C + [W_{k,1}(m,l+1,0) - W_{k,1}(m,l,0)](\tau_k - lT_C)\} \cdot \\
&\quad \{W_{k,1}(m,l,q) \cdot T_C + [W_{k,1}(m,l+1,q+1) - W_{k,1}(m,l,q+1)] \cdot (\tau_k - lT_C) + \\
&\quad [H_{k,1}(m,l,N+q) - H_{k,1}(m,l,q)] \cdot \Delta\nu\}\Big\} \\
&= \frac{1}{N_L N T_C} \sum_{m=0}^{N_L-1} \sum_{l=0}^{N-1} \int_{lT_C}^{lT_C+\Delta\nu} \{W_{k,1}(m,l,0) W_{k,1}(m,l,q) \cdot T_C^2 + \\
&\quad W_{k,1}(m,l,q)[W_{k,1}(m,l+1,0) - W_{k,1}(m,l,0)] \cdot T_C \cdot (\tau_k - lT_C) + \\
&\quad W_{k,1}(m,l,0)[W_{k,1}(m,l+1,q+1) - W_{k,1}(m,l,q+1)] \cdot T_C \cdot (\tau_k - lT_C) + \\
&\quad [W_{k,1}(m,l+1,0) - W_{k,1}(m,l,0)] \cdot [W_{k,1}(m,l+1,q+1) - W_{k,1}(m,l,q+1)] \cdot \\
&\quad (\tau_k - lT_C)^2 + W_{k,1}(m,l,0) \cdot [H_{k,1}(m,l,N+q) - H_{k,1}(m,l,q)] \cdot T_C \cdot \Delta\nu + \\
&\quad [W_{k,1}(m,l+1,0) - W_{k,1}(m,l,0)][H_{k,1}(m,l,N+q) - \\
&\quad H_{k,1}(m,l,q)] \cdot (\tau_k - lT_C) \cdot \Delta\nu\} d\tau_k
\end{aligned}
\tag{4-36}
$$

After integration, in the range $0 \le \Delta\tau \le \Delta\nu$, the autocorrelation function can be written as

$$
\begin{aligned}
R_{Lb}(\nu) &= \sum_{k=2}^{K} \frac{P_k}{4} E[Z_{k,1}^{L}(\tau_k,0) Z_{k,1}^{L}(\tau_k,\nu)] \\
&= \frac{1}{N_L N T_C} \sum_{k=2}^{K} \sum_{m=0}^{N_L-1} \sum_{l=0}^{N-1} \frac{P_k}{4} \{ W_{k,1}(m,l,0) W_{k,1}(m,l,q) \cdot T_C^2 \cdot \Delta\nu + \\
&\quad W_{k,1}(m,l,q)[W_{k,1}(m,l+1,0) - W_{k,1}(m,l,0)] \cdot \Delta\nu^2 \cdot \frac{T_C}{2} + \\
&\quad W_{k,1}(m,l,0)[W_{k,1}(m,l+1,q+1) - W_{k,1}(m,l,q+1)] \cdot \Delta\nu^2 \cdot \frac{T_C}{2} + \\
&\quad [W_{k,1}(m,l+1,0) - W_{k,1}(m,l,0)] \cdot [W_{k,1}(m,l+1,q+1) - W_{k,1}(m,l,q+1)] \cdot \frac{1}{3} \cdot \Delta\nu^3 + \\
&\quad W_{k,1}(m,l,0) \cdot [H_{k,1}(m,l,N+q) - H_{k,1}(m,l,q)] \cdot T_C \cdot \Delta\nu^2 + \\
&\quad [W_{k,1}(m,l+1,0) - W_{k,1}(m,l,0)] \cdot [H_{k,1}(m,l,N+q) - H_{k,1}(m,l,q)] \cdot \frac{1}{2} \Delta\nu^3 \}
\end{aligned}
\tag{4-37}
$$

Therefore the autocorrelation function $R_L(\nu)$ of the component $\Lambda_L(\tau_k)$ can be written as $R_L(\nu) = R_{La}(\nu) + R_{Lb}(\nu)$. Given that $\Lambda_L(\tau_k)$ is white in the loop bandwidth region of interest and the autocorrelation function is zero at $|\nu| \le NT_C$ (Huang 1998), the one-side power spectral density of the component $\Lambda_L(\tau_k)$ can be written as

$$\mu_L = 2\int_{-NT_C}^{NT_C} R_L(v)dv = 2\int_{-NT_C}^{NT_C} [R_{La}(v) + R_{Lb}(v)]dv = 4\int_{0}^{NT_C} R_{La}(v)dv + 4\int_{0}^{NT_C} R_{Lb}(v)dv$$

$$= \frac{1}{N_L NT_C}\sum_{q=0}^{N-1}\sum_{k=2}^{K}\sum_{m=0}^{N_L-1}\sum_{l=0}^{N-1} P_k \int_{qT_C}^{(q+1)T_C} \{W_{k,1}(m,l,0)W_{k,1}(m,l,q)\cdot T_C^2[T_C - (v - qT_C)] +$$

$$W_{k,1}(m,l,q)[W_{k,1}(m,l+1,0) - W_{k,1}(m,l,0)]\cdot(T_C^2 - (v - qT_C)^2)\cdot\frac{T_C}{2} +$$

$$W_{k,1}(m,l,0)[W_{k,1}(m,l+1,q) - W_{k,1}(m,l,q)]\cdot[T_C^2 - (v - qT_C)^2]\cdot\frac{T_C}{2} +$$

$$[W_{k,1}(m,l+1,0) - W_{k,1}(m,l,0)]\cdot[W_{k,1}(m,l+1,q) - W_{k,1}(m,l,q)]\cdot\frac{1}{3}[T_C^3 - (v - qT_C)^3] +$$

$$W_{k,1}(m,l,0)\cdot[H_{k,1}(m,l+1,N+q) - H_{k,1}(m,l+1,q)]\cdot T_C\cdot(v - qT_C)\cdot[T_C - (v - qT_C)] +$$

$$[W_{k,1}(m,l+1,0) - W_{k,1}(m,l,0)][H_{k,1}(m,l+1,N+q) -$$

$$H_{k,1}(m,l+1,q)]\cdot\frac{1}{2}[T_C^2 - (v - qT_C)^2]\cdot(v - qT_C)\}dv +$$

$$\frac{1}{N_L NT_C}\sum_{q=0}^{N-1}\sum_{k=2}^{K}\sum_{m=0}^{N_L-1}\sum_{l=0}^{N-1} P_k \int_{qT_C}^{(q+1)T_C} \{W_{k,1}(m,l,0)W_{k,1}(m,l,q)\cdot T_C^2\cdot(v - qT_C) +$$

$$W_{k,1}(m,l,q)[W_{k,1}(m,l+1,0) - W_{k,1}(m,l,0)]\cdot(v - qT_C)^2\cdot\frac{T_C}{2} +$$

$$W_{k,1}(m,l,0)[W_{k,1}(m,l+1,q+1) - W_{k,1}(m,l,q+1)]\cdot(v - qT_C)^2\cdot\frac{T_C}{2} +$$

$$[W_{k,1}(m,l+1,0) - W_{k,1}(m,l,0)]\cdot[W_{k,1}(m,l+1,q+1) - W_{k,1}(m,l,q+1)]\cdot\frac{1}{3}\cdot(v - qT_C)^3 +$$

$$W_{k,1}(m,l,0)\cdot[H_{k,1}(m,l,N+q) - H_{k,1}(m,l,q)]\cdot T_C\cdot(v - qT_C)^2 +$$

$$[W_{k,1}(m,l+1,0) - W_{k,1}(m,l,0)]\cdot[H_{k,1}(m,l,N+q) - H_{k,1}(m,l,q)]\cdot\frac{1}{2}(v - qT_C)^3\}dv \quad (4\text{-}38)$$

After integration, Equation (4-38) becomes

$$\mu_L = \frac{1}{N_L N T_C}\sum_{q=0}^{N-1}\sum_{k=2}^{K}\sum_{m=0}^{N_L-1}\sum_{l=0}^{N-1} P_k\{W_{k,1}(m,l,0)W_{k,1}(m,l,q)\cdot\frac{1}{12}T_C^4 +$$

$$W_{k,1}(m,l,q)W_{k,1}(m,l+1,0)\frac{1}{12}T_C^4 + W_{k,1}(m,l,0)W_{k,1}(m,l+1,q)\frac{1}{12}T_C^4 +$$

$$W_{k,1}(m,l+1,0)W_{k,1}(m,l+1,q)\cdot\frac{1}{4}T_C^2 +$$

$$W_{k,1}(m,l,0)\cdot[H_{k,1}(m,l+1,N+q) - H_{k,1}(m,l+1,q)]\cdot\frac{1}{24}T_C^4 +$$

$$W_{k,1}(m,l+1,0)[H_{k,1}(m,l+1,N+q) - H_{k,1}(m,l+1,q)]\cdot\frac{1}{8}T_C^4\} +$$

$$\frac{1}{N_L N T_C}\sum_{q=0}^{N-1}\sum_{k=2}^{K}\sum_{m=0}^{N_L-1}\sum_{l=0}^{N-1} P_k\{W_{k,1}(m,l,0)W_{k,1}(m,l,q)\cdot\frac{1}{3}T_C^4 +$$

$$W_{k,1}(m,l,q)W_{k,1}(m,l+1,0)\frac{1}{6}T_C^4 +$$

$$[W_{k,1}(m,l+1,0) + W_{k,1}(m,l,0)]\cdot[W_{k,1}(m,l+1,q+1) - W_{k,1}(m,l,q+1)]\cdot\frac{1}{12}T_C^4 +$$

$$W_{k,1}(m,l,0)\cdot[H_{k,1}(m,l,N+q) - H_{k,1}(m,l,q)]\cdot\frac{5}{24}T_C^4 +$$

$$W_{k,1}(m,l+1,0)\cdot[H_{k,1}(m,l,N+q) - H_{k,1}(m,l,q)]\cdot\frac{1}{8}T_C^4\}$$

$$= \frac{T_C^3}{4N_L N}\sum_{q=0}^{N-1}\sum_{k=2}^{K}\sum_{m=0}^{N_L-1}\sum_{l=0}^{N-1} P_k\{W_{k,1}(m,l,0)W_{k,1}(m,l,q)\cdot\frac{5}{3} +$$

$$W_{k,1}(m,l+1,0)W_{k,1}(m,l,q) + W_{k,1}(m,l,0)W_{k,1}(m,l+1,q)\frac{1}{3} +$$

$$W_{k,1}(m,l+1,0)W_{k,1}(m,l+1,q)\cdot +$$

$$[W_{k,1}(m,l+1,0) + W_{k,1}(m,l,0)]\cdot[W_{k,1}(m,l+1,q+1) - W_{k,1}(m,l,q+1)]\cdot\frac{1}{3} +$$

$$W_{k,1}(m,l,0)\cdot[H_{k,1}(m,l+1,N+q) - H_{k,1}(m,l+1,q)]\cdot\frac{1}{6} +$$

$$W_{k,1}(m,l+1,0)[H_{k,1}(m,l+1,N+q) - H_{k,1}(m,l+1,q)]\cdot\frac{1}{2} +$$

$$W_{k,1}(m,l,0)\cdot[H_{k,1}(m,l,N+q) - H_{k,1}(m,l,q)]\cdot\frac{5}{6} +$$

$$W_{k,1}(m,l+1,0)\cdot[H_{k,1}(m,l,N+q) - H_{k,1}(m,l,q)]\cdot\frac{1}{2}\}$$

$$= \frac{P_1 T_C^3}{4N_L N} I_L \qquad (4\text{-}39)$$

where

$$
\begin{aligned}
I_L = \sum_{q=0}^{N-1} \sum_{k=2}^{K} \sum_{m=0}^{N_L-1} \sum_{l=0}^{N-1} \frac{P_k}{P_1} \{ & W_{k,1}(m,l,0) W_{k,1}(m,l,q) \cdot \frac{5}{3} + \\
& W_{k,1}(m,l+1,0) W_{k,1}(m,l,q) + W_{k,1}(m,l,0) W_{k,1}(m,l+1,q) \frac{1}{3} + \\
& W_{k,1}(m,l+1,0) W_{k,1}(m,l+1,q) \cdot + \\
& [W_{k,1}(m,l+1,0) + W_{k,1}(m,l,0)] \cdot [W_{k,1}(m,l+1,q+1) - W_{k,1}(m,l,q+1)] \cdot \frac{1}{3} + \\
& W_{k,1}(m,l,0) \cdot [H_{k,1}(m,l+1,N+q) - H_{k,1}(m,l+1,q)] \cdot \frac{1}{6} + \\
& W_{k,1}(m,l+1,0) [H_{k,1}(m,l+1,N+q) - H_{k,1}(m,l+1,q)] \cdot \frac{1}{2} + \\
& W_{k,1}(m,l,0) \cdot [H_{k,1}(m,l,N+q) - H_{k,1}(m,l,q)] \cdot \frac{5}{6} + \\
& W_{k,1}(m,l+1,0) \cdot [H_{k,1}(m,l,N+q) - H_{k,1}(m,l,q)] \cdot \frac{1}{2} \}
\end{aligned}
\quad . \quad \text{(4-40)}
$$

Because local CM chips with even number and incoming CL chips with odd number are all zeros, and N is an even number, one of $W_{k,1}(m,l,q)$ and $W_{k,1}(m,l+1,0)$ is zero. Therefore, in Equation (4-40), $W_{k,1}(m,l+1,0) W_{k,1}(m,l,q) = 0$. For the same reason, one has

$W_{k,1}(m,l,0) W_{k,1}(m,l+1,q) = 0$,

$W_{k,1}(m,l,0) [H_{k,1}(m,l+1,N+q) - H_{k,1}(m,l+1,q)] = 0$,

$W_{k,1}(m,l+1,0) [H_{k,1}(m,l,N+q) - H_{k,1}(m,l,q)] = 0$,

and

$$\sum_{m=0}^{N_L-1}\sum_{l=0}^{N-1}\frac{P_k}{P_1}[W_{k,1}(m,l,0)W_{k,1}(m,l,q)]=\sum_{m=0}^{N_L-1}\sum_{l=0}^{N-1}\frac{P_k}{P_1}[W_{k,1}(m,l+1,0)\cdot W_{k,1}(m,l+1,q)]\,,$$

$$\begin{aligned}&\sum_{m=0}^{N_L-1}\sum_{l=0}^{N-1}\frac{P_k}{P_1}[W_{k,1}(m,l+1,0)+W_{k,1}(m,l,0)]\cdot[W_{k,1}(m,l+1,q+1)-W_{k,1}(m,l,q+1)]\cdot\frac{1}{3}\\&=\sum_{m=0}^{N_L-1}\sum_{l=0}^{N-1}\frac{P_k}{3P_1}[W_{k,1}(m,l+1,0)\cdot W_{k,1}(m,l+1,q+1)-W_{k,1}(m,l,0)\cdot W_{k,1}(m,l,q+1)]\\&=\frac{P_k}{3P_1}\{\sum_{m=0}^{N_L-1}\sum_{l=0}^{N-1}[W_{k,1}(m,l+1,0)\cdot W_{k,1}(m,l+1,q+1)]\\&\quad-\sum_{m=0}^{N_L-1}\sum_{l=0}^{N-1}[W_{k,1}(m,l,0)\cdot W_{k,1}(m,l,q+1)]\}\\&=0\end{aligned}\,,$$

$$\begin{aligned}&\sum_{m=0}^{N_L-1}\sum_{l=0}^{N-1}\frac{P_k}{P_1}W_{k,1}(m,l,0)[H_{k,1}(m,l,N+q)-H_{k,1}(m,l,q)]\\&=\sum_{m=0}^{N_L-1}\sum_{l=0}^{N-1}\frac{P_k}{P_1}W_{k,1}(m,l+1,0)[H_{k,1}(m,l+1,N+q)-H_{k,1}(m,l+1,q)]\end{aligned}\,.$$

Therefore, Equation (4-40) can be rewritten as

$$\begin{aligned}I_L=\sum_{q=0}^{N-1}\sum_{k=2}^{K}\sum_{m=0}^{N_L-1}\sum_{l=0}^{N-1}\frac{P_k}{P_1}\{&\frac{8}{3}W_{k,1}(m,l,0)W_{k,1}(m,l,q)+\\&\frac{4}{3}W_{k,1}(m,l,0)\cdot[H_{k,1}(m,l,N+q)-H_{k,1}(m,l,q)]\}\end{aligned}\,. \qquad (4\text{-}41)$$

The one-sided power spectral density of the components $\Lambda_M(\tau_k)$, $\Lambda_L(\tau_k)$ and $\Lambda_G(\tau_k)$ is

$$\begin{aligned}\mu&=\mu_M+\mu_L+\mu_G\\&=\frac{P_1T_C^3}{4N}I_M+\frac{P_1T_C^3}{4N_LN}I_L+\frac{N_0(NT_C)^2}{4}\cdot\end{aligned} \qquad (4\text{-}42)$$

Referring to Equations (4-9) to (4-12), and given the desired signal power

$P_1(NT_C)^2/8$, the PLL phase error is

$$\begin{aligned}\sigma_\phi{}^2 &= \mu \cdot \frac{B_n}{P_1(NT_C)^2/8} \\ &= [\frac{2T_C}{N^3} I_M + \frac{2T_C}{N_L N^3} I_L + \frac{2N_0}{P_1}] \cdot B_n \ . \\ &= \sigma_{\phi M}^2 + \sigma_{\phi L}^2 + \sigma_{\phi n}^2 \\ &= \sigma_{\phi C}^2 + \sigma_{\phi n}^2\end{aligned} \tag{4-43}$$

where B_n is the PLL loop-noise bandwidth, $\sigma_{\phi M}^2 = \frac{2T_C}{N^3} I_M B_n$, $\sigma_{\phi L}^2 = \frac{2T_C}{N_L N^3} I_L B_n$, $\sigma_{\phi n}^2 = \frac{2N_0}{P_1} B_n$ and $\sigma_{\phi C}^2 = \sigma_{\phi M}^2 + \sigma_{\phi L}^2$.

4.3 Simulation of the Average PLL Phase Error under Cross-Correlation and White Gaussian Noise

The PLL phase error in the above analyses includes the effects of white Gaussian noise and of the cross-correlation. In the following simulation, the interferences are first considered separately, then as a combined effect.

4.3.1 Simulation Scheme

In the simulation, the local CM code is assumed to match the desired incoming CM code well, with no code delay between the local CM code and the incoming CM code. This simulation includes two parts: input signal simulation and PLL simulation. Assuming that the signal is on baseband, the simulated signal includes

the desired signal, undesired signals from other satellites, and AWGN. In the simulation of the signal, the code delays between the local CM code and incoming CM and CL codes are considered to be random parameters uniformly distributed in the range [0, T]. For the incoming CM codes, there are navigation data that have random values of +1 or -1 on the CM codes, depending on the code delays. For the incoming CL codes, the m parameters are also considered to be random values uniformly distributed in the range [0, 74]. The phase differences between the local carrier and those of undesired signals are also considered to be random parameters, and they are uniformly distributed in the range [0, 2π]. After the incoming signal is simulated, it is multiplied with a local signal. Then the output of this correlation is sent to the simulated PLL tracking loop.

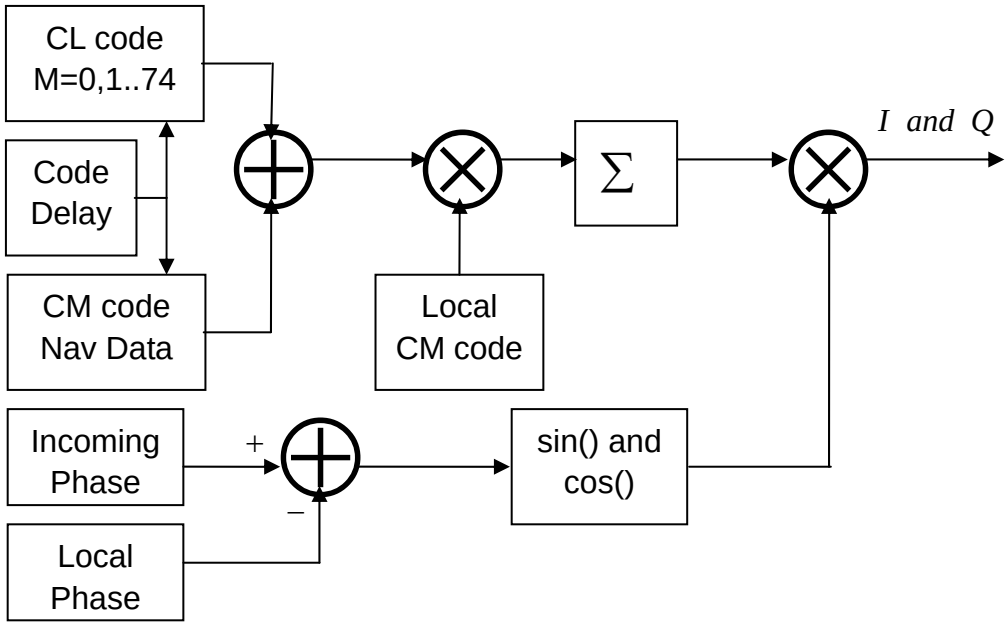

Figure 4.4 Simulated Base-band Signal for Phase-Locked Loop

The first simulation process is shown in Figure 4.4. This simulation is to generate the I and Q components as the input of phase locked loop. By using Matlab, first, the L2C code is generated by the summation of CM and CL code. The CM code is simulated with code delay, and it includes navigation data. The CL code is also simulated with the same code delay, and m is a random value ranging from 0 to 74. Then the incoming L2C code is multiplied by the local CM code. After correlation and integration, the output is multiplied by the sine of the phase difference and the cosine of the phase difference to generate quadrature-phase and in-phase components.

Figure 4.5 shows that the simulated PLL tracking loop includes a discriminator,

loop filter, and NCO. In this simulation, by using Matlab, the discriminator $\Psi = sign(I) \cdot Q$ is used. This discriminator is used because it can be analysed theoretically by using linear method. The product of the sign estimation of the in-phase component and quadrature-phase component is sent to the loop filter to generate a control signal. This output of the filter controls the NCO to produce a phase prediction $\theta_2(t)$. Here, the loop noise bandwidth is set to be a typical value 10 Hz.

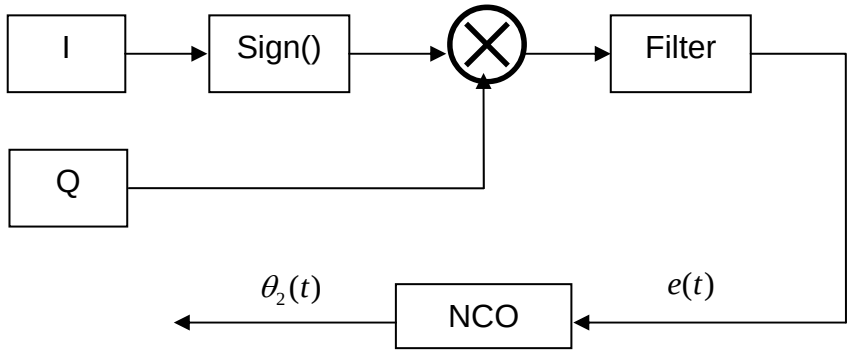

Figure 4.5 Simulated Phase-Locked Loop

4.3.2 Simulation Results and Analysis

In this section, three situations are discussed: the PLL error under the white Gaussian noise only, the PLL error under the cross-correlations only, and the PLL error under the two types of interferences combined.

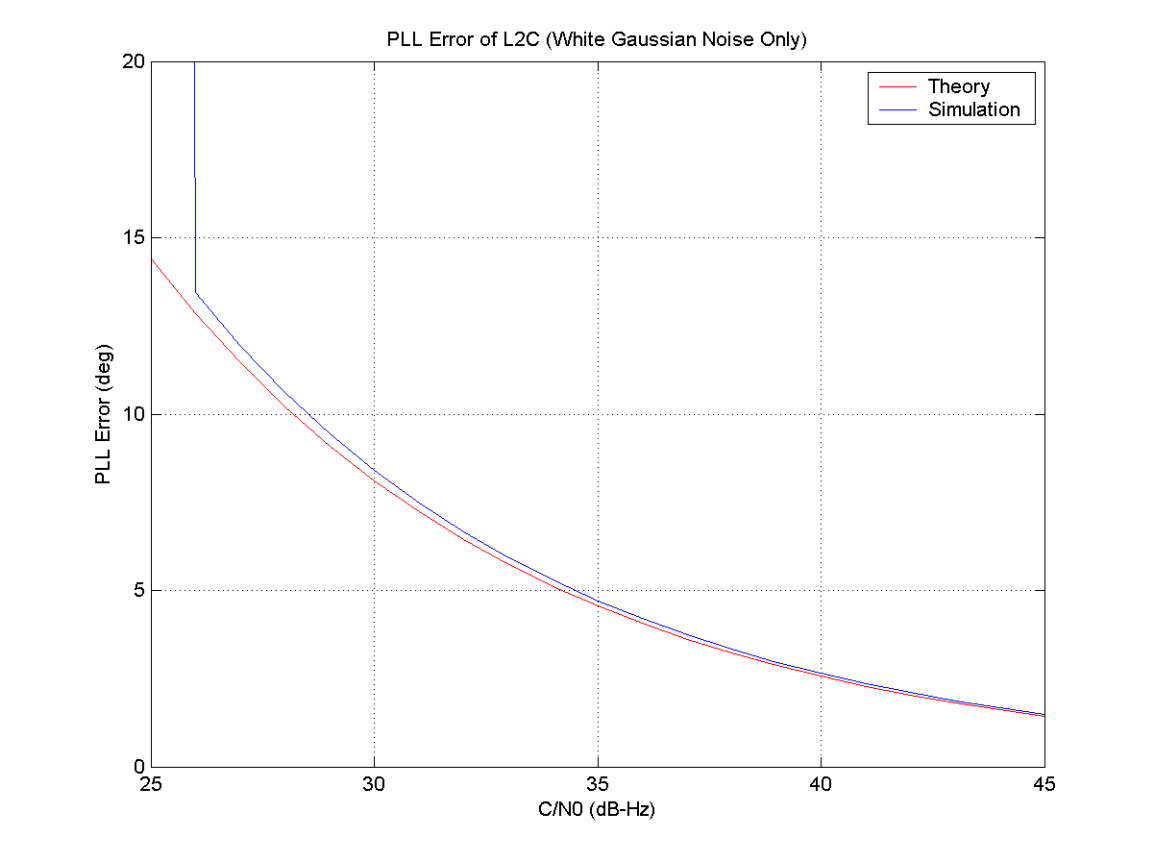

Figure 4.6 PLL Errors with White Gaussian Noise Only

Figure 4.6 shows the PLL error under white Gaussian noise only. The carrier-to-noise ratio is 25 to 45 dB-Hz; the phase-locked loop noise bandwidth B_n is 10 Hz. The PLL error is small in the normal situation (C/N_0 is about 42 dB-Hz), that is about 2 to 3 degrees. In the range C/N_0 from 45 to 34 dB-Hz, the PLL error increases slowly and the difference is less than 4 dB-Hz. Under high band-limited WGN (C/N_0 less than 34 dB-Hz), the PLL error is more than 5 degrees and grows rapidly with the decrease of C/N_0. In the range 34 to 25 dB-Hz, the PLL error increases to almost 10 degrees. When the C/N_0 is reduced to almost 25 dB-Hz, the PLL error reaches 15 degrees. Finally, when the C/N_0 is 25 dB-Hz, the PLL error is divergent, and the loop loses lock. In Figure 4.6, the difference between the

theoretical value and simulation value becomes large with a decrease of C/N_0, and the effect of the non-linear phase-locked loop is obvious.

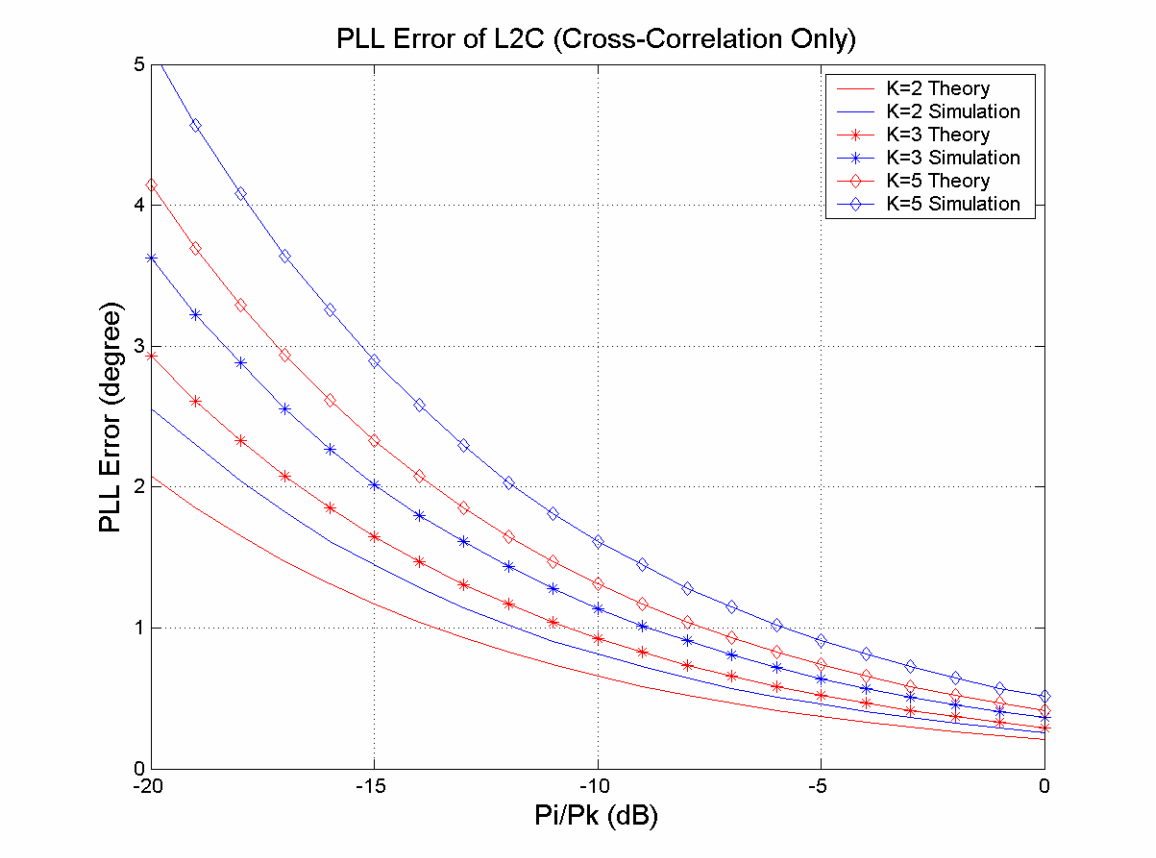

Figure 4.7 PLL Errors with Cross-Correlations Only

Figure 4.7 displays the PLL error with the cross-correlations only. When the ratio P_i / P_k is in the range [-10 0], the PLL error is less than 1.7 degrees. If the ratio P_i / P_k lies in the range [-20 -10], the PLL error increases rapidly. In the range [-20 0], if there is only one cross-correlation, the PLL error increases only to 2.2 degrees, while under the four cross-correlations, the PLL error increases up to 4.5 degrees. Therefore, under the situation with more high power undesired signals, the cross-correlation effect is large. When the signal power difference

between the desired and the unwanted signal is small, the effect of cross-correlation is minor. But with an increase of the undesired signal power, the power difference grows and the PLL error increases rapidly. The cross-correlation effect grows rapidly. The difference between the theoretical value and simulation value becomes large with a decrease of the ratio P_i / P_k, and the effect of the non-linear phase-locked loop is also obvious.

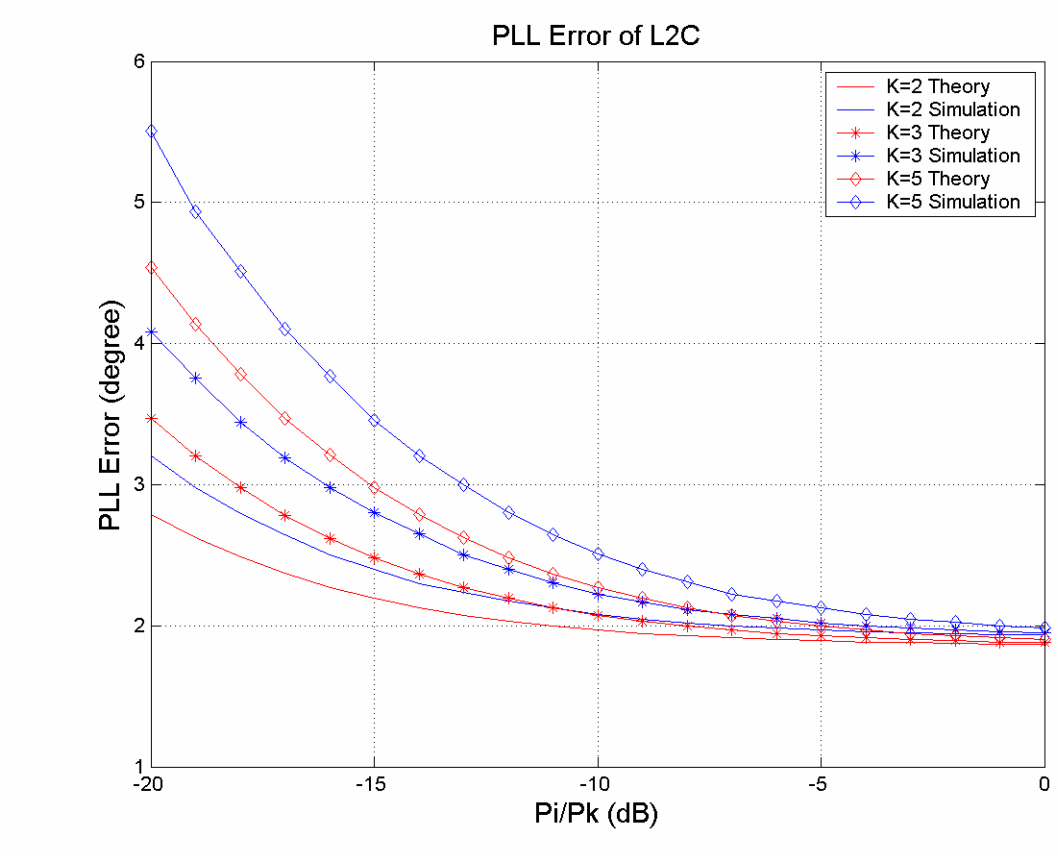

Figure 4.8 PLL Errors with Cross-Correlations and White Gaussian Noise

Figure 4.8 shows the PLL error under cross-correlations and band-limited WGN combined. In this simulation, the C/N_0 is 42.8 dB-Hz. The PLL error increases when the ratio P_i / P_k is reduced. When the ratio P_i / P_k equals 0 dB on the right

hand side in the figure, the theoretical values differ from the simulation values. The reason is that there is a non-linear effect in the simulation under this C/N_0 level. When C/N_0 is 42.8 dB-Hz, the difference between the simulated PLL error and theoretical PLL error is small. Figure 4.6 reflects the difference. In Figure 4.9, if the C/N_0 is chosen to be 30 dB-Hz, the difference is obvious. This phenomenon can be compared with the situation in Figure 4.6. Because of the non-linearity in the simulations, the difference between the simulation and the theoretical value increases when the C/N_0 decreases. So the large difference between the simulation and theoretical results is due to the non-linearity of the phase-locked loop under the lower C/N_0. When there is no band-limited WGN, as shown in Figure 4.7, the PLL errors increase to 2.2 degrees with one cross-correlation, and 4.5 degrees with four cross-correlations. But if there is band-limited WGN, as shown in Figure 4.8, when the C/N_0=42.8 dB-Hz the PLL errors increase to 1.2 degrees with one cross-correlation, and to 3.5 degrees with four cross-correlations. If the band-limited WGN becomes larger, as shown in Figure 4.9, and C/N_0=30 dB-Hz, the PLL errors increase to 0.4 degrees with one cross-correlation, and to 1.7 degrees with four cross-correlations. The reason is that the band-limited WGN increases and becomes an overwhelming factor that affects the performance of the phase-locked loop, even as the ratio P_i / P_k reaches -20 dB. Because from Figure 4.6, when C/N_0=30 dB-Hz, the PLL error affected by band-limited WGN only is about 8 degrees, while from Figure 4.7, even for P_i / P_k is -20 dB (the worst case in Figure 4.7) the PLL error affected by cross-correlation only is from 2 to 5 degrees depending on the cross-correlation

numbers. This can be explained by considering Equation (4-43). One has $\sigma_\phi = \sqrt{\sigma_{\phi C}^2 + \sigma_{\phi n}^2}$ and if there is no band-limited WGN, $\sigma_\phi = \sigma_{\phi C}$. But if the phase-locked loop is affected by the band-limited WGN and combined cross-correlations, and if the C/N_0 is also a constant, the change of the PLL error can be estimated approximately by

$$\Delta\sigma_\phi = \frac{d(\sqrt{\sigma_{\phi C}^2 + \sigma_{\phi n}^2})}{d\sigma_{\phi C}} \Delta\sigma_{\phi C} = \frac{\sigma_{\phi C}}{\sqrt{\sigma_{\phi C}^2 + \sigma_{\phi n}^2}} \Delta\sigma_{\phi C}.$$

Here, $\frac{\sigma_{\phi C}}{\sqrt{\sigma_{\phi C}^2 + \sigma_{\phi n}^2}} < 1$ such that $\Delta\sigma_\phi < \Delta\sigma_{\phi C}$. The total change of the PLL error is less than the change generated only by cross-correlation. In the worst case in Figure 4.7, P_i / P_k is -20 dB. $\Delta\sigma_{\phi n}$ is about 2 times $\Delta\sigma_{\phi C}$ depending on cross-correlation numbers, that is the PLL error reflected the band-limited WGN effect only is about 2 times the PLL error affected by cross-correlation only. The ratio becomes $\frac{\sigma_{\phi C}}{\sqrt{\sigma_{\phi C}^2 + \sigma_{\phi n}^2}} = \frac{1}{\sqrt{5}} < \frac{1}{2}$ such that $\Delta\sigma_\phi < \frac{1}{2}\Delta\sigma_{\phi C}$. In the cases $P_i / P_k > -12$ dB, the PLL error generated by cross-correlation only is less than 2 degrees. The ratio becomes $\frac{\sigma_{\phi C}}{\sqrt{\sigma_{\phi C}^2 + \sigma_{\phi n}^2}} < \frac{1}{4}$ and $\Delta\sigma_\phi < \frac{1}{4}\Delta\sigma_{\phi C}$ and, when $\sigma_{\phi n} >> \sigma_{\phi C}$, $\frac{\sigma_{\phi C}}{\sqrt{\sigma_{\phi C}^2 + \sigma_{\phi n}^2}} << 1$. We then have $\Delta\sigma_\phi << \Delta\sigma_{\phi C}$. This is why in Figure 4.9, when the C/N_0 is low (=30 dB-Hz), the change of PLL error is low.

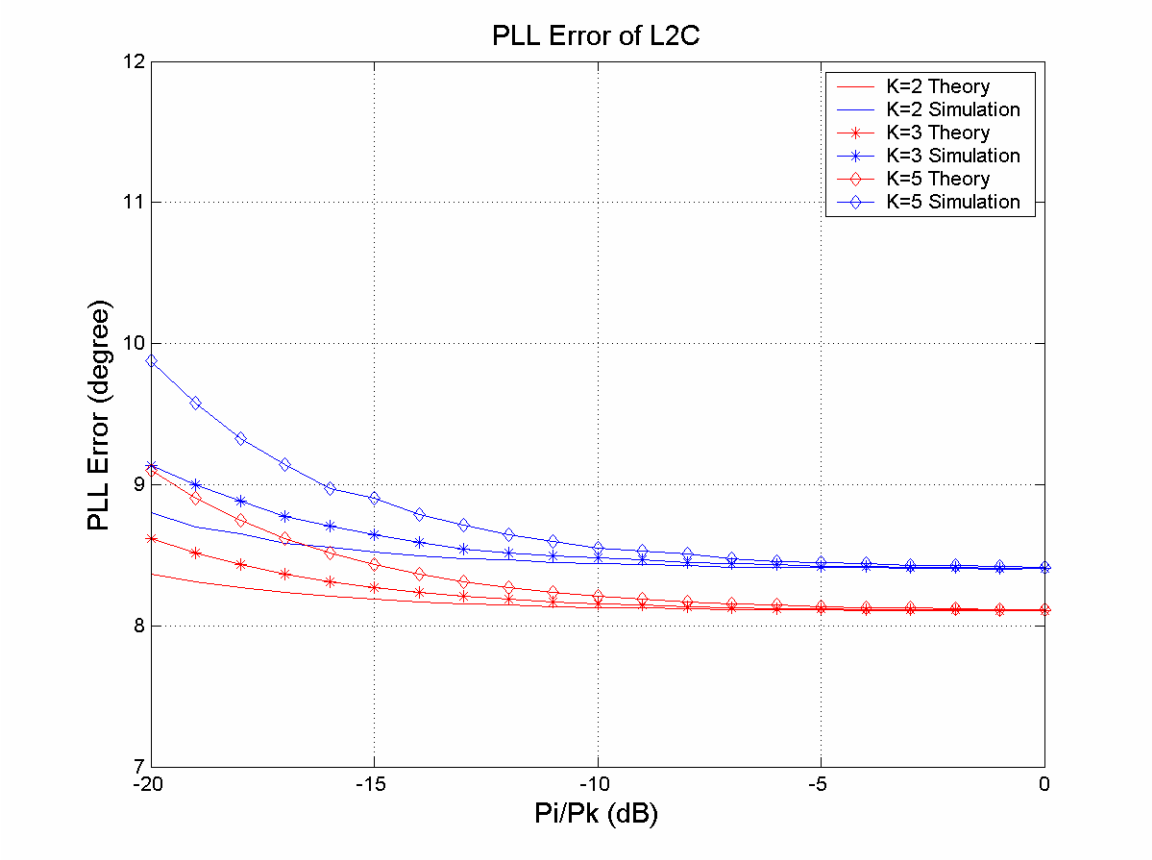

Figure 4.9 PLL Errors with Cross-Correlations and White Gaussian Noise

4.4 Conclusions

In this chapter, the PLL jitter was theoretically derived. To justify the theoretical results, a simulation is carried out to compare the theoretical derivation. The results describe the changes of PLL errors in three situations. Under band-limited WGN only, when the C/N_0 is normal (equal to 42.8 dB-Hz), the theoretical and simulation value match well. Under a low C/N_0, because of the non-linear nature of a phase-locked loop, the differences between theoretical and simulation results become large. Under the cross-correlations only, the PLL error increases rapidly with the decrease of P_i / P_k when $P_i / P_k < -10$ dB. Under the band-limited WGN

and cross-correlations combined, when the band-limited WGN becomes large (low C/N_0), the changes of PLL error generated by cross-correlations increase slowly as a function of P_i / P_k. The reason is that the effects of large band-limited WGN overwhelm the effects of cross-correlations.

Chapter 5

Conclusions and Recommendations

5.1 Conclusions

The main purpose of this thesis is to study the effects of RF interferences, such as cross-correlations and white Gaussian noise, on GPS L2C signal acquisition and carrier tracking, using both theoretical and simulated studies. The research is focused on the CM code acquisition and tracking under RF interference.

The probability of CM code detection under cross-correlation and white Gaussian noise was derived and simulated. Under the band-limited WGN only or the band-limited WGN and one worst cross-correlation combined, the non-coherent integration with M=3 has a 3 to 4 dB-Hz better ability to detect the desired signal than the one with M=1. With the same non-coherent integration number M, the detection abilities under band-limited WGN only is about 1 dB-Hz higher than the detection abilities under one worst cross-correlation and band-limited WGN combined. The worst-case cross-correlation was derived theoretically. The worst-case cross-correlation is between a local CM code (PRN=26) and incoming CL code (PRN=4), with a value of -31.1 dB. The practical calculation is done and the worst cross-correlation case is used in CM code detection and the sign evaluation of the in-phase component.

The error probability of information data estimation in the worst case is derived under cross-correlation and white Gaussian noise combined. When the power of

the desired signal is the same as the power of the undesired signal, the difference of the maximum error probabilities of information data estimation generated by the cross-correlations is not very large. The main effect on maximum error probabilities comes from band-limited WGN. Under the situation of a weak desired signal, if the unwanted signal power is higher than the desired signal power (more than 8 dB), the maximum error probabilities of information data estimation grow very fast with the decrease of the ratio Pi/Pk, especially when $K \geq 4$.

The SNR simulation results support the SNR theoretical derivation well. Under the band-limited WGN only, the SNR is linearly reduced from 26 dB to 6 dB with the reduction of the desired incoming signal power from -160 dBW to -180 dBW. The RMS error of the simulation from Figure 3.5 is less than 0.19 dB. When the desired incoming signal power is -160 dBW, the SNR is about 26 dB. Under the cross-correlations and band-limited WGN combined, when the unwanted signal power is almost the same as the desired signal power, the SNR is near 26 dB. The two results are almost the same. The effects from the cross-correlations can be ignored as compared to the effects of band-limited WGN. With an increase in the ratio of the unwanted signal power to the desired signal, the cross-correlations become an important factor on the SNR result. It cannot be ignored compared to the effects of band-limited WGN.

In PLL performance analyses of both theory and simulation, it is assumed that the DLL tracking is ideal. The local CM code exactly matches the incoming CM code, and there is no error from DLL tracking to affect the PLL performance. There are

estimation errors in the PLL performance analyses, especially in the situation of low C/N_0 or low ratio of desired signal power to unwanted signal power from other satellites P_i / P_k. The estimation errors occur because in the theoretical model, only linear status is considered. The model is assumed only in the small phase error environment. The phase error ϕ is used instead of its sinusoid. So when the phase error becomes large under strong interference, the simulation results display the non-linear property of PLL. Then the estimation error is generated and grows large when the interferences become strong; but if we compare the estimation errors with the PLL errors, it is still small.

In the analyses of PLL performance, under the band-limited WGN only, the PLL error for simulations match the theoretical result very well when the C/N_0 is normal (=42.8 dB-Hz). With the decrease of C/N_0, the difference between the simulation result and theoretical result becomes large because of the non-linear property of the PLL tracking loop. Under the cross-correlations only, the PLL error increases rapidly with the decrease of P_i / P_k when $P_i / P_k < -10$ dB. Because of the PLL's non-linear property, the estimation error becomes large when P_i / P_k is low. In the situation of the two interferences combined, because the band-limited WGN is larger than cross-correlation in general, especially under the low C/N_0 (=30 dB-Hz), the PLL error comes mainly from the band-limited WGN effects. The estimation error becomes large because of the non-linear PLL property. Therefore the simulation results and theoretical results are considered separately when the estimation error made by nonlinear property is larger than the error made by

cross-correlation.

5.2 Recommendations

Considering the findings from this thesis, it is recommended that advanced research be performed in the following areas.

First, CL code acquisition and tracking should be studied, because only CM code acquisition and tracking is studied in this thesis. The CL code is long, with a 1.5 s period. There is no navigation data on the CL code. If the CL code is analysed, a longer coherent integration time can be used, helping to increase SNR in signal detection.

Second, DLL tracking performance should be considered, because in this thesis only PLL performance is analysed and it is assumed that the DLL tracking is correct. In the real-world case, PLL tracking and DLL tracking errors affect the PLL and DLL tracking performance and vice versa, such that considering only one of them is not sufficient. If there are errors in the two tracking loops under cross-correlations and white Gausssian noise conditions, performance of the PLL should be different than the results for which only PLL error is considered.

The SNR analysis is done under the assumption that there is no code delay and no carrier offset for the desired signal. The worst case of cross-correlations and the average SNR is studied in the ideal situation. In fact, in the normal situation, there is not only code delay, but also carrier offset for the desired signal. There is loss of desired signal power, and the average SNR should be degraded.

Third, the discriminator should be studied further, because in this thesis only one type of discriminator is analysed and the linear model in used in small phase error conditions. If other discriminators are considered, can the linear model be used? If the discriminator must be analysed in non-linear status, can the non-linear model be simplified so as to analyse the PLL or DLL performance theoretically? These are questions that should be addressed.

REFERENCES

Bastide, F., O. Julien, C. Macabiau, and B. Roturier, (2002) “Analysis of L5/E5 Acquisition, Tracking and Data Demodulation Thresholds,” in *Proceeding of ION* 24-27 September, Portland, OR, pp. 2196-2207, U.S. Institute of Navigation, Fairfax, VA

Best, R. E. (2003), *Phase-Locked Loops Design, Simulation, and Applications*, McGraw-Hill, New York

Cho, D. J., C. Park, and S. J. Lee, (2004) “An Assisted GPS Acquisition Method using L2 Civil Signal in Weak Signal Environment,” *The 2004 International Symposium on GPS/GNSS* 6-8 December, Sydney, Australia

Deshpande, S. and M.E. Cannon (2004a) “Interference Effects on the GPS Signal Acquisition,” in *Proceeding of ION NTM* 26-28 January, San Diego, CA, pp. 1027-1036, U.S. Institute of Navigation, Fairfax, VA

Deshpande, S. (2004b) “Modulated Signal Interference in GPS Acquisition,” in *Proceeding of ION* 21-24 September, Long Beach, CA, pp. 76-86, U.S. Institute of Navigation, Fairfax, VA

Fontana, R.D., W. Cheung, P. M. Novak, and T. A. Stansell (2001) “The New L2 Civil Signal,” in *Proceeding of ION* 11-14 September, Salt Lake City, UT, pp. 617-631, U.S. Institute of Navigation, Fairfax, VA

Hegarty, C., A. J. Van Dierendonck, D. Bobyn, M. Tran, T. Kim, and J. Grabowski (2000) “Suppression of Pulsed Interference through Blanking,” in *Proceeding of the IAIN World Congress in Assoiation with the U.S. ION Annual Meeting* 26-28 June, San Diego, CA, pp. 399-408, U.S. Institute of Navigation, Fairfax, VA

Holmes, J. K. (1990), *Coherent Spread Spectrum Systems,* Wiley & Sons, New York, NY

Huang, W., I. Andonovic, and M. Nakagawa (1998) “PLL Performance of DS-CDMA Systems in the Presence of Phase Noise, Multiuser Interference, and Additive Gaussian Noise,” *IEEE Transactions on Communications*, Volume 46, No. 11, November, pp. 1507-1515

IS-GPS-200D (2004) *NAVSTAR GPS Space Segment / Navigation User Interfaces,* Space and Missile Systems Center (SMC) and Navstar GPS Joint Program Office (SMC/GP)

Kaplan, E.D. (1996), *Understanding GPS: Principles and Applications*, Artech House, Norwood, MA

Kumar, R., S. H. Raghavan, M. Zeitzew, P. Munjal and S. Lazar (1999) “Analysis of Code Cross Correlation Noise in GPS Receivers Operating in Augmented GPS Systems,” in *Proceeding of ION NTM* 25-27 January, San Diego, CA, pp. 295-304, U.S. Institute of Navigation, Fairfax, VA

Parkison, B.W. and J.J. Spilker Jr (1996), *Global Positioning System: Theory and Applications*, American Institute of Aeronautics and Astronautics, Washington

Peterson, W. W. (1962) *Error-Correcting Codes*, The M.I.T. Press

Pursley, M. B. (1977) “Performance Evaluation for Phase-Coded Spread-Spectrum Multiple-Access Communication—Part I: System Analysis,” *IEEE Transactions on Communications*, Volume 25, No. 8, August, pp. 795-799

Tang, B. and D. E. Dodds (2006) “Weak Signal GPS Synchronization For Locating In-Building Cellular Telephones,” *IEEE CCECE/CCGEI*, pp. 928-931

Tran, M. and C. Hegarty (2003) “Performance Evaluations of the New GPS L5 and L2 Civil (L2C) Signals,” in *Proceeding of ION NTM* 22-24 January, Anaheim, CA, pp. 521-535, U.S. Institute of Navigation, Fairfax, VA

Viterbi, Andrew J. (1966) *Principles of Coherent Communication*, McGraw-Hill, Inc.

Zhu, Z. and F. van Graas (2005) “Effects of Cross Correlation on High Performance C/A Code Tracking,” in *proceedings of ION NTM* 24-26 January, San Diego, CA, pp. 1053-1061, U.S. Institute of Navigation, Fairfax, VA